6-29-2012 12:00 AM

Uncovering Dual Roles for PERK Signaling During Experimentally Induced Pancreatitis

Elena Fazio, *The University of Western Ontario*

Supervisor: Dr. Christopher L. Pin, *The University of Western Ontario*

A thesis submitted in partial fulfillment of the requirements for the Doctor of Philosophy degree in Physiology

Uncovering dual roles for PERK signaling during experimentally induced pancreatitis

(Spine title: Examination of PERK signaling in the exocrine pancreas)

(Thesis format: Integrated Article)

by

Elena Norine Fazio

Graduate Program in Physiology and Pharmacology, Developmental Biology

A thesis submitted in partial fulfillment

of the requirements for the degree of

Doctor of Philosophy

The School of Graduate and Postdoctoral Studies

The University of Western Ontario

London, Ontario, Canada

THE UNIVERSITY OF WESTERN ONTARIO

School of Graduate and Postdoctoral Studies

CERTIFICATE OF EXAMINATION

Supervisor	Examiners
_____	_____
Dr. Christopher Pin	Dr. John Williams
Supervisory Committee	
_____	_____
Dr. Nathalie Bérubé	Dr. Frank Beier
_____	_____
Dr. Gerald Kidder	Dr. Nica Borradaile
_____	_____
Dr. Barry Tepperman	Dr. Joe Torchia

The thesis by

Elena Norine Fazio

entitled:

Uncovering dual roles for PERK signaling during experimentally induced pancreatitis

is accepted in partial fulfillment of the requirements for the degree of

Doctor of Philosophy

_____	_____
Date	Chair of the Thesis Examination Board

Abstract

Pancreatitis is characterized by inappropriate activation of digestive enzyme precursors, or zymogens, local and systemic inflammation, dysregulation of cellular calcium (Ca^{2+}), and induction of the unfolded protein response (UPR). The UPR consists of three distinct pathways all of which are activated during pancreatitis. However, the molecular roles of each remain unclear. The protein kinase RNA (PKR)-like ER kinase (PERK) pathway reduces general protein translation by phosphorylating eIF2α, and is activated within minutes of initiating pancreatic damage. Microarray analysis carried out by our lab revealed robust upregulation of the PERK pathways members Activating Transcription Factor (ATF) 3 and stanniocalcin (STC) 2. The roles of ATF3 and STC2 within the context of PERK signaling and pancreatitis are not well known. Thus, the goal of this study was to define the roles of STC2 and ATF3 during pancreatitis. Gene expression analysis revealed significant increases in STC2 during cerulein induced pancreatitis (CIP) and mice overexpressing STC2 ($STC2^{Tg}$) exhibited decreased pancreatitis severity as evidenced by the maintenance of acinar cell differentiation markers, lower levels of serum amylase compared to wild type (WT) and a decreased necrosis to apoptosis ratio. Conversely, ATF3 appears to function in an opposite fashion to STC2 during pancreatitis. Chromatin immunoprecipitation (ChIP) of pancreatic tissue following CIP showed that ATF3 bound the *Mist1* promoter, recruited Histone Deacteylasee (HDAC) 5 and repressed *Mist1* expression, leading to loss of the acinar cell phenotype. Human and mouse pancreatitis tissue samples reveal mutually exclusive expression of ATF3 and MIST1, illustrating clinical relevance for

ATF3. Mice lacking *Atf3* (*Atf3*$^{-/-}$) exhibited a similar phenotype to *STC2*^{Tg} mice, with increased maintenance of cellular junctions and cell polarity. These findings suggest that these mediators of the PERK pathway lead to opposing outcomes, and that this pathway plays a dual role of both protection and injury during pancreatitis.

Keywords

Pancreatitis, unfolded protein response, PERK pathway, STC2, ATF3, transcription, acinar cell differentiation

Co-Authorship Statement (where applicable)

Chapter 2 is a published body of work. Northern blot analysis of *Stc2* was carried out by S.A. Chadi and RT-PCR for *Atf3* and *Stc2* was carried out by K. Kernohan. Chapter 5 contains human sample immunohistochemistry that was carried out by C.L. Johnson. All other experimental work presented here was carried out by E.N. Fazio.

Acknowledgments

I am a slow walker, but I never walk backwards. – Abraham Lincoln

The completion of this thesis would not have been possible without the help of a tremendous number of people. First, I'd like to thank Christopher Pin for taking a chance on me many years ago, giving me the opportunity to rediscover science. You've been a wonderful mentor whose guidance has allowed me to become confident in my ideas to develop my own scientific mind. While, on one hand, I'm sad to be leaving, the fact that we were starting to finish each others' sentences meant that it was time to go. I can't thank you enough for what you've taught me, and for providing an environment in which I could grow.

To the members of the Pin Lab, past and present, thanks for always laughing at my jokes, and for not touching anything marked with green tape. And to Charis Johnson, it's not often that people are able to go to work and hang out with such a great friend everyday. Even though I'm just a floor away, I miss having you right there, even if you were always spoiling the jokes I would play on people!

I'd also like to thank the Children's Health Research Institute and the Department of Physiology and Pharmacology for providing me with unending support during my graduate career. I'd specifically like to thank Drs. Tom Drysdale, Gabriel DiMattia and Andy Watson for always being infallibly encouraging, and for always being interested in helping me along the way. I'd also like to thank my advisory committee,

Drs. Barry Tepperman, Nathalie Bérubé, and Gerald Kidder for providing me with valuable advice and always keeping me on task.

To all of my friends, I'd like to thank you for being so supportive of me over the years, and for being unendingly understanding when I would throw myself into my work and be out of touch for long stretches of time. I appreciate all of you, and am so lucky to be able to call you my friends.

Finally, I'd like to thank my entire family, and specifically, my parents, Valerio and Onoria Fazio. The person I am today is the result of your unending love, support and nurturing throughout my life. I wouldn't be who I am, or where I am without you, and I owe everything to you both. Mom and Dad, there's no way I can thank you sufficiently, just know that I love you and appreciate everything that you've done for me.

One quick and final thank you goes out to all of the mice that died in the name of this research (see, I told you guys I would do it…).

Table of Contents

List of Abbreviations

-/-	Knock out
AARE	Amino acid response element
AcH3	Acetylated histone H3
ANOVA	Analysis of variance
aPKC	Atypical protein kinase C
ASIP	Atypical PKC Isotype-specific Interacting Protein
ASK1	Apoptosis signal-regulating kinase 1
ATF	Activating transcription factor
Atf3$^{-/-}$	Activating transcription factor 3 knockout
ATF3ΔZip	Activating transcription factor 3 leucine zipper mutant
ATF6(N)	Activating transcription factor 6 (nuclear)
AUC	Area under curve
Bcl-2	B-cell lymphoma-2
bHLH	Basic helix-loop-helix
BiP	Binding protein
BK 5	Bovine keratin 5
bp	base pairs
bZIP	Basic leucine zipper
Ca^{2+}	Calcium ion

cAMP	Cyclic adenosine monophosphate
CCK	Cholecystokinin
Cdc42	Cell division control protein 42
CE	Cytoplasmic extract
CFTR	Cystic fibrosis transmembrane receptor
ChIP	Chromatin immunoprecipitation
ChIP	Chromatin Immunoprecipitation
ChIP-Seq	Chromatin immunoprecipitation-Sequencing
CHOP	C/EBP homologous protein
CIP	Cerulein induced pancreatitis
CP	Chronic pancreatitis
CPA	procarboxypeptidase A
CREB	cAMP response element binding
$Cre^{ER/T2}$	Cyclization recombinase
Cx32	Connexin 32
DAG	Diacylglycerol
DAPI	4',6-diamidino-2-phenylindole
DMEM	Dulbecco's modified Eagle medium
DNA	Deoxyribonucleic acid
DNAJB	DnaJ (Hsp40) homolog, subfamily B

EDEM	Endoplasmic Reticulum Degradation Enhancing Alpha-Mannosidase-Like
EDTA	Ethylenediaminetetraacetic acid
eIF2α	Elongation initiation factor 2 alpha
EMSA	Electrophoretic mobility shift assay
ER	Endoplasmic reticulum
ERAD	Endoplasmic reticulum associated protein degradation
ERSE	Endoplasmic reticulum stress response element
FAEE	Fatty acid ethyl ester
FITC	Fluorescein isothiocyanate
Fwd	Forward
GADD	Growth arrest and DNA damage inducible
GDP	Guanosine diphosphate
GEF	Guanine exchange factor
GFP	Green fluorescence protein
GFP	Green fluorescene protein
GLUT-2	Glucose transporter-2
GPCR	G-protein coupled receptor
GRP78	Glucose regulated protein 78
GRP78	Glucose-regulated protein 78

GTP	Guanosine triphosphate
H&E	Hematoxylin and eosin
H_2O	Water
HAC1	Homolog of ATF/CREB-1
HDAC	Histone deacetylase
HepG2	Hepatocellular carcinoma cell
HMGB1	High-mobility group protein B1
HRP	Horseradish peroxidase
Hsp	Heat shock protein
HUVEC	Human unbilical vein endothelial cell
IDV	Integrated density value
IF	Immunofluorescence
IgG	Immunoglobulin G
IKK	IkappaB kinase
IL	Interleukin
IP	Immunoprecipitation
IP_3	Inositol trisphosphate
IP_3R	Inositol trisphosphate receptor
IRE1	Inositol requiring enzyme-1
JNK	Jun kinase

kDa	Kilodalton
kg	Kilogram
LC3	Myosin associated protein 1 light chain 3
LiCl	Lithium chloride
Me-tRNA	Methionyl-transfer ribonucleic acid
mg	Milligrams
$MgCl_2$	Magnesium chloride
mL	millilitre
mL	Millilitres
mM	Millimolar
mRNA	Messenger ribonucleic acid
Munc18	Mammalian uncoordinated-18
Myd116	Myeloid differentiation primary response gene 116
n	n-value
Na	Sodium
NaCl	Sodium chloride
NADPH	Nicotinamide adenine dinucleotide phosphate
$NaHCO_3$	Sodium bicarbonate
NE	Nuclear extract
Nf-κB	Nuclear factor kappa-B

NFDM	Nonfat dry milk
NK-1R	Neurokinin-1 receptor
NP-40	Nonidet P-40
OCT	Optimal cutting temperature
ORF	Open reading frame
osb	Osteoblast
PAF	Platelet activating factor
PAR	Partitioning-defective 3
PBS	Phosphate buffered saline
PBS-T	Phosphate buffered saline-Tween 20
PCR	Polymerase chain reaction
PDAC	Pancreatic ductal adenocarcinoma
PDI	Protein disulfide isomerase
PDI	Protein disulphide isomerase
PDX1	Pancreas duodenal homeobox-1
PEPCK	Phosphoenolpyruvate carboxykinase
PERK	Protein kinase RNA-like endoplasmic reticulum kinase
pH	power of Hydrogen
PKCδ	Protein kinase C delta
PKCζ	PKC zeta

PKR	Protein Kinase RNA (ribonucleic acid)
PLC	Phospholipase C
PMSF	Phenylmethanesulfonylfluoride
PN	Postnatal day
PP-cell	Pancreatic polypeptide cell
PP1c	Protein phosphatase 1c
Ppp1r15a	Protein phosphatase 1 regulatory subunit 15A
PRSS1	Protease, serine 1 (trypsin 1)
PVDF	Polyvinylidene fluoride
qPCR	quantitative polymerase chain reaction
RNase	Ribonuclease
rpm	rotations per minute
RT-PCR	Reverse transcriptase polymerase chain reaction
Rvs	Reverse
S1P	Site 1 protease
S2P	Site 2 protease
SAL	Saline
SBDS	Shwachman Bodian Diamond Syndrome
SDS	Sodium dodecyl sulfate
SDS/PAGE	Sodium dodecyl sulfate/polyacrylamide gel electrophoresis

Ser51	Serine 51
SNAP	Soluble N-ethylmaleimide-sensitive fusion protein Attachment Protein
SNARE	Soluble N-ethylmaleimide-sensitive fusion protein Attachment Protein receptor
SPINK1	Serine protease inhibitor Kazal type-1
STC	Stanniocalcin
STC2^{Tg}	Stanniocalcin 2 over-expresser
STIM1	Stromal interaction molecule 1
t-SNARE	Target soluble N-ethylmaleimide-sensitive fusion protein Attachment Protein receptor
TE	Tris-EDTA
TEM	Transmission electron micrograph
TEM	Transmission electron microscopy
TF	Transcription factor
Tg	Transgenic
Tm	Tunicamycin
TNFα	Tumour necrosis factor alpha
TRAF2	Tumour nerosis factor receptor-associated factor 2
TRITC	Tetramethylrhodamine isothiocyanate
tRNA	Transfer ribonucleic acid

TTR	Transthyretin
TUNEL	Terminal deoxynucleotidyl transferase dUTP nick end labeling
UPR	Unfolded protein response
v-SNARE	Vesicular soluble N-ethylmaleimide-sensitive fusion protein A attachment Protein receptor
VAMP	Vesicle-associated membrane protein
w/v	weight/volume
WT	Wild type
XBP1	X-box protein-1
XBP1s	X-box protein-1 spliced
XBP1u	X-box protein-1 unspliced
ZO-1	Zona occludens-1
α-cell	Alpha cell
β-cell	Beta cell
δ-cell	Delta cell
ε-cell	Epsilon cell
µg	Microgram
µL	microliter
µm	Microns

List of Tables

List of Figures

List of Appendices

Chapter 1

1 « Historical Review»

1.1 « Pancreatic Structure and Function »

The pancreas is a dually functioning organ that serves to aid in the exocrine process of food digestion and the endocrine process of blood glucose homeostasis. To efficiently perform these two functions, the pancreas is composed of two discrete tissue types.

1.1.1 « The Endocrine Pancreas »

The endocrine pancreas represents approximately 2% of total pancreatic tissue. The functional unit of the endocrine pancreas is the islet of Langerhans, which is composed of multiple cell types with varying functions. Pancreatic β-cells make up the bulk of the islet, and function to produce and secret insulin to combat elevated blood glucose levels. Pancreatic α-cells envelop the islet, and produce and release glucagon to elevate blood glucose levels. Pancreatic δ-cells, pancreatic polypeptide cells (PP-cells) and ε-cells produce somatostatin, pancreatic polypeptide and ghrelin, respectively. Each of these three cell types makes up a small portion of the pancreatic islet.

1.1.2 « The Exocrine Pancreas »

The exocrine pancreas is a compound acinar gland (Langerhans, 1869) that comprises 98% of total pancreatic tissue and produces enzymes required for digestion. The functional unit of the exocrine pancreas is the acinus, composed of pancreatic acinar cells, centroacinar cells and duct cells. Pancreatic acinar cells are organized into discrete functional units called acini. Multiple acini are grouped together to form a pancreatic lobule. Within each acinus, the acinar cells are arranged with their apical ends adjacent to a central lumen that associates the cells with a pancreatic duct (Takahashi, 1984). This organization allows for co-ordinated secretion of enzymes from the cells directly into the pancreatic ductal network. Pancreatic duct cells are important not only because they form the structure of the pancreatic ductal network that delivers digestive enzymes to the gut, but also because they secrete bicarbonate. Bicarbonate is essential to the digestive process since it helps to neutralize the acid that moves from the stomach to the intestines during digestion. Centroacinar cells reside between the acinar cells and duct cells, and while their role is not fully understood but it is thought that they may contribute to electrolyte secretion as well as growth and homeostasis of proximal duct structures.

The duct network of the pancreas starts with the short, intercalated ducts associated with individual acini and collect secreted digestive enzymes. Intercalated ducts drain into intralobular ducts, which collect secretions

from acini situated in the same lobule. Intralobular ducts merge with the larger, interlobular ducts that collect acinar secretions from multiple lobules and deliver them to the main pancreatic duct that runs the entire length of the pancreas. The main pancreatic duct merges with the bile duct prior to emptying into the duodenum (Figure 1.1).

1.1.2.1 « Pancreatic Acinar Cells»

Pancreatic acinar cells are polarized cells that produce and secrete digestive enzymes in response to hormonal stimulation. These protein-producing factories synthesize both mature digestive enzymes (amylase, lipase, elastase) and inactive digestive enzyme precursors, termed zymogens. Within the acinar cell, zymogens and digestive enzymes are restricted to vesicles called zymogen granules. Containment of these proteins within zymogen granules prohibits activation of the enzymes and their exposure to the cell itself, limiting cellular digestion. Mature digestive enzymes do not require further processing to become active, but become active only in the intestines. Zymogens produced by pancreatic acinar cells include trypsinogen, chymotrypsinogen and procarboxypeptidase. After delivery to the small intestine, trypsinogen is cleaved to active trypsin by enteropeptidase in the intestinal mucosa. Trypsin subsequently cleaves the other zymogens, forming chymotrypsin and carboxypeptidase.

Figure 1.1. Anatomy of the Exocrine Pancreas. (A) Branching architecture of the exocrine pancreas. Individual acini are grouped into grape-like lobules. Ducts emerging from singular acini. are intercalated ducts that then merge into intralobular ducts that further drain into interlobular ducts. (B) Duct cells and centroacinar cells penetrate acini to facilitate digestive enzyme delivery to the small intestine. Acini are composed of individual acinar cells that are organized with their apical ends toward the centre. Nuclei are basally localized and zymogen granules are apically located. Modified from **(Bardeesy and DePinho, 2002).**

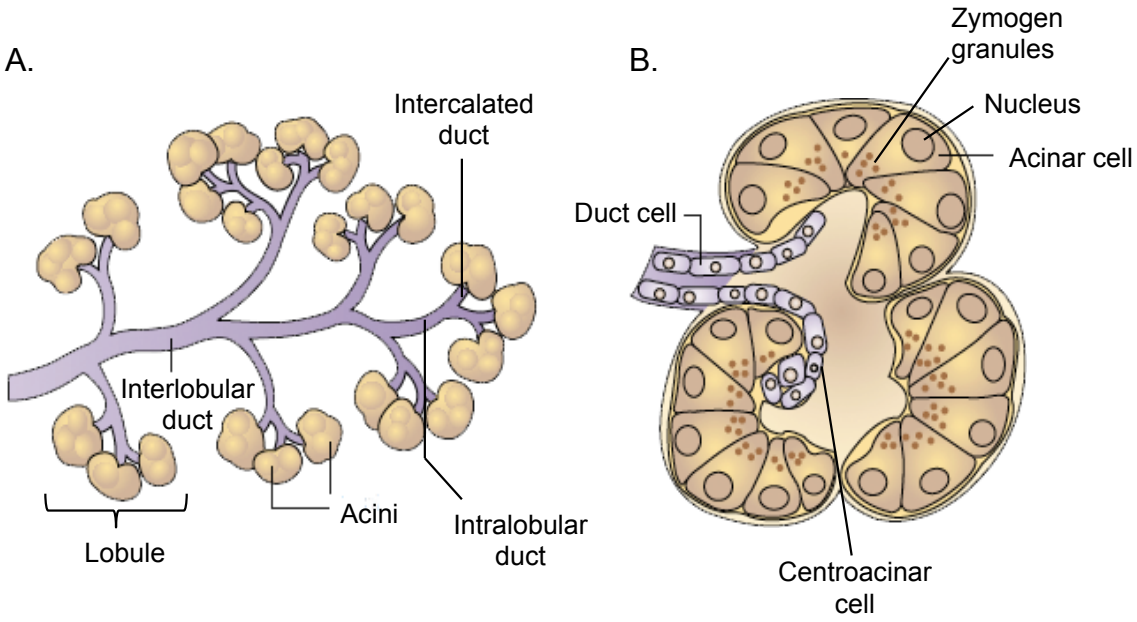

Figure 1.1. Anatomy of the Exocrine Pancreas.

The organization of the pancreatic acinar cell is such that digestive enzymes are released from the apical aspect of the cells under normal conditions. This allows for directed exocytosis into pancreatic ducts prohibiting indiscriminant enzyme release from other cell surfaces that can result in tissue damage and inflammation. To this end, pancreatic acinar cells are polarized, in that the cell nucleus is localized to the basal aspect of the cell (Ekholm, 1962), surrounded by the endoplasmic reticulum and the Golgi (reviewed in (Motta et al., 1997)). A hallmark of the apical aspect of acinar cells is the accumulation of zymogen granules (McCuskey and Chapman, 1969). Additionally, pancreatic acinar cells are associated via tight junctions near their apical ends (Friend and Gilula, 1972; Galli et al., 1976), resulting in the formation of a fluid impermeable barrier around the acinar lumen. This barrier functions to contain secreted digestive enzymes in the acinar lumen. Tight junctions also form a functional barrier, maintaining cell polarity by restricting diffusion of apical specific membrane proteins.

The partitioning-defective (PAR)-atypical protein kinase C (aPKC) complex is required for establishment of cell polarity in the epithelial cell types of many species. Most work defining the PAR-aPKC complex has been carried out in *Saccharomyces cerevisiae* and *Drosophila melanogaster;* however, mammalian homologs of PAR-aPKC proteins have been identified. In mammals, PAR-6 interacts with aPKC and agouti

signaling peptide (ASIP)/PAR-3, and this complex colocalizes with Zona occludens-1 (ZO-1), a component of tight junctions (Izumi et al., 1998). PAR-6 further interacts with cell division control protein 42 (Cdc42) (Qiu et al., 2000), which establishes cell polarity by regulating polarized transport of secretory vesicles (Adamo et al., 2001) that is important for regulated exocytosis in pancreatic acinar cells. aPKC is required for establishment of apical-basal polarity and assembly of tight junctions, since lack of aPKC expression results in mis-localization of PAR-6, ASIP and ZO-1, resulting in loss of polarity and tight junction barrier function (Suzuki et al., 2001). In mammals, PKCζ is an atypical PKC and has been implicated in cell polarity through interactions with partitioning (PAR) proteins 3 and 6, which are involved in asymmetric cell division.

1.1.2.2 « Regulated Exocytosis»

The process by which digestive enzymes are secreted from acinar cells is called regulated exocytosis. Regulated exocytosis in acinar cells is a tightly controlled process that is initiated by hormonal or neuronal stimuli. When chyme enters the duodenum, cells of the intestinal epithelium release secretagogues, one of which is cholecystokinin (CCK), a hormonal regulator of pancreatic acinar cell secretion. Pancreatic acinar cells, and to a lesser extent, neurons of the central nervous system possess CCK-A receptors, which are G-protein coupled receptors (GPCRs) from the Gq family. GPCRs interact with the trimeric G protein complex, which

includes α, β and γ subunits. Binding of CCK to the CCK-A receptor leads to dissociation of the α-subunit from the G-protein complex, and subsequent activation of phospholipase C-β (PLC-β), and cleavage of phosphatidylinositol 4,5-bisphosphate into inositol triphosphate (IP_3) and diacylglycerol (DAG; (Matozaki and Williams, 1989)). IP_3 binds to IP_3 receptors (IP_3R) located on the ER with the acinar cell. The IP3R is a ligand gated ion channel, and binding of IP3 results in a conformational change that allows stored calcium ions (Ca^{2+}) to flow from the ER into the cytoplasm. This initial wave of Ca^{2+} release results in stimulation of ryanodine receptors to increase Ca^{2+} release from ER stores, resulting in a massive Ca^{2+} influx into the cytoplasm. This apically restricted change in cytoplasmic Ca^{2+} concentration is required for the endpoint of zymogen granule exocytosis. However, DAG also plays a role in zymogen granule exocytosis by activating PKC in acinar cells.

For exocytosis of digestive enzymes to occur, the zymogen granule membrane must fuse with the apical cell membrane to allow release of its contents. Membrane fusion is regulated by soluble N-ethylmaleimide-sensitive factor attachment protein (SNAP) receptors, or SNAREs. In the SNARE hypothesis, transport vesicles of secretory pathways are equipped with vesicular SNAREs (v-SNAREs) that interact with proteins on the target membrane (t-SNAREs) to enable membrane fusion and release of vesicular contents (reviewed in (Gaisano, 2000)). The SNARE complex consists of three protein types; the vesicle-associated membrane protein

(VAMP) and SNAP proteins, both present on the vesicular membrane, and a plasma membrane localized syntaxin. Initial experiments involving the SNARE hypothesis were performed in bacterial and neuronal systems. However, non-neuronal SNARE proteins have been identified. SNAREs postulated to be involved with apical exocytosis in pancreatic acinar cells include the t-SNARE syntaxin 2 and the v-SNAREs, VAMP 2 (Gaisano et al., 1994), VAMP 8 (Wang et al., 2004), and synaptobrevin 2 (Hansen et al., 1999) and synaptotagmin 1 (Falkowski et al., 2011).

In pancreatic acinar cells syntaxin 2, which is anchored to the cell membrane is maintained in a closed conformation through association with mammalian uncoordinated-18 (Munc18). When the cytosolic Ca^{2+} concentration increases, Ca^{2+} associates with Munc18, changing its conformation and dissociating it from syntaxin 2, allowing syntaxin 2 to remain in an open conformation that is receptive to interaction with v-SNAREs. The v-SNARE with which syntaxin 2 interacts is still unidentified, however, cleavage of VAMP2 using tetanus toxin resulted in a 30% decrease in Ca^{2+} stimulated amylase secretion (Gaisano et al., 1994), and knockout of VAMP8 abolishes secretagogue stimulated secretion (Wang et al., 2004) illustrating the importance of these proteins in the secretory process. Additionally, activation of PKCδ by DAG results in phosphorylation of VAMP2, synaptotagmin 1 and syntaxin, allowing for their association and subsequent fusion of the zymogen granule and cell membranes resulting in digestive enzyme exocytosis. Therefore, PKCδ

provides a mechanistic link between acinar cell polarity and regulated exocytosis.

1.2 « Pancreatitis»

The exocrine pancreas is susceptible to numerous pathologies including cystic fibrosis, Schwachmann Diamond Syndrome, pancreatitis and exocrine pancreas cancers. Cystic fibrosis and Schwachmann Diamond Syndrome are characterized by genetic mutations in the cystic fibrosis transmembrane receptor (CFTR) (Kerem et al., 1989; Riordan et al., 1989; Rommens et al., 1989) and the Schwachmann-Bodian-Diamond-syndrome (SBDS) (Nicolis et al., 2005) genes, respectively. These two disorders are also the most common exocrine pancreas pathologies diagnosed in children, and result in exocrine pancreas insufficiency (Guy-Crotte et al., 1996; Shwachman et al., 1964). Exocrine pancreatic cancer is predominantly diagnosed in adults, and often arises from ductal cells as pancreatic ductal adenocarcinoma. Other less predominant forms of exocrine pancreas cancer include, but are not limited to, acinar cell carcinoma, epithelial-derived papillary tumours, pancreatoblastoma, which is predominant in children. Exocrine pancreatic cancer is often fatal due to late stage diagnosis arising from a lack of early detection mechanisms. However, a current predictor of pancreatic cancer is chronic pancreatitis (Lowenfels et al., 1993).

Pancreatitis, or inflammation of the pancreas, is a disease of the exocrine pancreas that can manifest in both acute and chronic forms. Pancreatitis is a result of autodigestion, where pancreatic enzymes are prematurely activated within the tissue. As the disease progresses, infection may occur, resulting in organ bleeding and tissue necrosis. Twenty percent of cases are severe, where pancreatic enzymes and toxins enter the bloodstream and cause sepsis and multi-organ failure. As mentioned, pancreatitis can also be a precursor to pancreatic cancer. Statistics reveal that over approximately 200,000 and 50,000 Americans are hospitalized with acute or chronic pancreatitis respectively, with a mortality rate of 5-20% depending on disease severity (Bank et al., 2002).

Acute pancreatitis refers to a rapid-onset, reversible inflammation of the pancreas that can vary in severity from a mild, self-limiting form, to a more aggressive phenotype. Chronic pancreatitis involves long-term inflammation, where tissue damage is irreversible. In both situations, patients experience severe abdominal pain and swelling, accompanied by nausea and vomiting.

1.2.1 «Etiology»

Pancreatitis can arise from environmental or genetic factors. There are multiple environmental influences that can lead to development of pancreatitis, including the development of gallstones, and exposure to excessive ethanol or tobacco smoke. The fact that not all people exposed

to ethanol or tobacco smoke develop pancreatitis indicates that there is a hereditary component to the disease. Work from our lab has shown an increased sensitivity to ethanol exposure in mice lacking the exocrine pancreas transcription factor MIST1 (Alahari et al., 2011), illustrating an interaction between genetic and environmental factors. Furthermore, other genetic factors associated with pancreatitis include mutations in genes encoding *cationic trypsinogen* (*PRSS1*), and *serine protease inhibitor Kazal-type 1* (*SPINK1*).

1.2.1.1 «Environmental Factors»

Gall stones are the most common cause of pancreatitis in men and women (Yadav and Lowenfels, 2006). The presence of a gallstone in the bile duct can obstruct drainage of pancreatic digestive enzymes, since the main pancreatic duct and bile duct both empty through the sphincter of Oddi. Inability to properly clear digestive enzymes from the main pancreatic duct results in accumulation of digestive enzymes that can damage pancreatic tissue and lead to pancreatic inflammation.

Other environmental risk factors include smoking and excessive alcohol consumption. Most knowledge correlating smoking to pancreatitis is epidemiological, where there is a dose dependent response to tobacco smoke exposure and a synergistic effect with alcohol consumption (Lindkvist et al., 2008; Tolstrup et al., 2009; Yadav et al., 2009). Little has been done to experimentally investigate the contribution of smoking to the

development of pancreatitis; however, one study showed that 58% of rats exposed to tobacco smoke for 12 weeks developed chronic pancreatic inflammation with fibrosis and scarring of acinar structures (Wittel et al., 2006).

The precise mechanism of alcohol-induced pancreatitis is still unclear, especially since not all heavy drinkers develop pancreatitis. However, products of ethanol metabolism are thought to contribute to the development of pancreatitis. The main site of alcohol metabolism is the liver, where ethanol undergoes oxidative metabolism to acetaldehyde and acetate (Badger et al., 2003). The pancreas' capacity for oxidative metabolism is much lower (Laposata and Lange, 1986) and uses an alternative metabolic pathway that converts ethanol into fatty-acid ethanol ester (FAEE) intermediates (Gukovskaya et al., 2002; Haber et al., 2004; Laposata and Lange, 1986). When infused into rats, FAEEs cause a pancreatitis response with pancreatic edema, acinar cell vacuolization, intracellular trypsin activation (Werner et al., 2002) and induction of proinflammatory transcription factors (Gukovskaya et al., 2002). Additionally, cell stress pathways are activated after chronic exposure to ethanol in mice, and may contribute to observed acinar cell pathology. Specifically, administration of an ethanol diet in mice results in activation of the unfolded protein response (UPR) (Alahari et al., 2011; Lugea et al., 2011).

While there is a clear association of environmental factors and the development of pancreatitis, not all people chronically exposed to ethanol or tobacco smoke develop pancreatitis, intimating the involvement of a genetic component.

1.2.1.2 «Genetic Factors»

Hereditary pancreatitis is classified as an autosomal dominant condition that starts as bouts of acute pancreatitis, progressing to chronic pancreatitis, often at a young age. Most patients with hereditary pancreatitis have one of two mutations (R122H or N29I) in the *cationic trypsinogen* gene (*PRSS1*) (Gorry et al., 1997; Whitcomb et al., 1996). In the R122H mutation, arginine 122 is replaced with a histidine (Sahin-Toth and Toth, 2000) perturbing the Arg122-Val123 association that is required for degradation of prematurely activated trypsin in the pancreas (Sahin-Toth and Toth, 2000; Varallyay et al., 1998; Whitcomb et al., 1996). Further analysis revealed that this mutation increases the auto-activation and stabilization of prematurely activated trypsin (Kukor et al., 2002). The N29I mutation results in the replacement of an asparagine residue with an isoleucine residue. This mutation results in increased trypsinogen auto-activation without increasing its stability (Sahin-Toth and Toth, 2000; Szilagyi et al., 2001; Teich et al., 2005). Thus, the accepted mechanism of *PRSS1* mutations is uncontrolled trypsin auto-activation leading to tissue damage.

Mutation of a second gene, *serine protease inhibitor Kazal-type 1* (*SPINK1*), has also been linked to familial forms of chronic pancreatitis (Witt et al., 2000). SPINK1 is a protease inhibitor that targets activated intrapancreatic trypsin. The *SPINK1* mutation, N34S, induces a conformational change that does not independently lead to pancreatitis. However, the N34S mutation is associated to alcoholic pancreatitis, indicating it is part of a larger pathological mechanism (Kuwata et al., 2002; Wittel et al., 2006).

1.2.2 «Pathology»

The pathology of pancreatitis includes inappropriate activation of zymogens, inflammatory response, dysregulation of Ca^{2+} and induction of endoplasmic reticulum (ER) stress.

1.2.2.1 «Enzyme Activation»

Acinar cells produce digestive enzymes that are synthesized and stored as inactive zymogens to prevent tissue autodigestion. While a low level of intracellular zymogen activation takes place under physiologic conditions, protective intracellular mechanisms are in place to prevent cell damage, including the presence of trypsin inhibitors, proteases to degrade enzymes, and suboptimal enzyme activation pH.

Even with these protective mechanisms in place, secretagogue hyperstimulation leads to intracellular enzyme activation. Colocalization of

zymogen granules with lysosomes plays a role in this activation, where cathepsin B is redistributed from the lysosome to the zymogen granule and subsequently activates trypsin (Saluja et al., 1987; Watanabe et al., 1984). Treatment of isolated acini with cathepsin B inhibitors E-64d or CA-074me abolished trypsin activation associated with cerulein hyperstimulation (Saluja et al., 1997; Van Acker et al., 2002). Hyperstimulation of *cathepsin B* knockout mice with cerulein showed an 80% reduction in trypsin activation compared with wild type counterparts. Parameters indicative of pancreatic damage, including necrosis, serum amylase and serum lipase, were also decreased in these animals (Halangk et al., 2000).

The activation of trypsin and other enzymes is an early initiating event of pancreatitis, where trypsin activity is detected as early as 10 minutes after hyperstimulation with cerulein in rats, with detection of carboxypeptidase by 15 minutes (Grady et al., 1996; Mithofer et al., 1998). Other hallmarks of pancreatitis, including cell vacuolization and edema, were detected within 30 minutes of hyperstimulation, indicating that enzyme activation is an initiating event in pancreatitis. The impact of enzyme activation on pancreatitis pathology is illustrated by the observation that pretreatment with protease inhibitors reduces the severity of pancreatitis in animals hyperstimulated with secretagogues (Suzuki et al., 1992).

1.2.2.2 «Inflammatory Response»

Unlike enzyme activation, the inflammatory response induced by pancreatitis is not an immediate response, occurring one hour after initiating experimental pancreatitis in mice. During pancreatitis, acinar cells activate transcription factors that induce the production and release of various chemokines and cytokines that attract inflammatory cells (Grady et al., 1997). The recruitment of various inflammatory cells potentiates expression of proinflammatory mediators including tumor necrosis factor (TNF) - α , and interleukins (IL) 1, 2 and 6 (Makhija and Kingsnorth, 2002).

Platelet activating factor (PAF) is a proinflammatory mediator upregulated in secretagogue-induced pancreatitis (Sandoval et al., 1996; Zhou et al., 1993; Zhou et al., 1990) as well as in human disease. PAF has a role in wound healing, physiological inflammation and apoptosis (Liu and Xia, 2006), and is produced by various inflammatory cells (Ishii and Shimizu, 2000), as well as in pancreatic acini in response to cerulein (Ishii and Shimizu, 2000; Stafforini et al., 2003; Zhou et al., 1993). The importance of PAF in pancreatitis pathology was illustrated when treatment with PAF antagonists resulted in decreased serum amylase levels, decreased cell vacuolization (Ais et al., 1992; Hofbauer et al., 1998; Lane et al., 2001) and decreased pancreatic inflammation (Lane et al., 2001) after hyperstimulation with cerulein.

Substance P has also been implicated in the inflammatory response to pancreatitis. Substance P is important for inflammatory processes (Bowden et al., 1994), and its expression is increased during cerulein induced pancreatitis, along with expression of it's associated receptor, the neurokinin-1 receptor (NK-1R). Mice lacking the NK-1R exhibited decreased severity of pancreatitis when hyperstimulated with cerulein (Bhatia et al., 1998), indicating that Substance P plays an important role in the pathogenesis of pancreatitis.

One of the earliest immune response is the recruitment of neutrophils, which contribute to the pathogenesis of pancreatitis. Neutrophil depletion resulted in decreased severity of cerulein induced pancreatitis in mice (Pastor et al., 2006). The influence of neutrophils in the pathogenesis of pancreatitis is twofold. First, the neutrophil's NADPH oxidase system for generating reactive oxygen species contributes to trypsin activation and cellular necrosis. This is evident in neutrophil depletion studies during pancreatitis where the cell death mechanism switches to apoptosis from necrosis (Pastor et al., 2006), and trypsin activation is decreased (Gukovskaya et al., 2002; Pastor et al., 2006). Secondly, elastase produced by neutrophils proteolytically cleaves the junctional protein E-cadherin (Mayerle et al., 2005), allowing for neutrophil transmigration into the pancreas and inhibition of neutrophil elastase results in decreased severity of pancreatitis (Mayerle et al., 2005; Song et al., 1999).

1.2.2.3 «Dysregulation of Ca^{2+}»

The resting physiologic concentration of Ca^{2+} in the acinar cell cytosol is much lower than that found in the extracellular fluid and within intracellular Ca^{2+} stores (Petersen et al., 1998). Due to this dichotomy, acinar cells are responsive to small increases in cytosolic Ca^{2+} concentrations, allowing Ca^{2+} signals to control intracellular events. Regulated exocytosis initiated by CCK relies on a specific pattern of cytosolic Ca^{2+} oscillations, where short-lived spikes in the apical pole are followed by longer lasting transients that radiate throughout the cell. Each of these oscillations associate with a burst of exocytosis and release of zymogens into the acinar lumen (Maruyama and Petersen, 1994). Hyperstimulation of acinar cells, as seen in pancreatitis, results in a different pattern of Ca^{2+} release, where Ca^{2+} release is no longer restricted to the apical border, and physiologic oscillations are replaced by a large rise in Ca^{2+} followed by sustained elevation at a lower level.

Pathologic Ca^{2+} release patterns occur early in the pathogenesis of secretagogue-induced pancreatitis. Inhibition of hyperstimulatory Ca^{2+} elevations using Ca^{2+} chelators inhibits zymogen activation, illustrating a requirement for Ca^{2+} in premature enzyme activation (Kruger et al., 2000; Raraty et al., 2000; Saluja et al., 1999). Additionally, pathologic activation of trypsinogen is attenuated in the absence of extracellular Ca^{2+}, illustrating

that Ca^{2+} release from intracellular Ca^{2+} stores alone is not sufficient for enzyme activation (Kruger et al., 2000; Saluja et al., 1999). However, cytosolic Ca^{2+} concentration alone is not sufficient for enzyme activation to occur, suggesting that other outcomes of secretagogue hyperstimulation also play a role in pancreatitis-associated trypsinogen activation (Raraty et al., 2000).

1.2.2.4 «Induction of Endoplasmic Reticulum Stress»

In mammalian cells, the endoplasmic reticulum (ER) serves as a site of protein folding, maturation and transport, and as a Ca^{2+} store. Pancreatic acinar cell function relies heavily on the ER for two reasons. First, since acinar cells produce large amounts of secreted proteins, their ER must be able to process these proteins with high fidelity. Secondly, proper zymogen secretion relies on changes in intracellular Ca^{2+}, which occur, in part, through ER store operated Ca^{2+} release.

In order for the ER to process secreted proteins efficiently, ER Ca^{2+} homeostasis must be maintained. During pancreatitis, the prolonged increase in cytosolic Ca^{2+} results in depletion of ER Ca^{2+} stores and subsequent loss of ER homeostasis. This results in ER stress, which occurs when there is an imbalance in ER protein handling. A main outcome of ER stress is activation of the unfolded protein response (UPR)

to restore protein-folding homeostasis in the ER. Our lab and others have shown that the UPR is activated during pancreatitis (Kowalik et al., 2007; Kubisch and Logsdon, 2007; Tashiro et al., 2001). While activation of the UPR during pancreatitis may be clearly linked to ER Ca^{2+} homeostasis it is interesting to note that, in addition to restoring protein folding homeostasis, the UPR activates inflammatory responses, suggesting its involvement in contradictory outcomes related to pancreatitis pathology. Therefore, it is important to know what outcomes are specifically dependent on the UPR during pancreatic injury.

1.3 « The Unfolded Protein Response»

In eukaryotic cells, the lumen of the ER is the site of protein folding and maturation of secreted and transmembrane proteins. The rate of unfolded protein entry into the ER can change rapidly based on the physiological state of the individual cell. Secretory cells are required to be responsive to physiological and pathological stimuli that result in increased protein production and secretion. For example, when pancreatic acinar cells are hormonally stimulated, they are triggered to produce and secrete digestive enzymes in quantities that exceed the capabilities of the maturation and folding machinery already present in the ER. Additionally, folding and maturation machinery require appropriate [Ca^{2+}]. In instances where the protein-folding load of a cell is rapidly increased, cell signaling cascades

are activated to adjust the protein folding capacity of the ER to ensure that the quality of secreted and transmembrane proteins is maintained. The unfolded protein response (UPR) is a set of three molecular cascades activated within the cell when its protein folding demand exceeds protein folding capacity. Activation of the UPR eases the protein load on the cell through (1) inhibition of protein translation (reviewed in (Brostrom and Brostrom, 1998; Kaufman, 1999)) (2) increasing protein folding capacity through heightened synthesis of protein folding chaperones (Haze et al., 2001; Okada et al., 2002) and increased production of lipids to expand ER compartments (Cox et al., 1997), (3) degradation of improperly folded proteins (Yoshida et al., 2003) and (4) activation of apoptosis (reviewed in (Schroder and Kaufman, 2005)).

Three transducers of the UPR have been identified, and each mediates a distinct arm of the response. These transducers are inositol-requiring protein-1 (IRE-1), activating transcription factor 6 (ATF6) and protein kinase RNA (PKR)-like ER kinase (PERK) (Figure 1.2). The UPR transducers are localized to the ER membrane, where they have an ER luminal domain that senses accumulating unfolded and misfolded proteins, and a cytosolic domain that elicits appropriate signaling mechanisms to accommodate the sensed increased protein load. The ER luminal domain associates with glucose responsive protein 78 (GRP78; BiP), which maintains the transducers in an inactive state. There are two models describing activation of UPR transducers. The first relies on

competition for BiP by accumulating of unfolded proteins in the ER lumen. Dissociation of BiP from the UPR transducers results in their activation and subsequent initiation of signaling cascades. The second model illustrates that transducer activation involves direct binding of unfolded proteins to its ER luminal domain of transducers (Gardner and Walter, 2011). This model is based on the observation that the IRE1 protein contains a groove for peptide binding (Credle et al., 2005), and that an IRE1 mutant incapable of binding BiP can activate signaling effectively (Kimata et al., 2007; Pincus et al., 2010).

1.3.1 « Activating Transcription Factor 6 (ATF6)»

ATF6 is a transcription factor synthesized as an inactive precursor localized to the ER membrane and contains a 272 amino acid ER luminal domain. While the luminal domain interacts with BiP as a sensor for accumulation of unfolded proteins, inter- and intramolecular disulfide bonds within this luminal domain act as redox sensors that monitor the ER environment (Walter and Ron, 2011). Accumulation of misfolded proteins causes ATF6 to associate with transport vesicles and translocate from the ER to the Golgi apparatus (Schindler and Schekman, 2009).

Figure1.2. The Unfolded Protein Response. The UPR consists of three pathways that are maintained in an inactive state by association with BiP. Activation of PERK, IRE1 and ATF6 results in co-ordination of numerous transcription factors that function to alleviate excess protein folding load in the ER by inhibiting translation, increasing expression of protein folding chaperones, increased protein degradation and inducing apoptosis.

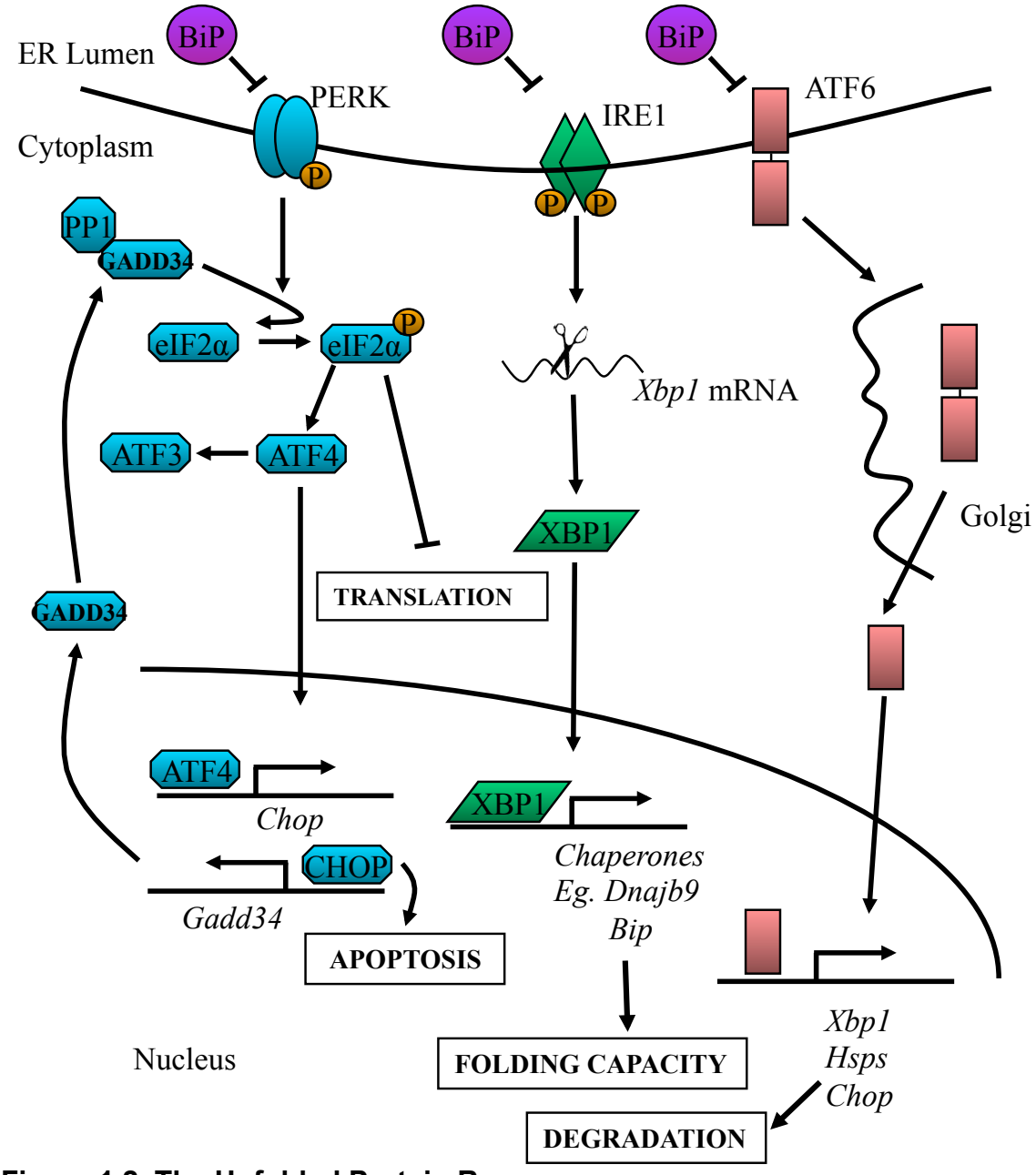

Figure 1.2. The Unfolded Protein Response.

Sequential processing by site-1 protease (S1P) and S2P (Ye et al., 2000) results in the removal of both the ATF6 luminal and transmembrane domains (Haze et al., 1999; Ye et al., 2000), liberating the 378 amino acid N-terminal cytoplasmic domain (ATF6(N)). ATF6(N) then translocates to the nucleus to activate transcription of UPR target genes including *protein disulfide isomerase* (*PDI*) to aid in protein folding, *BiP*, and the UPR transcription factor *X-box binding protein-1* (*Xbp1*) (Lee et al., 2002).

1.3.2 « Inositol Requiring Enzyme-1 (IRE1)»

Of the three pathways, the IRE1 pathway is the most highly conserved throughout species, existing in all organisms studied to date, and initially discovered in yeast. IRE1 has a bifunctional role as both a kinase and an endoribonuclease. The only known phosphorylation event mediated by IRE1 is trans-autophosphorylation of its juxtaposed kinase domains after oligomerization (Papa et al., 2003; Shamu and Walter, 1996).

Trans-autophosphorylation activates IRE1's endoribonuclease activity, the only known substrate for which is *Xbp1* (*Hac1* in yeast; (Calfon et al., 2002; Yoshida et al., 2001)), which encodes X Binding Protein 1, a basic-helix-loop-helix (bHLH) transcription factor. IRE1 mediates endonucleolytic cleavage of a 26 base pair intron within *Xbp1* mRNA. After excision, the 5' and 3' fragments are ligated by a yet unknown mechanism in metazoans, but appears to be similar to the mechanism in yeast where ligation occurs by tRNA ligase (Sidrauski et al., 1996). Prior to

cleavage, translation of unspliced *Xbp1* (*Xbp1u*) mRNA is results in the generation of a highly labile protein (Yoshida et al., 2006). The cleavage event that generates spliced *Xbp1* (*Xbp1s*) results in a frameshift mutation that shifts the stop codon and results in the translation of a more stable protein containing a nuclear localization signal and transactivation domain (Yoshida et al., 2001; Yoshida et al., 2006). After translocation to the nucleus, XBP1 activates expression of a number of genes, including protein folding chaperones, genes involved in ER associated degradation (ERAD) and genes that regulate lipid biosynthesis, thereby stimulating ER expansion. In contrast, XBP1u acts as a negative regulator of the UPR by binding XBP1s and sequestering it from the nucleus, thereby inhibiting its transcriptional activation abilities (Yoshida et al., 2006).

Events downstream of IRE1 oligomerization include binding of TRAF2 (Urano et al., 2000). The IRE1-TRAF2 complex can recruit multiple factors, including IκB kinase (IKK), and apoptosis signal regulating kinase 1(ASK1). Recruitment and activation of IKK results in phosphorylation and subsequent degradation of IκB, releasing nuclear factor-κB (NF-κB), which translocates to the nucleus (Hu et al., 2006). The TRAF2-IRE1 complex recruits ASK1, which further activates c-Jun N-terminal kinase (JNK) (Davis, 2000; Nishitoh et al., 1998). Subsequent transcriptional regulation by both NF-κB and JNK plays a role in expression of inflammatory genes in conditions of cell stress and accumulated unfolded proteins (Urano et al., 2000).

1.3.3 « Protein Kinase RNA (PKR)-Like ER Kinase (PERK)»

PERK is an ER resident transmembrane kinase that, when activated, oligomerizes and undergoes trans-autophosphorylation, much like IRE1. When activated, PERK phosphorylates elongation initiation factor 2α (eIF2α) at serine 51. Phosphorylation of eIF2α inhibits general protein translation. When eIF2α is not phosphorylated, the GTP-bound eIF2 heterotrimer recruits Met-tRNA to the translational start site, allowing protein translation to proceed. Once translation is initiated, GTP undergoes hydrolysis to GDP, leaving eIF2 in an inactive GDP bound form. The eIF2Bε subunit of the eIF2B complex acts as a guanine nucleotide exchange factor (GEF) and is required to recycle eIF2 into its active, GTP bound form. When eIF2α becomes phosphorylated at Ser51, it acts as a competitive inhibitor of eIF2B, preventing reactivation of eIF2 and a subsequent decrease in recruitment of Met-tRNA to translational start sites, resulting in a overall decrease in translation (Figure 1.3; (Harding et al., 1999)). Decreased translation relieves the protein folding load for the cell and conserves amino acid pools for essential functions (Anthony et al., 2004; Zhang et al., 2002). While general protein translation is repressed by the phosphorylation of eIF2α, mRNAs with small open reading frames (ORFs) in their 5' region are preferentially translated. Activating transcription factor 4 (ATF4) is one such mRNA that is preferentially translated. ATF4 regulates the expression of multiple UPR-related target genes, including *CCAAT/enhancer homologous protein*

(*CHOP*)/*Growth arrest and DNA-Damage-inducible 153* (*GADD153*) (Harding et al., 2000; Ma et al., 2002b), *Growth Arrest and DNA Damage-inducible 34* (*GADD34*) (Ma and Hendershot, 2003), *Stanniocalcin 2* (*STC2*) (Ito et al., 2004) and *Activating transcription factor 3* (*ATF3*) (Jiang et al., 2004).

CHOP/GADD153 is a basic leucine zipper (bZIP) transcription factor that is part of the apoptotic response of the UPR. In most cells, CHOP is expressed at low levels, and increases only following induction of ER stress. In addition to ATF4, ATF6 (Yoshida et al., 2000) and XBP1s can regulate *Chop* expression. The responsiveness of *Chop* to all three factors is due to the presence of two amino- acid-regulatory elements (AAREs) (Bruhat et al., 2000) and two ER stress response elements (ERSEs) within the *Chop* promoter (Ubeda and Habener, 2000). While ATF6, XBP1s and ATF4 can all bind the *Chop* promoter, ablation of the PERK pathway results in nearly complete ablation of *Chop* induction during ER stress, indicating that the PERK/ATF4 axis is required during stress conditions, and the other pathways are required for maximal induction of *Chop* (Harding et al., 2000; Okada et al., 2002; Scheuner et al., 2001). CHOP is a pro-apoptotic factor since it represses Bcl-2 expression (McCullough et al., 2001), allowing the increased Ca^{2+} flux from the ER into the mitochondria (Filippin et al., 2003) thereby resulting in mitochondrial membrane

Figure 1.3. Mechanism of translational Inhibition by the UPR. Under normal conditions, the eIF2Bε subunit of the eIF2B complex recycles GDP to GTP on the γ subunit of eIF2. GTP-eIF2 recruits met-tRNA to the translational start site and translation proceeds. Induction of the UPR results in dimerization and activation of PERK, which then phosphorylates eIF2α at serine 51. This phosphorylation event renders eIF2 a competitive inhibitor of eIF2B, resulting in decreased recycling of GDP to GTP on eIF2, decreasing the recruitment of met-tRNA to translational start sites.

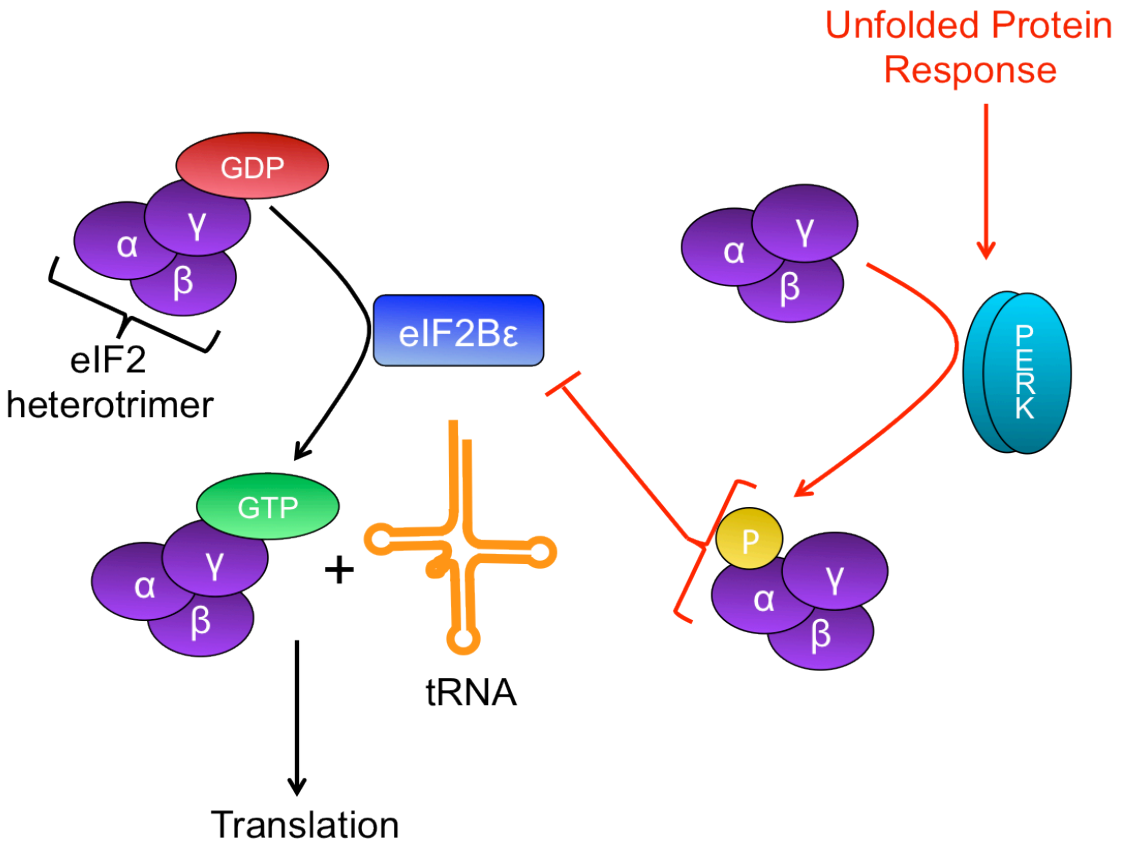

Figure 1.3. Mechanism of Translational Inhibition by the UPR.

depolarization (Annis et al., 2001; Hacki et al., 2000). This apoptotic mechanism occurs when other mitigating outcomes of the UPR have failed. Protein phosphatase 1 regulatory subunit 15A (Ppp1r15a; or Growth arrest and DNA damage inducible (GADD34)) is an ER stress-inducible factor. ATF4 regulates expression of *Gadd34* by binding to the unfolded protein response element (UPRE) that is upstream of the transcriptional start site (Gardner and Walter, 2011; Ma and Hendershot, 2003). When GADD34 is expressed, it acts as a regulatory subunit for protein phosphatase-1 (PP1c), which dephosphorylates eIF2α both in vitro and in vivo. Thus, GADD34 acts as a negative feedback mechanism for the PERK pathway by mediating dephosphorylation of eIF2α and promoting re-initiation of general translation (He et al., 1996; Novoa et al., 2001).

1.3.3.1 « Stanniocalcin 2 (STC2)»

The stanniocalcin (STC) family of secreted glycoproteins consists of two members – STC1 and STC2 – that have 35% conserved identity and conservation of exon/intron boundaries, indicating that they are paralogs (Moore et al., 1999). STC was first discovered in fish and shown to be involved in Ca^{2+} homeostasis through effects on Ca^{2+} influx (Flik et al., 1990; Sundell et al., 1992). *Stc2* mRNA is expressed in a wide variety of mammalian tissues, including the heart, prostate, uterus, pancreas, and skeletal muscle (Gagliardi et al., 2005; Shin and Sohn, 2009). In mammals STC2 is undetectable in the circulation, thus STC2-related regulation of

Ca^{2+} is thought to take place at the cellular level. Transgenic mice over-expressing a human *STC2 (STC2^{Tg})* exhibit dwarf phenotypes (Gagliardi et al., 2005; Johnston et al., 2010) related to negative effects on bone and muscle development (41). Recent work with mice lacking *Stc2 (Stc2$^{-/-}$)* identified STC2 as a negative regulator of Ca^{2+} influx into the cytosol from ER stores, and as an interactor with the ER Ca^{2+} sensor stromal interaction molecule 1 (STIM1)(Zeiger et al., 2011). Additionally, *STC2* expression is upregulated upon induction of ER stress in N2a neuroblastoma cells (Law and Wong, 2009). This increase in *STC2* expression was reliant on the concomitant increase of ATF4 (Ito et al., 2004). While the exact function of STC2 in relation to the PERK pathway is unknown, studies using cultured fibroblasts isolated from *Stc2$^{-/-}$* mice have revealed that STC2 expression is a prosurvival mechanism of the UPR (Zeiger et al., 2011). To date, no relationship between PERK signaling and STC2 activation has been identified *in vivo*.

1.3.3.2 « Activating Transcription Factor 3 (ATF3)»

ATF3 is a bZIP transcription factor that belongs to the ATF/cAMP response element binding (CREB) family of proteins that bind to a core consensus sequence (TGACGT) in target promoters (Deutsch et al., 1988; Montminy and Bilezikjian, 1987). ATF3 dimerizes at the leucine zipper motif to regulate transcription. When homodimerized, ATF3 represses transcription of target genes, whereas heterodimerization can result in

different outcomes based on the binding partner. Heterodimerization with CHOP results in the formation of an inactive dimer that cannot regulate transcription (Chen et al., 1996). However, association with c-Jun results in activation of a transcriptional program in neurons (Nakagomi et al., 2003; Pearson et al., 2003).

The outcome of ATF3 acting as a transcriptional activator or repressor may be dictated by the isoform of ATF3 that is expressed or whether an ATF/CRE site is present in the promoter of the gene being regulated. ATF3 binds to promoter regions with ATF/CRE sites and stabilizes inhibitory cofactors resulting in gene repression.

The discovery of various ATF3 isoforms has uncovered a role for ATF3 in transcriptional activation. ATF3 isoforms lack the leucine zipper domain to varying degrees, resulting in finability to dimerize (Figure 1.4A). ATF3ΔZip was the first isoform to be identified and is the product of alternative splicing of the *ATF3* gene. While full length ATF3 acts as a transcriptional repressor, ATF3ΔZip does not bind DNA and acts as a transcriptional activator (Chen et al., 1994), which led to a cofactor model of ATF3 gene activation. In this model, ATF3 sequesters inhibitory cofactors from promoters, bypassing transcriptional repression (Chen et al., 1994; Hashimoto et al., 2002) (Figure 1.4B).

Second and third ATF3 splice variants (ATF3ΔZip2a,b) were discovered in human umbilical vein endothelial cells (HUVECs) and have confirmed that

Figure 1.4. ATF3 Isoforms and Mechanisms of Transcriptional Regulation. A. ATF3 contains two activation domains (A), one repression domain (R), a basic region and leucine zipper (Zip). The truncated ATF3ΔZip and ATF3ΔZip2 isoforms lack the leucine zipper domain. B. ATF3 represses transcription of genes containing ATF/CRE sites in their promoters by recruiting inhibitory factors (I). ATF3 activates transcription at genes that do not contain ATF/CRE sites in their promoters by sequestering inhibitory factors. Truncated ATF3 isoforms also sequester inhibitory factors to activate transcription. Modified from (Chen et al., 1994; Hashimoto et al., 2002).

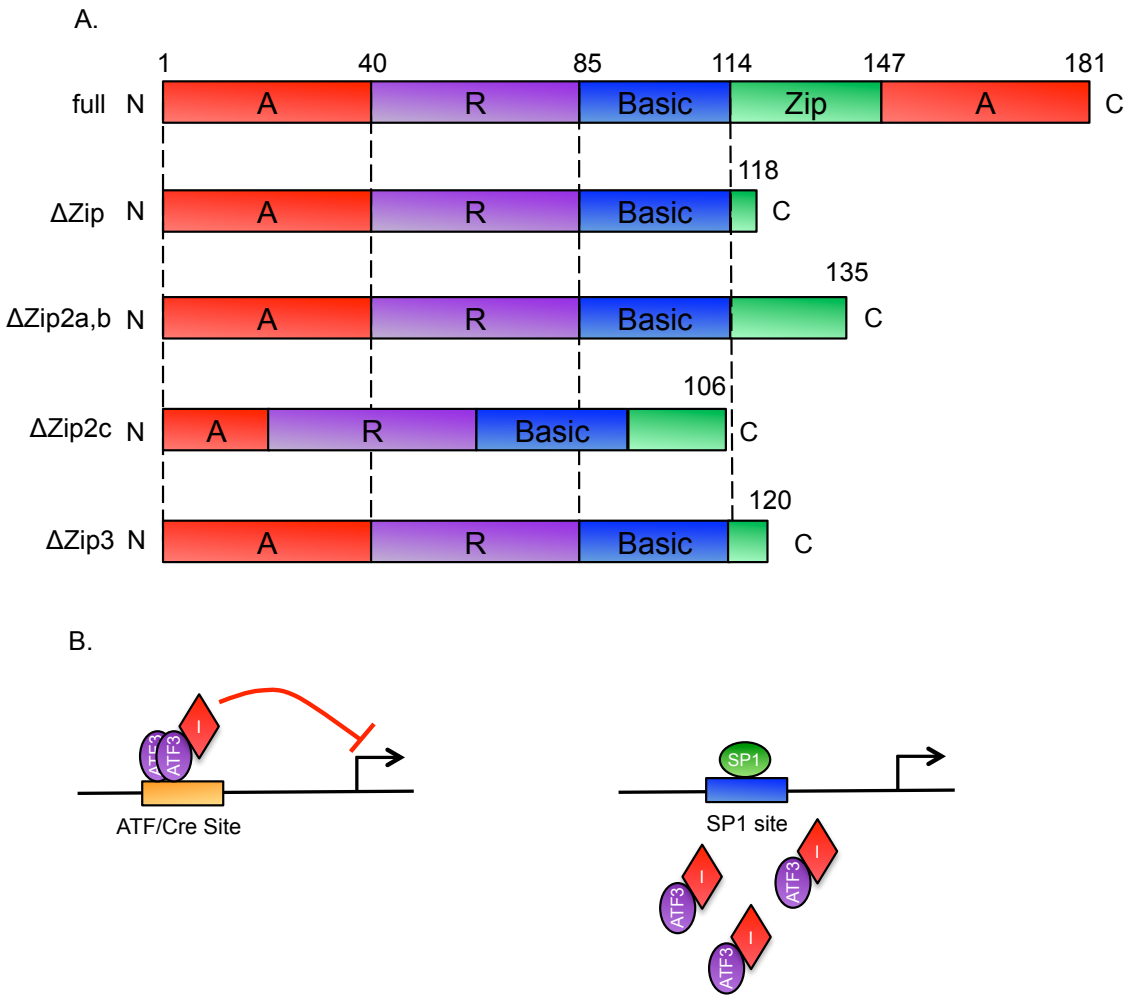

Figure 1.4. Isoforms of ATF3 and Mechanisms of Transcriptional Regulation.

ATF3ΔZip isoforms counteract transcriptional repression conferred by ATF3 (Hashimoto et al., 2002) (Figure 1.4). ATF3ΔZip2c and ATF3ΔZip3 were both identified in hepatocellular carcinoma (HepG2) cells during analysis for ATF3ΔZip2 expression, and while ATF3ΔZip2c conferred no transcriptional regulation ranscriptional transcriptional regulation in this system, ATF3ΔZip3 was able to stimulate transcription (Pan et al., 2003). However, the in vivo mechanisms by which ATF3 confers transcriptional regulation are still unclear.

A recent study revealed that ATF3 recruits HDAC1 to the *IL-6* and *IL-12b* gene promoters during ischemia/reperfusion injury in the kidney cell line NRK-52E (Li et al., 2010), providing a mechanism by which ATF3 confers transcriptional repression.

Mice lacking *Atf3* (*Atf3*$^{-/-}$) exhibit no obvious phenotypes, consistent with the idea that ATF3 is a stress-inducible gene not required for normal physiological processes (Hartman et al., 2004). Further studies with *Atf3*$^{-/-}$ mice revealed a role for ATF3 in numerous disease states where ATF3 promotes apoptosis in cytokine stressed pancreatic islets (Hartman et al., 2004), protects against cardiac hypertrophy, dysfunction and fibrosis (Zhou et al., 2011), and protects against ischemia/reperfusion injury in the kidney (Li et al., 2010).

Three different lines of mice overexpressing ATF3 have been generated. Over-expression of ATF3 using the *bovine keratin V* (*BK5*) promoter

(*BK5.ATF3*), which promotes ATF3 expression in epithelial cells, leads to ATF3 accumulation in the epidermis, mammary gland, tongue, thymus, stomach and pancreas. *BK5.ATF3* mice exhibit a sparse hair phenotype, and develop oral carcinoma (Wang et al., 2007) and mammary metaplastic lesions or tumours (Wang et al., 2008) indicative of a role for ATF3 in cancer progression.

ATF3 expression driven by the *transthyretin* (*TTR*) promoter (*TTR-ATF3*), increases accumulation in the liver and choroid plexus, but can also show expression in the endocrine pancreas. *TTR-ATF3* mice experience perinatal lethality and die between 30 minutes and 4 hours after birth. After crossing founder mice with wild types and generating an ATF3 over-expressing hybrid, it was determined that endocrine pancreas development was altered by inappropriate ATF3 expression. The degree of the phenotype varied from one founder line completely lacking pancreatic islets, to other founder lines exhibiting decreased numbers of all pancreatic endocrine cells (Allen-Jennings et al., 2001). Since TTR is also expressed in the liver, *TTR-ATF3* mice exhibited liver dysfunction that resulted in decreased expression on phophoenolpyruvate carboxykinase (PEPCK), an enzyme involved in gluconeogenesis. Inhibited expression of PEPCK in *TTR-ATF3* animals resulted in hypoglycemia, contributing to the perinatal lethality of these animals(Allen-Jennings et al., 2002).

Expression of ATF3 from the *pancreas duodenal homeobox 1* (*Pdx1*) promoter (*Pdx1-ATF3*) targeted accumulation to developing islets and

pancreatic β-cells after birth. *Pdx1-ATF3* mice experience early postnatal lethality and decreased overall size. These mice exhibited altered endocrine pancreas development, including smaller islet size, altered islet morphology and decreased numbers of insulin positive cells (Hartman et al., 2004).

While it appears that extensive work has been aimed at determining the role of ATF3 in the endocrine pancreas, little is known about ATF3's role in the exocrine pancreas.

1.4 «Gene Transcription»

Transcriptional regulation is a complex process whereby multiple factors determine expression of a gene. While transcription factors, like ATF3, are thought to be important in the cell-specificity and developmental regulation of gene expression, other factors, such as transcriptional coactivators and corepressors are also critical to this process, in that they determine whether transcription will be activated or repressed at a given gene promoter.

1.4.1 « Transcription Factors»

Transcription factors are molecules that bind to promoters or enhancers of a given gene resulting in gene activation or gene repression.

The mechanisms through which transcription factors exert these influences include: 1) stabilization or inhibition of RNA polymerase II binding to the promoter or enhancer; 2) acetylation or deacetylation of core histones, which can be performed by the transcription factor itself, or by recruitment of histone acetyltransferases (HATs) or histone deacetyltransferases (HDACs); and finally, by 3) recruitment of transcriptional coactivator or corepressor molecules.

1.4.2 «Gene Activation»

Within chromosomes genes are packaged as nucleosomes, a structure where DNA is tightly wound around core histones. The condensation of DNA in this manner serves as a level of transcriptional control in that, when condensed, DNA is inaccessible to transcription factors to promote transcription. Activation of gene expression involves recruitment of transcriptional coactivators that fall into two distinct groups. Histone acetyltransferases (HATs) function to acetylate conserved lysine residues in the amino terminal tails of core histones tails, neutralizing their positive charge and decreasing their affinity for DNA (Hong et al., 1993). This leads to a relaxed DNA conformation that permits accessibility of transcription factors. Common HATs include CREB binding protein/E1A binding protein p300 (CBP/p300) and p300/CBP associated factor (PCAF).

Unlike HATs, which target the histone amino terminal lysines, the second category of transcriptional coactivators destabilizes the core of the

histone via ATP-dependent mechanisms. This results in a shift of the nucleosome, creating a nucleosome free area that exposes transcriptional enhancers to transcriptional activation (Hargreaves and Crabtree, 2011). Members of this class of transcriptional coactivators include Switch/Sucrose non-fermentable (Swi/Snf) and imitation switch (ISWI).

Coincident with the discovery that histone acetylation is associated with transcriptional activation, was the discovery of the reverse mechanism where histone deacetylation results in transcriptional repression.

1.4.3 «Gene Repression»

The tightly wound nucleosomal structure results on repression of genes due to multiple different factors. First, this condensed conformation disallows interaction of various proteins including transcription factors, polymerases, coactivators and corepressors with gene promoters (Workman and Kingston, 1998). Second, chains of nucleosomes can become further folded into higher order structures that can repress entire chromosomal regions (Bell and Felsenfeld, 1999; Ramakrishnan, 1997). Finally, nucleosomes can interact with chromosomal proteins to further repress gene expression in a heritable manner (Grunstein, 1998).

Further gene repression mechanisms involve the deacetylation of active gene promoter regions. Histone deacetylation is carried out by a group of proteins called histone deacetylases (HDACs). HDACs function

by removing the acetyl group from histone tails, leading to decreased space between histones and surrounding DNA and subsequent condensation of DNA resulting in inaccessibility of transcriptional proteins to gene promoters.

There are three main classes of HDACs, that are defined by their cellular localization. Of importance to this work are class I and class II HDACs. Class I HDACs include HDAC 1, 2, 3 and 8, and are characterized based on their homology to the yeast RPD3 gene, their predominantly nuclear localization and their ubiquitous expression in human tissues. Class II HDACs include HDAC 4, 5, 6, 7, 9, 10 and 11 and are characterized by their similarity to the yeast HDA1, their nuclear or cytoplasmic localization, and their restriction to specific tissue types.

Interestingly, HDAC1 has been linked to the UPR in that, in the kidney during ischemia-reperfusion injury, it associates with ATF3 to suppress transcription of inflammatory genes (Li et al., 2010)q. While this is an intriguing finding, the role of HDACs and their association with ATF3 in model systems of injury in other tissues is yet to be examined.

1.5 « The Unfolded Protein Response and Pancreatic Physiology and Pathology»

The role of the UPR in exocrine pancreas physiology and pathology has not been thoroughly investigated. However, it is known that multiple UPR factors, including ATF4 and XBP1s are normally expressed in exocrine pancreas tissues during normal physiology. Development of a XBP1s reporter mouse where a variant of GFP is fused to XBP1s protein confirmed the presence of XBP1s in the exocrine pancreas under normal physiological circumstances (Iwawaki et al., 2004).

Multiple knockout and transgenic mouse lines have been generated for different molecules involved in the UPR. Only a few mutant mouse lines have been used to assess the role of the UPR in exocrine pancreas physiology and pathology, including mice lacking *Xbp1* (*Xbp1*$^{-/-}$), or *Perk* (*Perk*$^{-/-}$).

1.5.1 « XBP1 mutants»

Xbp1 expression is first detected in the mouse pancreas at embryonic day (E) 12.5. XBP1 expression peaks by E14.5, and then is reduced by E18.5 (Clauss et al., 1993), suggesting a developmental role for XBP1. A global *Xbp1* knockout (*Xbp1*$^{-/-}$) in mice is embryonic lethal with no viable *Xbp1*$^{-/-}$ embryos obtained after E14.5. Embryonic lethality was rescued when XBP1 was re-expressed in the liver (*Xbp1*$^{-/-}$*; Liver*^{Xbp1}). Gross

morphological analysis of *Xbp1*$^{-/-}$;*Liv*^{Xbp1} pancreata revealed a 90% decrease in pancreas size when compared to wild type (WT) littermates, and pancreatic tissue consisted of sparsely distributed acini in a loose mesenchymal structure. Transmission electron microscopy (TEM) revealed proper organization of *Xbp1*$^{-/-}$;*Liv*^{Xbp1} acinar cells around a lumen, but with significantly fewer and smaller zymogen granules compared to WT litter mates. Additionally, the ER in mutant cells was poorly developed with few cisternae. Pancreatic tissue from *Xbp1*$^{-/-}$;*Liv*^{Xbp1} mice showed drastic reductions in amylase and trypsin accumulation and significant acinar cell apoptosis by E18.5 due to dysregulated ER stress (Lee et al., 2005). Interestingly, development of the endocrine pancreas was unaffected in *Xbp1*$^{-/-}$;*Liv*^{Xbp1} mice (Lee et al., 2005). Thus, this work established a role for XBP1 specifically in development of the exocrine pancreas.

To more thoroughly determine the role of XBP1 in the pancreatic acinar cell, *Xbp1*^{flox} (Lee et al., 2005) mice were crossed with a line that allowed for inducible cre-mediated recombination in pancreatic acini (*Mist1-Cre*$^{ER/T2}$) to allow for inducible deletion of *Xbp1* in adult acinar cells (*Xbp1*$^{\Delta Ex2}$) (Hess et al., 2011). Analysis of *Xbp1*$^{\Delta Ex2}$ mice four weeks after loss of XBP1 revealed a 60% decrease in expression of amylase and elastase, and increased activity of the UPR. Structurally, *Xbp1*$^{\Delta Ex2}$ acinar cells exhibited decreased accumulation of zymogen granules and decreased amounts of cytoplasm. Further analysis revealed poorly developed and distended ER

with disorganized cisternae, and ribosomes were not longer associated with the ER. Additionally, these cells showed increases in ER stress indicators and eventually succumbed to apoptotic cell death, indicating that XBP1 is essential for maintaining both the UPR and acinar cell homeostasis (Hess et al., 2011).

Transcriptional targets for XBP1 in the pancreas include *Sec61α*, ER degradation enhancer, mannosidase alpha-like (*Edem*), protein disulfide isomerase (*PDI*) and the pancreas-specific isoform *PDIp*. Sec61α is required for translocation of newly synthesized proteins across the ER membrane (Rapoport et al., 1996), whereas EDEM plays a role in the degradation of misfolded proteins in the ER (Hosokawa et al., 2001). As the name implies, the PDIs are required for disulfide bond formation and isomerization of newly synthesized proteins (Schwaller et al., 2003) within the ER. *PDIp* is exclusively expressed in the exocrine pancreas (Desilva et al., 1996) and is able to bind zymogens, suggesting an important role in zymogen folding (Volkmer et al., 1997). XBP1 also directly regulates expression of *Mist1*, an exocrine pancreas transcription factor (Acosta-Alvear et al., 2007). XBP1 binds to the *Mist1* promoter in the C2C12 myoblast cell line, plasma cells and in MIN6 insulinoma cells, and ectopic XBP1s expression induces MIST1 expression in these cells (Acosta-Alvear et al., 2007). While these studies were not carried out in an acinar cell environment, they indicate that XBP1 can regulate expression of *Mist1*.

Studies have also aimed at determining XBP1's role during pancreatic injury. Experimental induction of pancreatitis using L-arginine in rats or CCK analogs in isolated rat pancreatic acini induced splicing of *Xbp1* (Kubisch and Logsdon, 2007; Kubisch et al., 2006). Furthermore, studies from our lab and others have shown that prolonged exposure to ethanol initiated splicing of *Xbp1* in pancreatic tissue (Alahari et al., 2011; Lugea et al., 2011). While long-term ethanol feeding in mice does not lead to pancreatic deficiency, long-term ethanol feeding of *Xbp1* heterozygote (*Xbp1*$^{+/-}$) mice, which exhibit a 30% decrease in the level of pancreatic XBP1, resulted in areas of acinar cell necrosis, stroma deposition and the presence of tubular complexes. There was also a 25% decrease in the number of zymogen granules per cell and a 30% reduction in amylase expression in *Xbp1*$^{+/-}$ ethanol-fed mice. Other hallmarks of injury in *Xbp1*$^{+/-}$ mice included increased tissue inflammation, increased vacuolization of acinar cells and increased autophagy (Lugea et al., 2011). To date, transcriptional targets of XBP1 during pancreas injury have not been determined.

1.5.2 « PERK mutants»

Three different lines of *Perk*$^{-/-}$ mice exhibit a phenotype in the exocrine pancreas. A single study revealed that global *Perk* knockout (*Perk*$^{-/-}$) exhibited early postnatal lethality. However, backcrossing into the outbred Swiss Webster strain resulted in decreased mortality and recovery of half of the predicted number of *Perk*$^{-/-}$ pups at weaning. Exocrine pancreatic

tissue in *Perk*$^{-/-}$ mice displayed no gross morphological phenotype, however, closer inspection revealed ER that was segmented with distended lumens, indicative of impaired protein folding capabilities. Phosphorylation of eIF2α was significantly decreased in *Perk*$^{-/-}$ tissue, indicating that, under normal conditions, PERK is required for translational control in pancreatic tissue. Wild type mice exhibited limited fecal lipid content as assessed by Oil Red O staining, indicating that digestion was proceeding properly. *Perk*$^{-/-}$ mice exhibited significant increases in fecal lipid accumulation, indicative of impaired digestion and exocrine insufficiency in digestive enzyme release. Additionally, *Perk*$^{-/-}$ exocrine tissue displayed increased apoptosis and increased cell proliferation. Taken together, these observations indicate that PERK plays a role in the maintenance of pancreatic acinar cell integrity (Harding et al., 2001).

A conditional *Perk*$^{-/-}$ mouse with loxP sites inserted into intronic sequences flanking three exons that encode part of the luminal domain, the transmembrane domain, and part of the catalytic domain were crossed with mice carrying Cre recombinase driven by the adenoviral *Ella* promoter (*PKO*). Thirty seven percent of *PKO* mice survived perinatally and 23% of mice died prenatally. Surviving mice exhibited 40-50% growth retardation by postnatal day (PN) 7 and eIF2α phosphorylation levels were reduced in the pancreata of these mice between PN7 and PN12. Pancreata of *PKO* mice are morphologically normal within the first three weeks of birth, but then begin to display an exocrine pancreatic phenotype

similar to the complete *PKO* mice with greatly distended and fragmented ER containing fewer proteins. Over time, acinar cells became highly vacuolated and underwent massive apoptosis. In addition, expression of digestive enzymes was impaired at the protein level but not the mRNA level (Zhang et al., 2002).

Crossing *PKO* mice with mice expressing Cre recombinase driven by the *elastase-1* promoter, generated mice with a PERK deletion exclusively in the exocrine pancreas (*exPKO*). *exPKO* pups were indistinguishable from their littermates and at PN14 exhibited morphologically normal pancreata. By PN19 the discrete cell pockets in the exocrine pancreas of *exPKO* mice exhibited structural disorganization and cell death, where cells were swollen and degranulated with abnormal nuclei. By 3-4 months of age, the normally predominant population of acinar cells was replaced by fibroblasts, adipocytes, macrophages and leukocytes. Interestingly, these mice never became diabetic unlike their *PKO* counterparts, indicating that lack of PERK in the acinar cells specifically affects the exocrine pancreas. Interestingly, lack of PERK in acinar cells resulted in a pancreatitis like phenotype for a window of time, where pancreatitis associated gene expression is increased, followed by increased levels of serum amylase and cell apoptosis (Iida et al., 2007).

1.5.3 « ATF4 mutants»

To determine whether the phenotype observed in the *exPKO* mice was due to lack of ATF4 expression, the exocrine pancreas of mice lacking

ATF4 (*Atf4*$^{-/-}$) was examined. *Atf4*$^{-/-}$ mice exhibit retardation of postnatal growth and are blind due to defective lens development (Hettmann et al., 2000; Masuoka and Townes, 2002). Examination of the exocrine pancreas in *Atf4*$^{-/-}$ mice revealed a significant reduction in early postnatal exocrine pancreas development compared to wild type littermates. Additionally, *Atf4*$^{-/-}$ exocrine pancreas tissue did not display upregulation of pancreatitis-associated genes, and did not exhibit increased cell death. These observations indicate that the observed phenotype in *exPKO* mice was not due to a lack of ATF4 upregulation (Iida et al., 2007).

From these studies, it is clear that the PERK pathway is integral for both development and maintenance of the exocrine pancreas. Loss of PERK results in a pancreatitis phenotype that is not explained by loss of ATF4. Another transcription factor in the PERK pathway that might play a role in the generation of exocrine pancreas pancreatitis phenotypes is ATF3. As mentioned, *Atf3*$^{-/-}$ mice do not exhibit abnormal pancreatic development or progressive tissue degeneration. However, ATF3 may play a role in the maintenance of the acinar cell phenotype under stress conditions in the exocrine pancreas.

1.6 « Rationale»

While it is known that the UPR is activated during pancreatic pathology, the specific UPR molecules involved in pathologic responses, and the roles of these molecules, are still unclear. The goal of this study was to

determine the contribution of the PERK pathway to exocrine pancreas pathology and determine the transcriptional and molecular impact of the PERK pathways in this process.

The hypothesis of this study is that the PERK pathway regulates the acinar cell response to injury through transcriptional and non-transcriptional mechanisms. To test this, I used two genetically modified mouse lines. *Stc2*^{Tg} mice ubiquitously express the human *STC2* protein while *Atf3*$^{-/-}$ mice contain a targeted deletion of the *Atf3* gene.

Both signaling molecules and transcription factors are assessed, providing a well-rounded perspective of the effects of PERK pathway activation in exocrine injury. STC2 is a signaling molecule activated by the PERK pathway, and analysis of mice over-expressing STC2 will provide insight to how PERK pathway non-transcriptional mechanisms control exocrine injury. ATF3 is a transcription factor that is activated by PERK signaling. Unlike other UPR transcription factors, ATF3 is not expressed during normal exocrine pancreas physiology; however, it is robustly upregulated during exocrine injury, implying that it's sole role is in response to stress. ATF3 has been implicated in the differentiation program of various cell types, and may play an important role during pancreatitis since acinar cells are postulated to lose differentiation characteristics during injury. Thus, analysis of the role of ATF3 during exocrine pancreas injury may uncover a novel transcriptional role, not just for the PERK pathway, but for the UPR as a whole, in exocrine pancreas injury.

By characterizing *Stc2*^{Tg} and *Atf3*$^{-/-}$ mice under normal and pathological conditions, I have been able to provide novel insight into the contribution of PERK signaling during pancreatitis.

Chapter 2

2 « Over-expression of Stanniocalcin 2 alters PERK signaling and reduces cellular injury during cerulein induced pancreatitis in mice »

This chapter is composed of a manuscript published in *BMC Cell Biology* (Fazio et al., 2011). E. Fazio conceived experiments, performed >90% of the experimental work, provided theoretical input and wrote the manuscript. G. DiMattia conceived experiments, revised the manuscript and provided theoretical input. S. Chadi performed the *Stc2* Northern blot and K. Kernohan performed RT-PCR reactions for *Stc2* and *Atf3*, C.Pin conceived experiments, revised the manuscript and provided theoretical input.

2.1 « Introduction »

The stanniocalcin (STC) family of secreted glycoproteins consists of two members – STC1 and STC2 – that have 35% conserved identity and conservation of exon/intron boundaries, indicating that they are paralogs (Moore et al., 1999). STC was first discovered in fish and shown to be involved in calcium homeostasis through effects on calcium influx (Flik et al., 1990; Sundell et al., 1992). Although terrestrial mammals rarely experience hypercalcemia, alterations in subcellular compartmentalization of Ca^{2+} are found under pathological conditions such as the accumulation of improperly folded proteins.

STC2 expression is upregulated upon induction of hypoxic or endoplasmic reticulum (ER) stress in N2a neuroblastoma cells (Law and Wong, 2009). This increase in *Stc2* expression was reliant on the concomitant increase of Activating Transcription Factor (ATF4) (Ito et al., 2004), a protein integral to (PKR)-like endoplasmic reticulum kinase (PERK) signaling, which is part of the unfolded protein response (UPR). To date, no relationship between PERK signaling and STC2 activation has been identified *in vivo*.

The UPR is activated when ER homeostasis is disrupted. Alterations to proper functioning of ER machinery arise when protein load exceeds folding capacity, such as when luminal ER Ca^{2+} concentrations are perturbed. The UPR consists of three signaling pathways that are individually transduced by ATF6, inositol-requiring enzyme 1 (IRE1) or PERK (Bertolotti et al., 2000; Okamura et al., 2000). Each transducer is maintained in a repressed state by binding of the ER chaperone protein glucose regulated protein 78 (GRP78/BiP) (Bertolotti et al., 2000; Okamura et al., 2000). When unfolded proteins accumulate, they bind to GRP78/BiP resulting in its release from the UPR transducers (Freiden et al., 1992; Laitusis et al., 1999) . In the case of PERK, dissociation of GRP78/BiP leads to its homodimerization and autoactivation (Liu and Kaufman, 2003). Activation of PERK results in phosphorylation of eukaryotic translation initiation factor 2α (eIF2α) (Shi et al., 1998), limiting its ability to contribute to the protein translational complex, thereby inhibiting global protein translation and alleviating the protein load on the cell (Harding et al., 1999). Phosphorylation of eIF2a also

selectively upregulates translation of mRNAs from short upstream open reading frames (Hinnebusch, 1997). The predominant target mRNA for peIF2α is *Atf4*, which subsequently increases the expression of the transcriptional repressor *Atf3*, and *growth arrest and DNA damage-inducible* (*Gadd*) *34* (Jiang et al., 2004; Ma et al., 2002a). GADD34 (alternatively known as *Myd116; myeloid differentiation, primary response gene 116,* or *Ppp1r15a*; protein phosphatase 1, regulatory [inhibitor] subunit 15A) negatively regulates PERK signaling by combining with protein phosphatase 1 to dephosphorylate eIF2α, thereby restoring general translation (Ma and Hendershot, 2003; Novoa et al., 2001).

PERK is expressed in the exocrine and endocrine pancreas under normal conditions (Shi et al., 1998; Sood et al., 2000) and *Perk*$^{-/-}$ mice experience deterioration of glycemic control and exocrine insufficiency over time (Harding et al., 2001). Exocrine specific deletion of PERK revealed cellular disorganization and degranulation, increased serum amylase levels and increased cell death (Iida et al., 2007). Our laboratory identified rapid activation of PERK signaling following induction of pancreatitis by secretagogue hyperstimulation and correlated decreased activation of the pathway in mice that exhibit increased sensitivity to pancreatic injury (Kowalik et al., 2007). Together, these observations indicate that PERK signaling has important roles in both the physiology and pathology of the exocrine pancreas.

Given the relationship between PERK and STC2 *in vitro*, the objectives of this study were to (1) determine if a similar relationship exists in the exocrine pancreas and (2) gain insight into a role for STC2 as part of the UPR. Our results revealed a direct correlation of *Stc2* expression with PERK signaling *in vivo* only after initiating pancreatic injury. Transgenic over-expression of human STC2 in mice ($STC2^{Tg}$) (Gagliardi et al., 2005) resulted in altered PERK signaling and decreased signs of acinar cell damage associated with cerulein-induced pancreatitis (CIP). These observations indicate that STC2 is linked to PERK signaling in acinar cells and may have a role in limiting damage during pancreatic injury.

2.2 « Methodology »

2.2.1 « Mouse handling »

For characterization of *Stc2* expression during cerulein-induced pancreatitis (CIP), wild type and $Mist1^{-/-}$ mice were maintained on a C57/Bl6 background. For analysis of pancreatitis severity, $STC2^{Tg}$ and wild type mice are maintained on a C57/Bl6 x CBA background. Mice carrying a targeted ablation of the *Mist1* gene ($Mist1^{-/-}$) (Pin et al., 2001) or transgenic mice expressing the human *STC2* ($STC2^{Tg}$) from the cytomegalovirus (*CMV*) promoter + chicken *β-actin* promoter (Gagliardi et al., 2005), have previously been described. All experiments were approved by the Animal Care Committee at the University of Western Ontario

(Protocol #116-2008) and mice handled according to regulations stipulated by the Canadian Council on Animal Care.

2.2.2 « Induction of pancreatitis »

To induce pancreatic injury, 2-4 month-old female mice were given up to seven hourly intraperitoneal injections of cerulein (50 µg/kg body weight; Sigma-Aldrich). As a control, mice were injected with 0.9% saline. Mice were sacrificed 1, 4 or 8 hours after initial cerulein injection and pancreatic tissue from each was immediately processed to isolate RNA, protein, and tissue sections for histological or immunohistochemical analysis. To assess serum amylase, blood was obtained via cardiac puncture, placed on ice for 20 minutes and centrifuged at 4°C, 2500 rpm for 15 minutes. Serum amylase was quantified using a Phadebas amylase assay (Magle Life Sciences, Lund, Sweden) as per manufacturer's instructions.

2.2.3 « Tissue preparation and histology »

Pancreatic tissue was either directly embedded in OCT or incubated in formalin for 24 hours followed by paraffin embedding. For morphological analysis, paraffin embedded tissue was sectioned to 6 µM and stained with hematoxylin and eosin. Immunofluorescent (IF) analysis was performed on fresh frozen sections as described previously (Fazio and Pin, 2007). Primary antibodies and their dilutions

are listed in Table 1. Following primary antibody incubation, sections were incubated for 1 hour with the secondary antibodies of either anti-rabbit FITC or anti-mouse TRITC (1:250; Sigma-Aldrich). Sections were incubated with 4',6-diamidino-2-phenylindole (DAPI; 1:1000) and slides mounted with Vectashield (Vector Laboratories, Burlingame CA, USA). Histological staining was visualized with a Leica DMIOS upright microscope and images were captured using OpenLab 4.0.3 Software (PerkinElmer, Waltham, MA, USA).

2.2.4 « TUNEL analysis »

TUNEL analysis was used to identify apoptotic cells using the *In situ* Cell Death Detection kit (Roche, Laval, QC, Canada) following manufacturer's instructions. Briefly, frozen sections were fixed, washed and permeabilized before labelling with TUNEL reaction mixture for 60 minutes. After washing, sections were counterstained with DAPI, coverslipped and visualized using a Leica DMIOS upright microscope and images were captured using OpenLab 4.0.3 Software (PerkinElmer, Waltham, MA, USA). Analysis of percent apoptotic cells was carried out by comparing TUNEL positive cells to total cell number. Cell counts based on DAPI were done using Image J software, and TUNEL positive cells were determined manually. Ten random fields of view from 4 sections per animal were used for analysis.

2.2.5 « RNA isolation, Northern blotting and Real-Time RT-PCR »

RNA was isolated from the splenic portion of the pancreas and processed using TRIzol (Invitrogen, Burlington, ON, Canada) as described (Kowalik et al., 2007). Northern blotting was performed as previously described (Pin et al., 2001). Thirty µg of RNA was resolved by electrophoresis on a 1% agarose/formaldehyde gel and blotted onto Hybond membrane (GE Healthcare, Baie d'Urfe, QC, Canada). Membranes were hybridized overnight at 42°C with a α-^{32}PdCTP radiolabelled probe for *Stc2* or for *18S* rRNA as a loading control.

For RT-PCR, two µg of RNA was reverse transcribed using Improm-II reverse transcriptase and random primers (Promega, Madison WI, USA). RT-PCR for *Stc2*, *Atf3*, *amylase* and *b-actin* was performed with 1 µL of cDNA and *Taq* DNA polymerase (Promega, Madison WI, USA).

2.2.6 « Protein isolation and immunoblot analysis »

Protein extraction was carried out to obtain both nuclear and cytoplasmic fractions. Briefly, 5 volumes of buffer CE pH 7.6 (10 mm Hepes, 60 mM KCl, 1 mM EDTA, 0.075% v/v NP-40, 1 mM DTT, 1 mMPMSF) were added to whole pancreatic tissue prior to homogenization. Homogenized cells were centrifuged at 1000 rpm, 4°C for 4 minutes. The supernatant was removed and saved as cytoplasmic extract. The nuclear pellet was gently washed with CE buffer lacking NP-40 and centrifuged again. After removal of the supernatant, the nuclear

pellet was covered with 1 pellet volume of NE buffer (20 mm Tris-HCl, 420 mM NaCl, 1.5 mm $MgCl_2$, 0.2 mM EDTA, 1 mM PMSF, 25% w/v glycerol) and the NaCl concentration was adjusted to 400 mM for the entire volume. An additional pellet volume of NE buffer was added followed by vortexing for resuspension. The extract was incubated on ice for 10 minutes with intermittent vortexing. Both cytoplasmic and nuclear extracts were centrifuged at 14,000 rpm, 4°C, for 10 minutes to pellet any debris. Nuclear extracts were used for analysis of MIST1, PDX1, XBP1 and ATF4 levels, whereas cytoplasmic extracts were used for all other immunoblot analysis.

For immunoblot analysis, 40 to 60 µg of pancreatic protein was resolved by SDS/PAGE and transferred to PVDF membrane (Biorad, Mississauga, ON, Canada). Blots were blocked with 5% non-fat dry milk (NFDM) and probed with primary antibodies diluted in 5% NFDM overnight at 4^{o}C. For primary antibodies and their dilutions, see Table 2.1. Blots were washed three times in PBS supplemented with Tween-20 (PBS-T) then incubated with anti-rabbit or anti-mouse horseradish peroxidase conjugated secondary antibody (1:10,000 or 1:2000, Jackson Labs, Bar Harbor, ME, USA) in 5% NFDM for one hour. Blots were subjected to another series of washes in PBS-T, incubated with Western Lightning chemiluminescence substrate (Perkin Elmer, Waltham MA, USA), exposed to X-ray film (Fisher Scientific, Ottawa, ON, Canada) and developed. Denistometry was performed on immunoblot autoradiographs by analysis with a FluorChem 8800 documentation system and accompanying FluorChem 8800 software (Alpha Innotech, San Leandro CA, USA).

2.2.7 « Statistical Analyses »

All statistical analyses were performed using Graphpad Prism 4.02 (Graphpad Software, San Diego CA, USA). Carboxypeptidase cleavage and serum amylase levels were analyzed using a two-way ANOVA followed by a Bonferroni post-hoc test. Levels of phosphorylated eIF2α and LC3 cleavage were statistically analyzed using a Mann-Whitney test.

2.3 « Results»

2.3.1 « The PERK pathway, including STC2, is activated during cerulein induced pancreatitis»

To determine if PERK signaling is active in pancreatic tissue, we performed IF with an antibody that recognizes only the phosphorylated form of PERK (pPERK). The accumulation of pPERK was restricted to a tight apical portion of the acinar cells (Figure 2-1A) typical of where Ca^{2+} is released during the process of regulated exocytosis (Kasai and Augustine, 1990; Nathanson et al., 1992). Interestingly, CIP treatment led to a change in pPERK localization within four hours, with active PERK exhibiting a more diffuse and basally-restricted pattern of accumulation (Figure 2.1B). Increased accumulation of ATF3 protein was restricted to acinar cells in CIP-treated pancreatic tissue (Figure 2.1C, D). RT-PCR revealed no expression of *Stc2* in saline control pancreata (Figure 2.2A)

Figure 2.1. The PERK Pathway is Active in the Exocrine Pancreas During CIP. (A,B) Immunofluorescence (IF) for pPERK before (A) and 4 hours after (B) initiation of CIP. pPERK (arrowhead) localizes to the apical end of acinar cells under physiological conditions and more basally during CIP. Dotted line outlines an acinus. Magnification bar = 13 μM. DAPI was used to counter stain nuclei. (C, D) IF for ATF3 expression revealed limited accumulation before CIP (C) and acinar-specific expression afterwards (D). Magnification bar = 63 μM. I = islet.

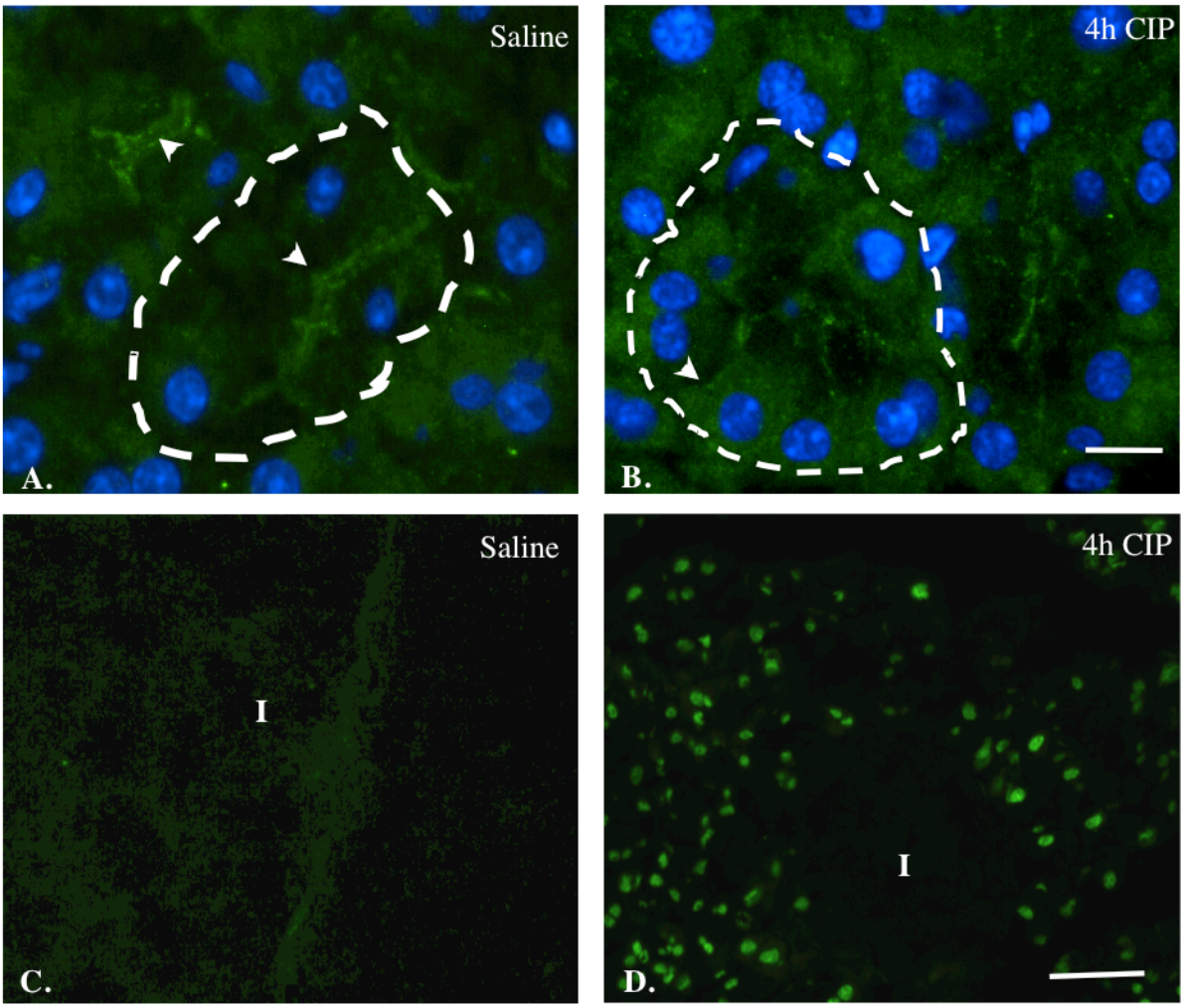

Figure 2.1. The PERK Pathway is Active in the Exocrine Pancreas During CIP.

suggesting that PERK activation under these conditions does not lead to *Stc2* expression. Similar results were obtained in control pancreata for *Atf3*, another downstream target of PERK signaling. Our laboratory has shown that PERK activity increases during pancreatic injury (Kowalik et al., 2007). To determine if the pathological activation of PERK leads to increased STC2 expression, pancreatic injury was initiated by cerulein-induced pancreatitis (CIP). Increased *Stc2* and *Atf3* mRNA accumulation was observedduring CIP (Figure 2.2A). Increased *Stc2* expression was confirmed by Northern blot analysis four hours after induction of pancreatitis (Figure 2.2B, saline WT vs. CIP WT). To support the link between elevated *Stc2* levels and injury-associated PERK activation, we examined the expression of *Stc2* in *Mist1*$^{-/-}$ mice, which exhibit minimal activation of PERK during injury (Kowalik et al., 2007). *Mist1* is a transcription factor required for terminal differentiation of pancreatic acinar cells, and its absence in exocrine tissue results in improper activation of UPR components both normally and during injury via an unknown mechanism (Kowalik et al., 2007). In sharp contrast to wild type mice, *Stc2* mRNA was virtually undetectable upon CIP treatment in *Mist1*$^{-/-}$ (Figure 2.2B; Saline *Mist1*$^{-/-}$ vs. CIP *Mist1*$^{-/-}$).

2.3.2 « Pancreatic morphology is not altered in STC2^{Tg} tissue»

These findings suggest that STC2 is co-induced with PERK in acinar cells only after injury and may protect the pancreas in response to CIP. To determine if STC2 could alter the acinar cell response to pancreatic injury, we examined a mouse model in which STC2 is constitutively expressed (*STC2*^{Tg};

Figure 2.2. STC2 Accumulation Increases in Pancreatic Tissue Following Induction of Pancreatic Injury. (A) RT-PCR of whole pancreatic RNA extracts from saline (S) and cerulein (C) treated mice showed increased accumulation of *Stc2* and *Atf3* mRNA after initiation of CIP in pancreatic tissue. Amplification of *Amylase* (*Amy*) was used as a positive control for RT reactions. (B) Northern blot analysis revealed elevated *Stc2* mRNA four hours after initial cerulein (CIP) or saline (S) injection. No increases in *Stc2* were observed in *Mist1*$^{-/-}$ (M-/-) pancreatic tissue under similar conditions.

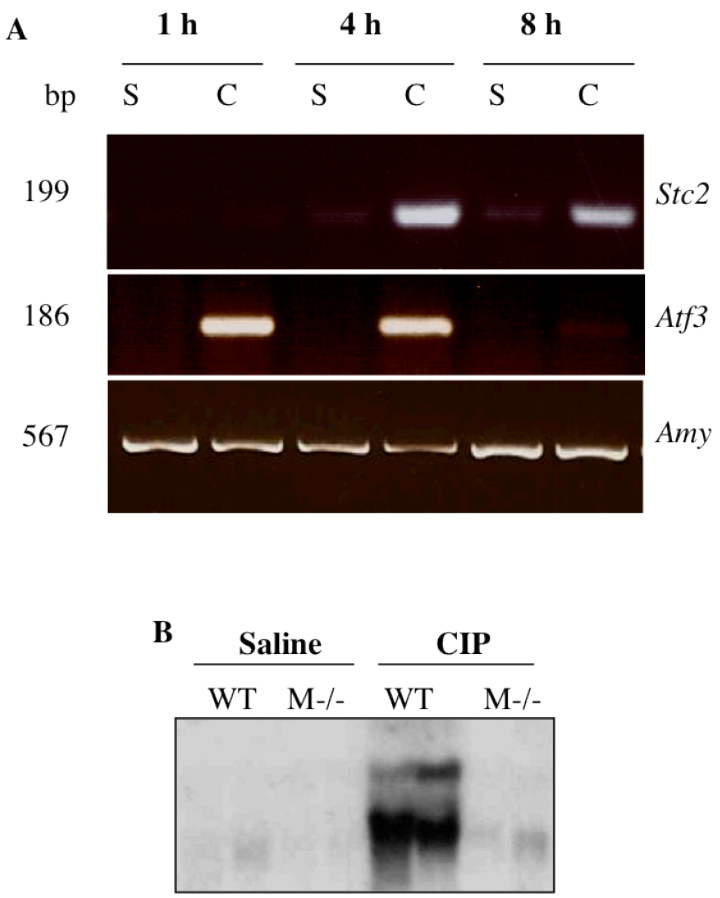

Figure 2.2. STC2 Accumulation Increases in Pancreatic Tissue Following Induction of Pancreatic Injury.

(Gagliardi et al., 2005)). IHC confirmed increased accumulation of STC2 in *STC2*^{Tg} pancreata compared to wild type (WT) tissue, with STC2 accumulation in islets and exocrine tissue (Figure 2.3B). H&E histology (Figure 2.3C, D) indicated that morphology was not overtly altered in *STC2*^{Tg} pancreatic tissue. IF staining for pancreatic differentiation markers MIST1 (exocrine, Figure 2.4A, B) and PDX1 (endocrine, Figure 2.4C, D) showed similar spatial localization and GLUT-2 accumulation was localized to the cell membrane of endocrine cells in both genotypes (Figure 2.4E, F). Western blot analysis confirmed equivalent levels of these markers, as well as amylase, between WT and *STC2*^{Tg} tissue (Figure 2.4G).

2.3.3 « Activation of the PERK pathway is altered in *STC2*^{Tg} pancreatic tissue»

We next examined PERK signaling in *STC2*^{Tg} pancreatic tissue. PERK activation results in phosphorylation of eIF2α and translation of ATF4 (Lu et al., 2004; Vattem and Wek, 2004). ATF4 is required for expression of *Gadd34*, *Atf3* and *Stc2* (Ito et al., 2004; Jiang et al., 2004; Ma and Hendershot, 2003). Western blot analysis of WT and *STC2*^{Tg} pancreatic tissue revealed decreased phosphorylation of both PERK and eIF2α (Figure 2.5A, B; n=4,animals $p < 0.01$) in *STC2*^{Tg} tissue. Surprisingly, ATF4 accumulated to higher levels in this *STC2*^{Tg} pancreas, suggesting dysregulation of PERK signaling (Figure 2.5C). To understand why activation of

Figure 2.3. Pancreatic Morphology is Unchanged in *STC2^{Tg}* Mice. (A, B) IHC for STC2 in WT (A) and *STC2^{Tg}* (B) pancreatic islets shows that STC2 accumulates in both acinar (*) and islet (I) tissue only in the *STC2^{Tg}* mice. Magnification bar = 27 μm. Tissue was counterstained with hematoxylin to reveal tissue morphology. (C, D) Hematoxylin and eosin staining comparing general histology of pancreatic tissue in WT (C) or *STC2^{Tg}* (D) pancreata. Magnification bar = 60 μM; I - islet.

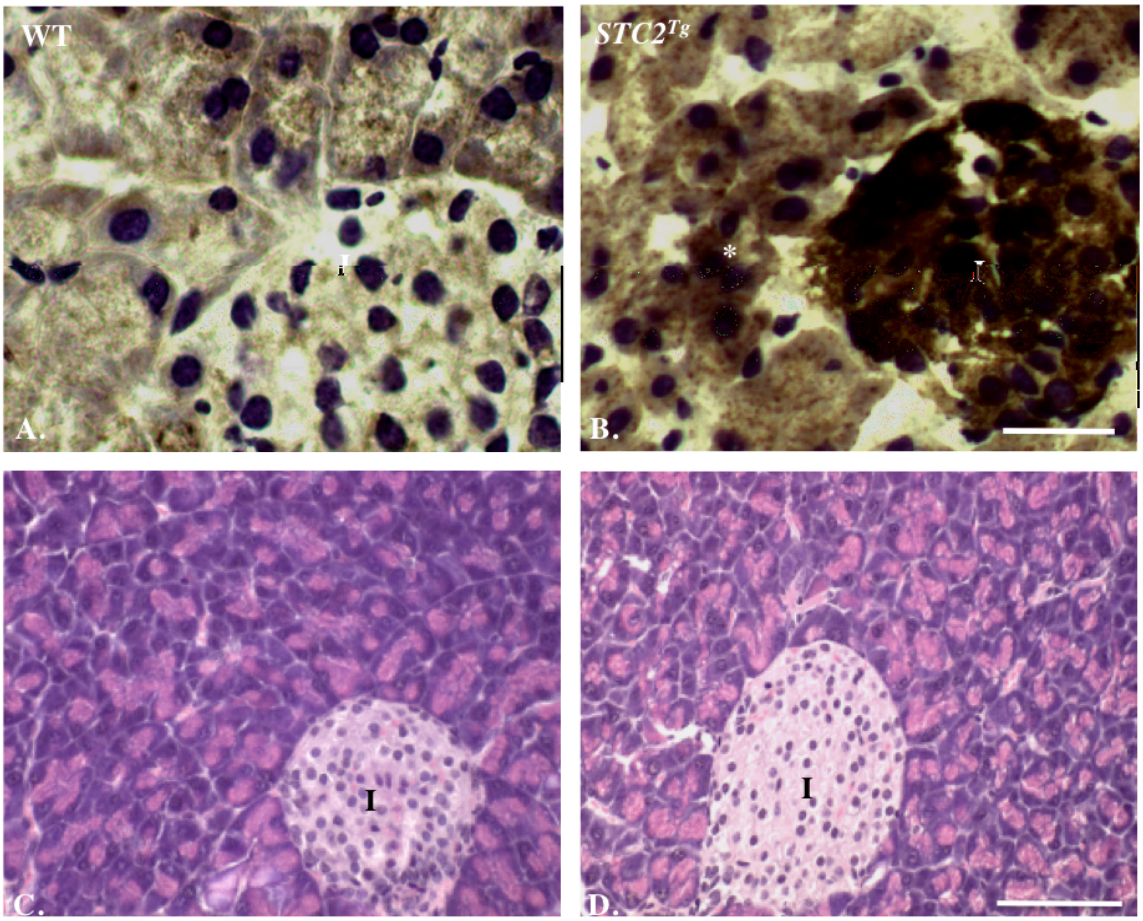

Figure 2.3. Pancreatic Morphology is Unchanged in *STC2*^{Tg} Mice.

Figure 2.4. Analysis of Protein Expression in *STC2*^{Tg} Pancreata. IF analysis for MIST1 (A, B), PDX1 (C, D) or GLUT2 (E, F) in WT (A, C, E) or *STC2*^{Tg} (B, D, F) pancreata. Magnification bar = 54 μm. (G) Representative Western blot analysis for pancreatic differentiation markers amylase, MIST1, PDX1 and GLUT2.

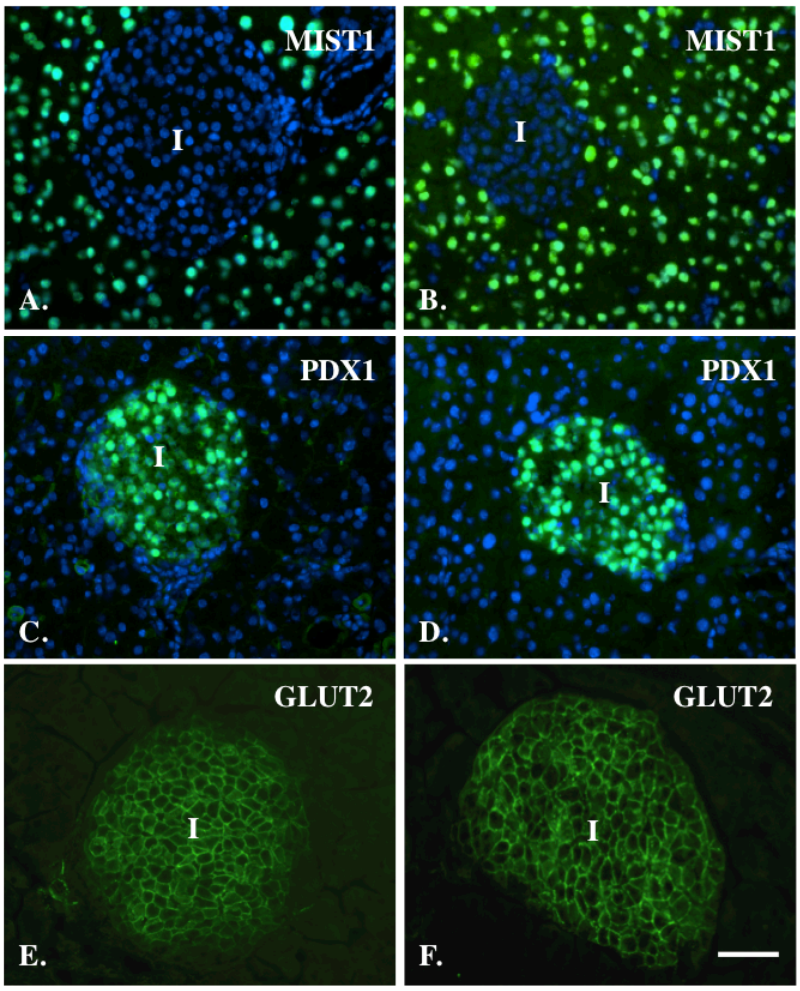

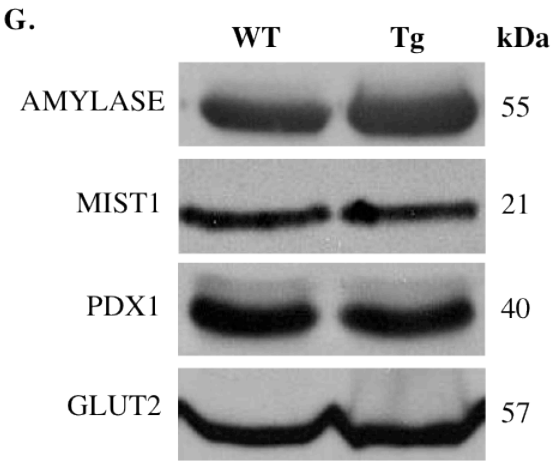

Figure 2.4. Analysis of Protein Expression in *STC2*^{Tg} Pancreata.

PERK and eIF2α appear reduced in STC2^{Tg} tissue, we examined regulators of these two proteins. The phosphorylation of eIF2α is reversed by GADD34 through its interaction with protein phosphatase 1 (PP1) and recent evidence indicates that calcineurin binds PERK and stimulates its autophosphorylation (Bollo et al., 2010). In *STC2*^{Tg} pancreatic tissue, the levels of GADD34 protein were significantly higher than wild type tissue (Figure 2.5C). Conversely, *STC2*^{Tg} calcineurin levels were considerably lower than WT counterparts. No changes in the ER resident protein calregulin were observed between genotypes (Figure 2.5C). Based on these results, it appears that over-expression of STC2 affected expression of mediators and feedback mechanisms in PERK signaling.

2.3.4 « Autophagy is enhanced in *STC2*^{Tg} tissue»

Alterations to PERK/ATF4 signaling should have an effect on cell autophagy, a long-term response to ER stress, which is regulated by ATF4 during hypoxia (Rzymski et al., 2010). Western blot analysis followed by densitometry revealed a significant increase in the cleaved form of the autophagy marker myosin associated protein 1 light chain 3 (LC3) in *STC2*^{Tg} pancreatic tissue (Figure 2.6A, B; n=4 animals, $P < 0.01$) consistent with increased accumulation of ATF4 in *STC2*^{Tg} mice. IF analysis corroborated increased autophagy as punctate LC3 staining is notably increased in *STC2*^{Tg} exocrine tissue (Figure 2.6C) when compared to WT tissue (Figure 2.6D).

Figure 2.5. Systemic Over-expression of STC2 (*STC2^{Tg}*) Alters the PERK Signaling Pathway in Pancreatic Tissue. (A) Representative Western blot analysis for mediators of PERK signaling pPERK, peIF2α, total (t) eIF2α and ATF4 in wild type (WT) and *STC2^{Tg}* (Tg), revealed decreased levels of pPERK and peIF2α and increased amounts of ATF4 in *STC2^{Tg}* mice. (B) Densitometry revealed that the ratio of peIF2a to total eIF2α is decreased in *STC2^{Tg}* extracts relative to WT tissue (n=3 animals; *$p<0.05$). (C) Similar western blot analysis revealed increased accumulation of GADD34 and decreased accumulation of calcineurin in *STC2^{Tg}* pancreatic protein extracts. No difference in calregulin accumulation was observed. Molecular weights (kDa) are provided.

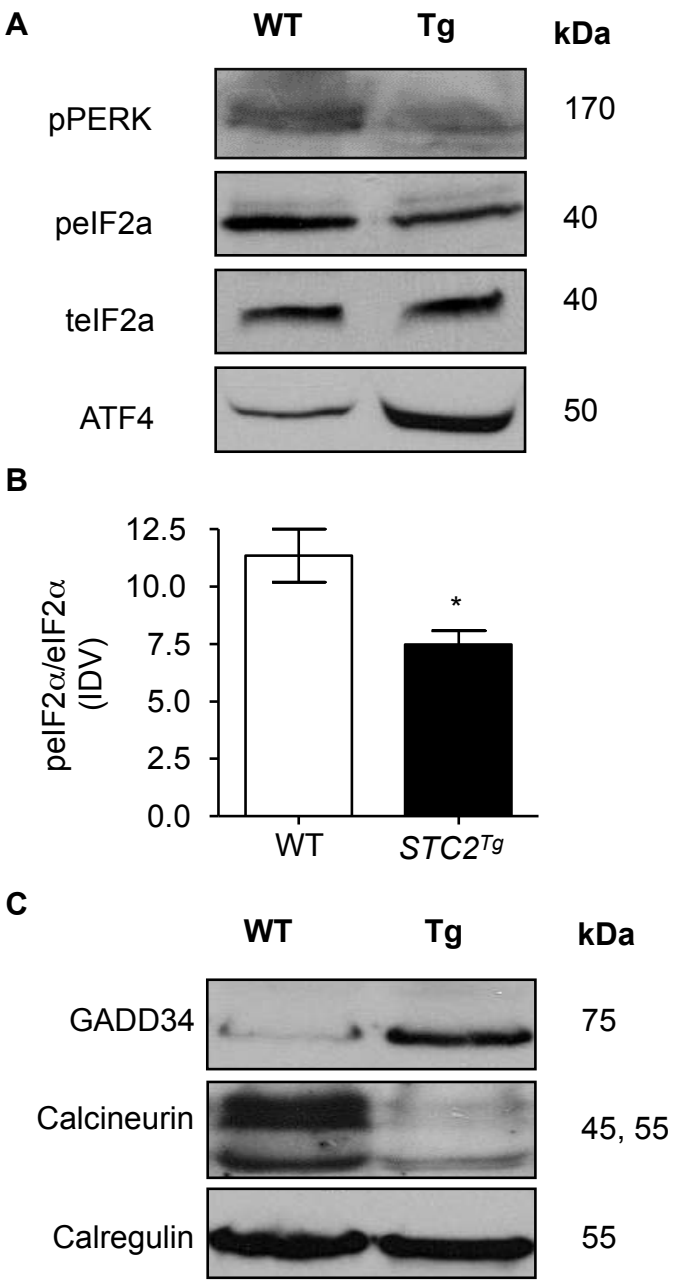

Figure 2.5. Systemic Over-expression of STC2 (*STC2*^{Tg}) Alters the PERK Signaling Pathway in Pancreatic Tissue.

Figure 2.6. *STC2*^{Tg} Acinar Cells Have Increased Autophagy. (A) Representative Western blot analysis for LC3 I and LC3 II accumulation in wild type (WT) and *STC2*^{Tg} pancreatic extracts revealed increased accumulation of cleaved LC3 II which was (B) quantified by densitometry (n=3 animals; *$p<0.05$). IF for LC3 cellular accumulations showed increased autophagic vesicles (arrowhead) in *STC2*^{Tg} pancreatic tissue. Magnification bar = 10 μm.

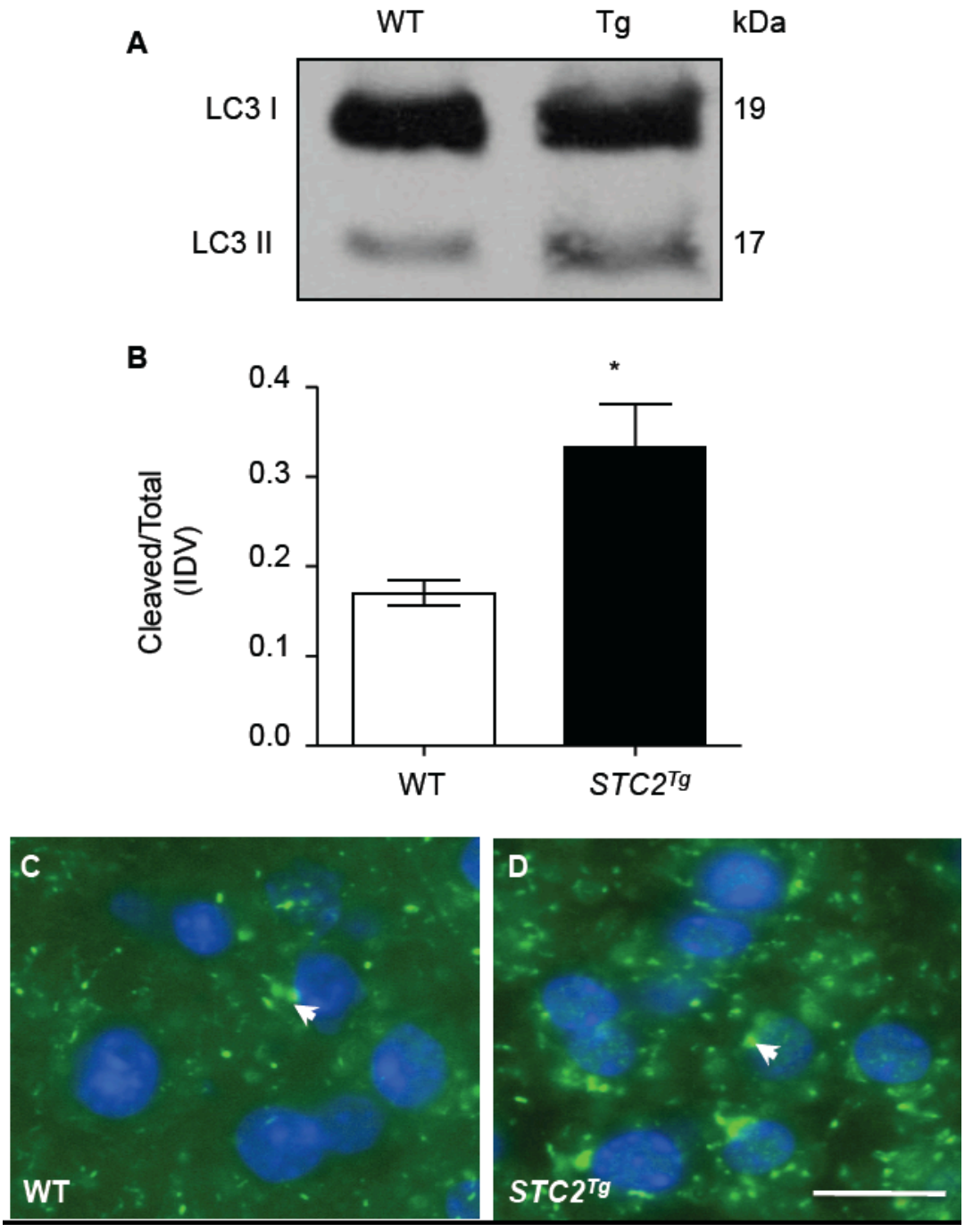

Figure 2.6. *STC2^{Tg}* Acinar Cell Have Increased Autophagy.

2.3.5 « Overexpression of STC2 results in decreased severity of exocrine cell injury»

The alterations in PERK signaling and cell autophagy suggested that *STC2*^{Tg} mice should have altered sensitivity to pancreatic injury. Four hours after the induction of pancreatitis, circulating serum amylase levels and tissue edema were compared between WT and *STC2*^{Tg} mice (Figure 2.5). While serum amylase levels were moderately higher in saline-treated *STC2*^{Tg} mice, the proportional increase in serum amylase levels following CIP was significantly lower in *STC2*^{Tg} mice when compared to WT mice, indicative of decreased sensitivity to pancreatic insult (Figure 2.7A; n=4 animals, $p < 0.05$). However, no difference was observed in tissue edema after CIP between genotypes (Figure 2.7B). We next examined the effects of pancreatic injury at the cellular level by examining enzyme activation and cell structures. Western blot analysis of procarboxypeptidase (CPA) activation revealed reduced levels of active CPA in CIP *STC2*^{Tg} pancreatic tissue when compared to WT cerulein-treated tissue (Figure 2.8). Interestingly, analysis of cell junction proteins showed continued expression in *STC2*^{Tg} tissue following CIP that was not evident in WT tissue.

In WT acinar cells, the expression of β-catenin decreased to negligible levels, indicative of a loss in adherens junctions between acinar cells as expected (Figure 2.9A, B). However, β-catenin remained readily detectable in *STC2*^{Tg} pancreatic tissue after induction of CIP (Figure 2.9C, D). Similarly, punctate connexin32 (Cx32) accumulation was lost in WT (Figure 2.9E, F) but not in

Figure 2.7. STC2 over-expression reduces severity of acinar cell damage during cerulein-induced pancreatic injury. (A) Analysis of serum amylase levels four hours into CIP treatment show that serum amylase levels rise approximately 3 fold in WT mice when compared to saline (•) whereas the increase in *STC2*^{Tg} mice is significantly lower at 2-fold (■; * $p < 0.01$). (B) Tissue edema analysis revealed significant increases for both WT and *STC2*^{Tg} tissue 4 hours into CIP (black bars) when compared to saline controls (white bars; n=4 animals). No difference between genotypes was observed. Error bars represent mean ± standard error.

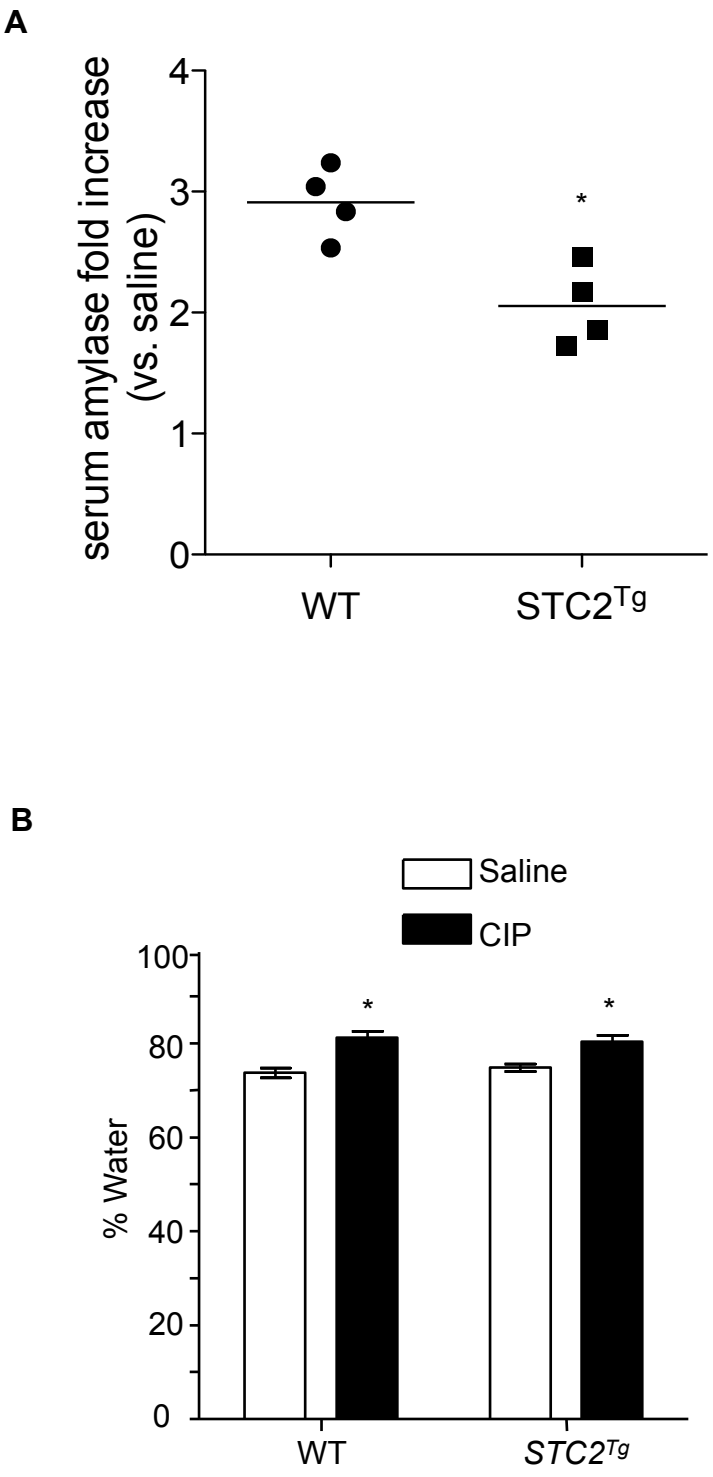

Figure 2.7. STC2 Over-expression Reduces Severity of Acinar Cell Damage During Cerulein Induced Pancreatic Injury.

Figure 2.8. During CIP *STC2*^{Tg} Pancreata Exhibit Decreased Activation of Carboxypeptidase. (A) Representative Western blot for procarboxypeptidase (47 kDa) and carboxypeptidase (CPA; 33 kDa) or trypsinogen four hours after initial saline (Sal.) or cerulein (CIP) injections showed decreased accumulation of activate CPA in *STC2*^{Tg} mice four hours into CIP. Quantification by densitometry (graph) comparing the ratio of cleaved (active; 33 kDa) to total CPA revealed a significant difference CPA activation between CIP treated WT and *STC2*^{Tg} mice (n=4 animals; different letters indicate statistically different values; $p<0.05$). Trypsinogen levels do not differ between genotypes. (B) Densitometric analysis revealed a significant increase in WT tissue, that was also observed in *STC2*^{Tg} tissue, but to a lower and significantly different extent (n=4 animals, letters represent significant differences).

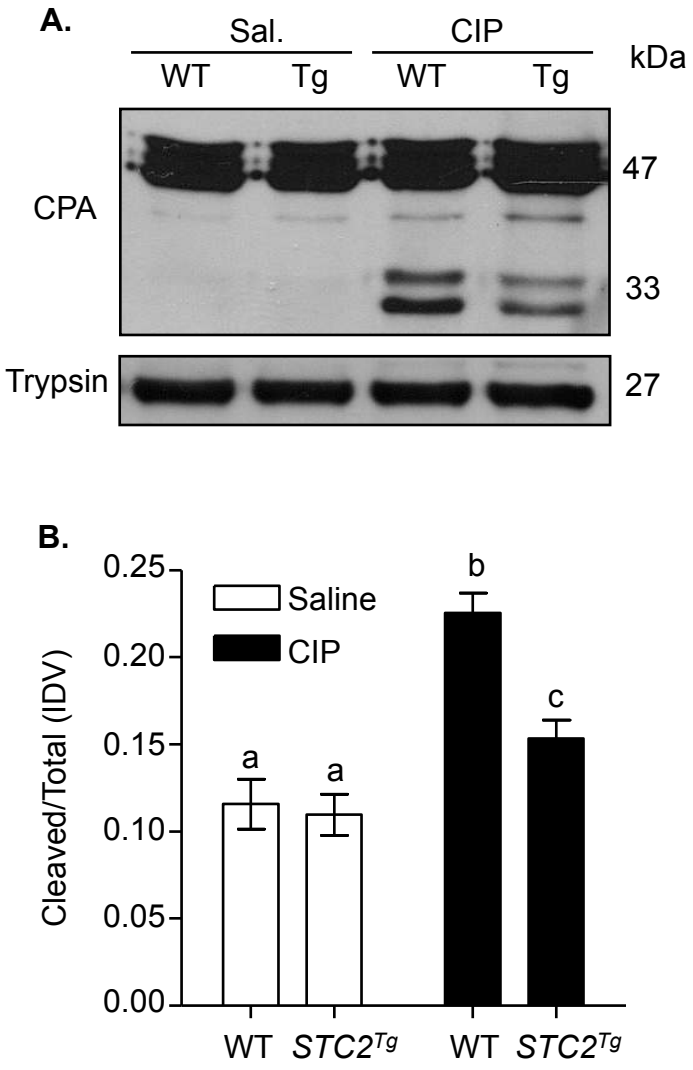

Figure 2.8. During CIP, STC2Tg Pancreata Exhibit Decreased Activation of Carboxypeptidase.

Figure 2.9. Cell junctions are maintained in *STC2*^{Tg} exocrine tissue during CIP. IF analysis for β-catenin (A-D) or Cx32 (E-H) in wild type (WT) or *STC2*^{Tg} (Tg) mice four hours after initial injection of saline (A, C, E, G) or cerulein (B, D, F, H) showing decreased accumulation only in WT tissue during CIP. (I) Representative Western blot analysis on pancreatic protein extracts 4 hours after initial saline or cerulein (CIP) injection confirm decreased β-catenin and Cx32 accumulation only in WT-CIP treated tissue (n=4).

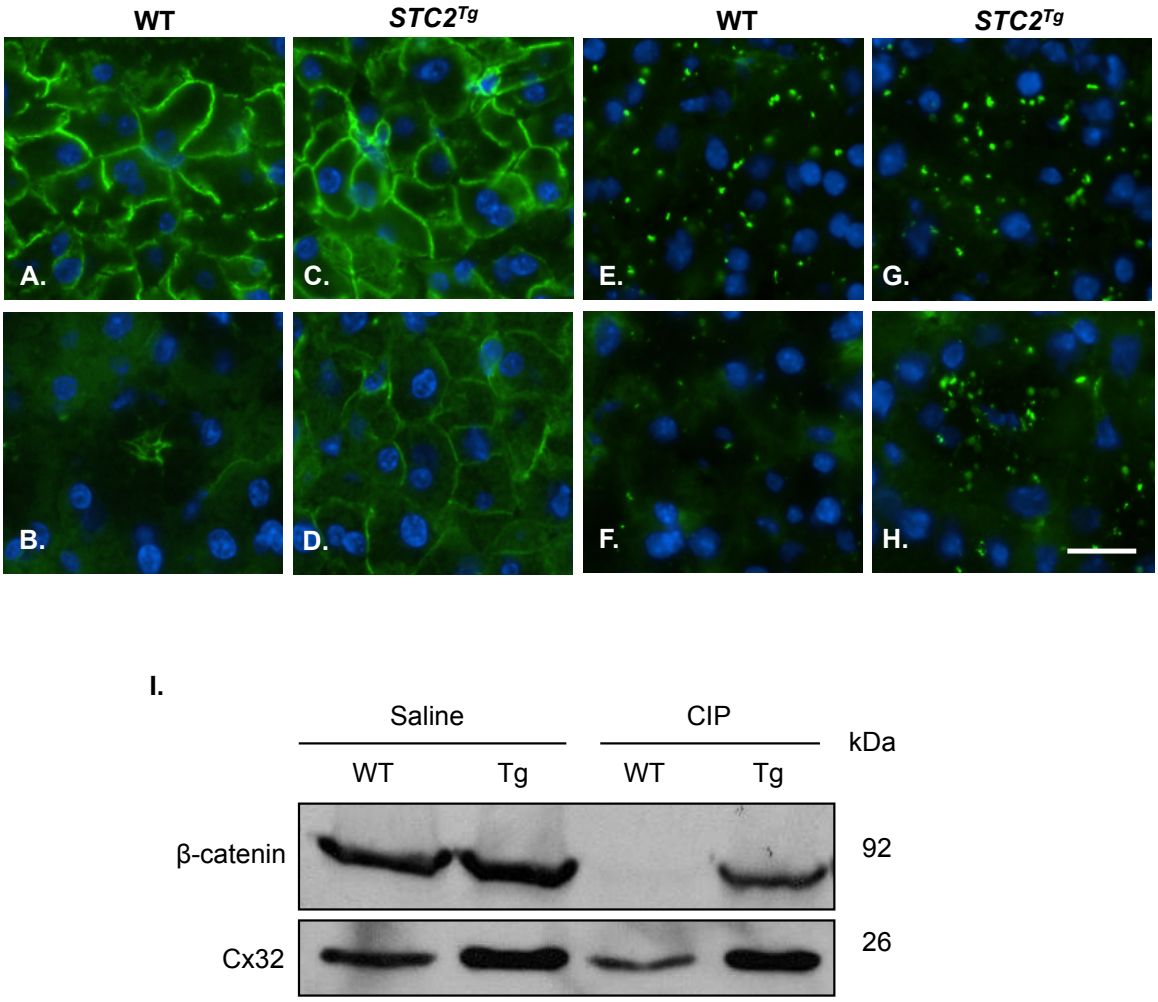

Figure 2.9. Cell Junctions are Maintained in *STC2*^{Tg} Exocrine Tissue During CIP.

STC2^{Tg} acini (Figure 2.9G, H) suggesting a greater disruption in gap junction complexes in WT acinar cells. Western blot analysis corroborated IF data with β-catenin and Cx32 accumulations significantly lower in WT extracts compared to *STC2*^{Tg} extracts four hours into CIP (Figure 2.9I) indicating that intercellular complexes were protected in *STC2*^{Tg} mice, suggestive of reduced cellular damage. Combined, these findings suggest that acinar cell integrity is maintained to higher degree when acini are exposed to higher than normal levels of STC2.

Visualization of apoptosis using TUNEL staining revealed increased apoptosis in both WT (Figure 2.10A, B; arrowheads) and *STC2*^{Tg} (Figure 2.10C, D; arrowheads) pancreatic tissue after induction of pancreatitis. Quantification of TUNEL positive cells revealed decreased apoptosis in *STC2*^{Tg} tissue that, although not statistically significant, may be of biological relevance (Figure 2.10E).

High mobility group protein b1 (HMGB1) is protein that translocates to the nucleus to interact with DNA, but upon necrotic stimulus, it is released from the nucleus and the cell to participate in inflammatory responses. Cytoplasmic staining of HMGB1 is routinely used as an indicator of cell necrosis. HMGB1 IF revealed the expected nuclear staining in both WT (Figure 2.11A) and *STC2*^{Tg} (Figure 2.11C) saline treated tissue. After induction of pancreatitis, punctate, cytoplasmic HMBG1 staining was observed in distinct patches of cells in WT tissue (Figure 2.11B). All *STC2*^{Tg} tissue analysed was devoid of punctate cytoplasmic HMGB1 staining indicating a lack of necrotic cells (Figure 2.11D).

Figure 2.10. Apoptosis is Decreased During CIP in *STC2*^{Tg} Tissue. TUNEL analysis revealed an increase in apoptosis in both WT (A vs. B; arrowheads) and *STC2*^{Tg} (C vs. D) pancreata after induction of pancreatitis (B, D) Magnification bar = 45 μM. Quantification of TUNEL positive cells revealed a trend toward decreased apoptosis in *STC2*^{Tg} tissue (I; n=4 animals; letters indicate significant differences). Bars represent mean ± standard error.

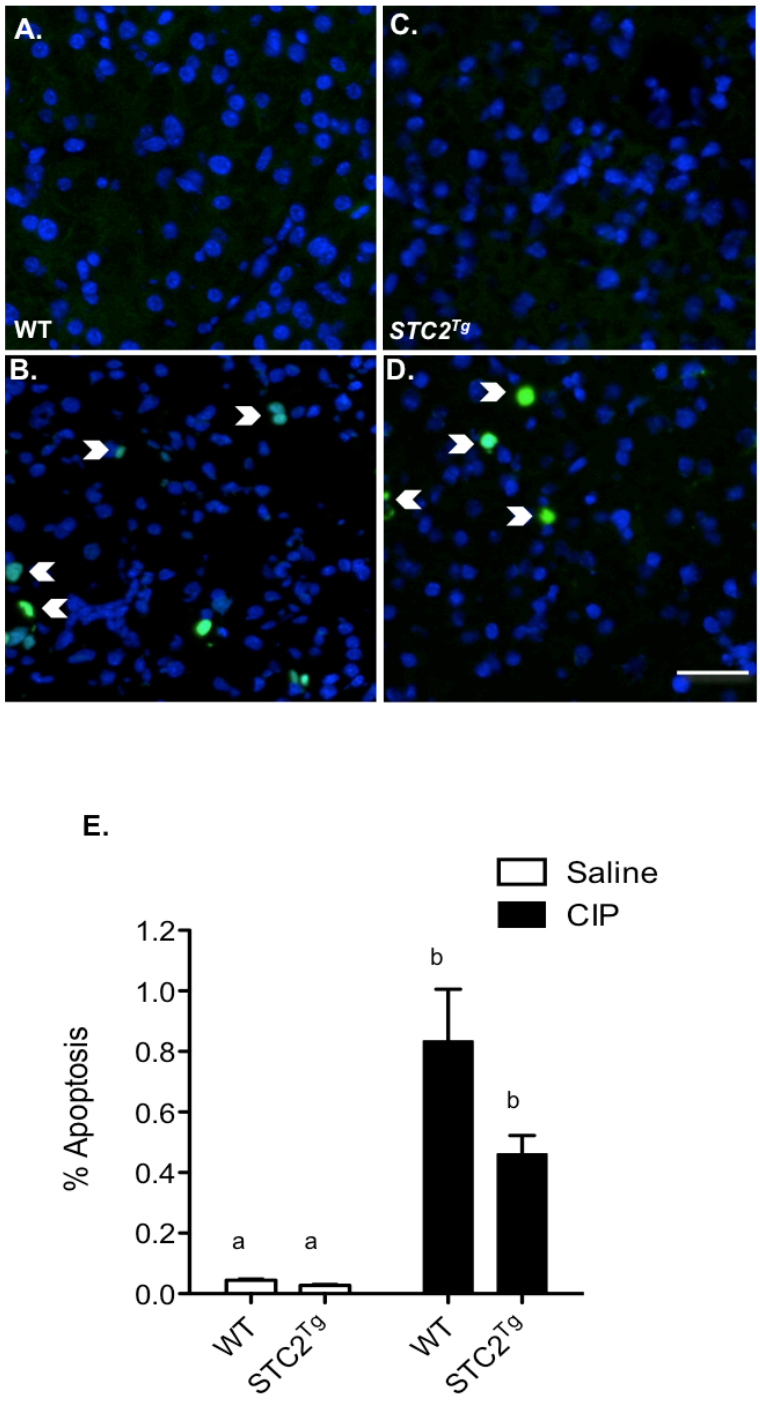

Figure 2.10. Apoptosis is Decreased During CIP in *STC2*^{Tg} Tissue.

Figure 2.11. Necrosis is decreased during CIP in *STC2*^{Tg} tissue. HMGB1 IF to identify necrosis revealed expected nuclear localization in saline conditions for WT (A; n=3 animals) and *STC2*^{Tg} (B; n=3 animals) tissue. After induction of pancreatitis, patches of cells with cytoplasmic, punctate HMGB1staining, indicative of necrosis, were observed in WT tissue (C; n=4 animals) but not in *STC2*^{Tg} tissue (D; n=4 animals). Magnification bar = 34 μM.

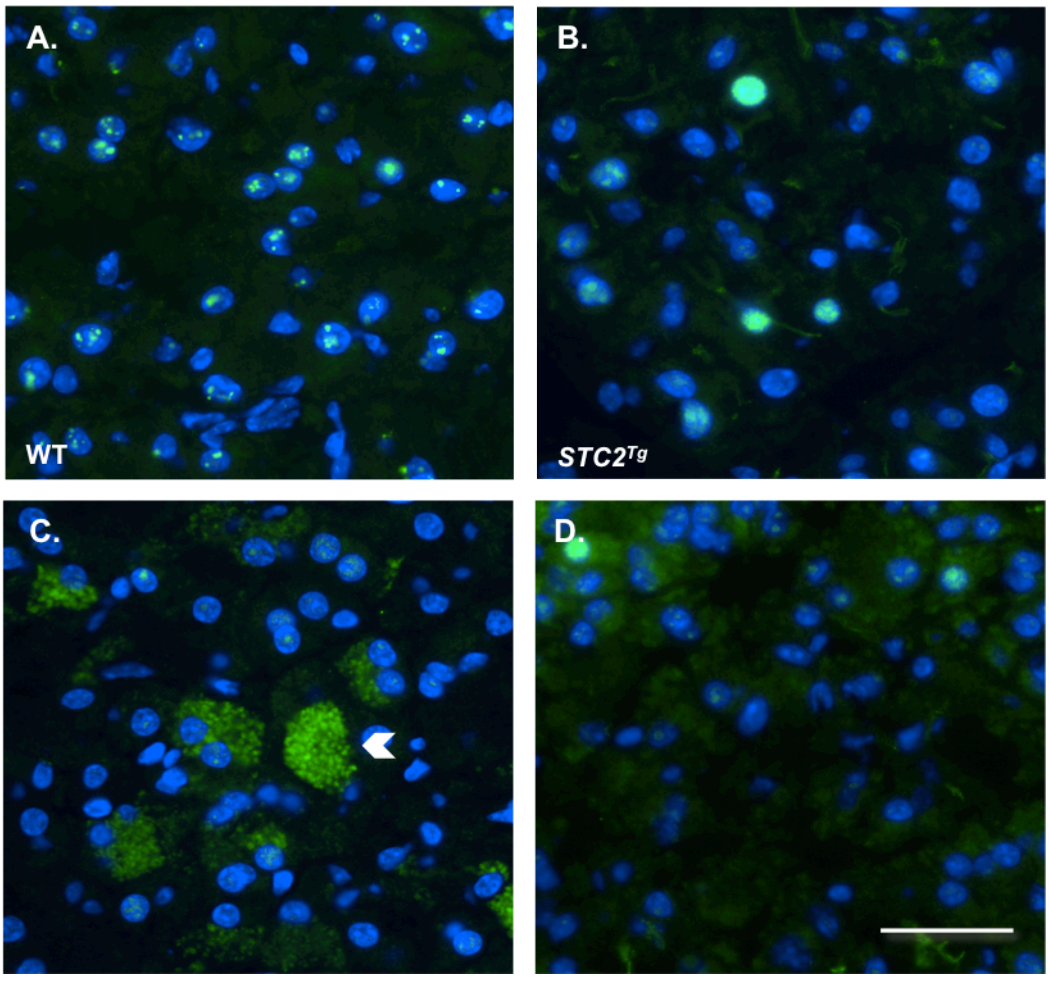

Figure 2.11. Necrosis is Decreased During CIP in *STC2*^{Tg} Tissue.

This analysis reveals that levels of both apoptosis and necrosis were decreased in *STC2*^{Tg} tissue, indicative of less tissue damage after CIP.

2.4 « Discussion»

STC2 is a secreted protein that, when expressed to high levels in mice, has profound effects leading to growth restriction (Gagliardi et al., 2005). However, ablation of *Stc2* in mice results in limited phenotypic alterations suggesting that STC2 functions may fall outside normal physiology (Chang et al., 2008). In support of such a hypothesis, *in vitro* analysis has identified increased *Stc2* accumulation following treatment with thapsigargin or tunicamycin, agents that activate ER stress pathways (Ito et al., 2004). STC2 is also up-regulated in response to hypoxic insult and is expressed to higher levels in many tumor-derived cell lines (Law and Wong, 2009, 2010). This suggests that STC2 may be involved in responding to external challenges that activate cell stress pathways. In this study, we have identified increased *Stc2* accumulation within four hours of inducing pancreatic injury that correlated with activation of the PERK signaling. Importantly, forced expression of STC2 in mice altered PERK signaling and reduced cellular damage in response to pancreatic injury. These results suggest a role for STC2 responding to and mediating the effects of cell stress in pancreatic tissue.

Studies assessing the expression of *Stc2* have revealed a limited expression pattern in adult tissues. In the human pancreas, *Stc2* is specifically expressed in alpha cells of the Islets of Langerhans and not in acinar tissue (Moore et al., 1999).

Our mRNA analysis revealed murine pancreatic expression of *Stc2* only after induction of pancreatitis by secretagogue stimulation. Unfortunately, IHC on CIP-treated tissue sections did not detect STC2 protein (data not shown) indicating that STC2 may be expressed at lower than detectable levels or that it is rapidly secreted into the circulation. While we have not definitively identified acini as the cell origin of *Stc2* expression, *Atf3*, a downstream mediator of PERK signaling, accumulated only in acinar cells during CIP. Therefore, it appears that CIP treatment leads to a cell autonomous activation of *Stc2*. As observed in HEK293 and N2a neuroblastoma cells, the increased accumulation of *Stc2* is consistent with activation of PERK signaling in response to injury (Ito et al., 2004). Induction of *Stc2* mRNA levels was not observed after CIP in *Mist1*$^{-/-}$ mice, which do not activate PERK or ATF3, and experience increased severity of CIP (Kowalik et al., 2007). These findings support the activation of *Stc2* as a protective mechanism, potentially as a mediator of the UPR.

While previous studies have correlated increased expression of STC2 as part of the UPR, the effects of STC2 on PERK signaling have not been examined. We have now identified that systemically high levels of STC2 reduce PERK activation. *STC2*^{Tg} mice showed decreased phosphorylation of PERK and eIF2α in pancreatic tissue suggesting that continued exposure to STC2 may lead to activation of negative feedback mechanisms. Since no change in total eIF2α is observed, this difference is peIF2α is specific to the phosphorylation event and not decreased eIF2α accumulation. Similar analysis of total PERK levels would extend this rationale to PERK phosphorylation.

We have identified at least two effectors of the PERK signaling pathway that were changed in *STC2*^{Tg} mice. First, GADD34, which combines with protein phosphatase 1 to reduce eIF2a phosphorylation (Novoa et al., 2001), accumulated to higher levels. Second, we observed significantly decreased accumulation of calcineurin, which stimulates PERK autophosphorylation, thereby increasing activity (Bollo et al., 2010). Whether these changes are reflective of a direct role for STC2 in their regulation or a response to other events caused by over exposure to STC2 is unclear. However, the altered expression of these factors suggests a role for STC2 in regulating Ca^{2+} homeostasis since both calcineurin and PERK are affected by altered Ca^{2+} sequestration in the ER.

In light of decreased PERK and eIF2α activation, it was surprising that increased accumulation of ATF4 was observed in the pancreas of *STC2*^{Tg} mice. Phosphorylation of eIF2a is known to stimulate translation of *Atf4* mRNA, leading to increased ATF4 protein accumulation. However, increased ATF4 expression, and the subsequent increase in GADD34 could be mediated by increased stability of the ATF4 protein. Recent studies have shown that ATF4 is stabilized by interaction with p300 through inhibition of ubiquitination (Lassot et al., 2005), and that association with p300/CBP enhances ATF4 transcriptional ability (Cherasse et al., 2007; Lassot et al., 2005). It is possible that in *STC2*^{Tg} mice, stabilization of ATF4 is enhanced regardless of decreased phosphorylation of eIF2α, accounting for its increased expression. Although there is little known

about non-peIF2α related transcriptional activation of ATF4, increased transcriptional activation by a yet to be identified factor cannot be ruled out.

Figure 2.12 summarizes a potential role of STC2's regulation of the UPR, where over-expression of STC2 directly or indirectly inhibits calcineurin expression, (Figure 2.12, dotted line), which then inhibits calcineurin-dependent phosphorylation of PERK. Decreased phosphorylation of PERK results in decreased phosphorylation of eIF2α, as observed in *STC2*^{Tg} pancreatic tissue. Although the increased expression of ATF4 in *STC2*^{Tg} tissue is not intuitive considering the phosphorylation of both PERK and eIF2α, it reveals a potential direct or indirect role for STC2 in ATF4 regulation (Figure 7, dotted arrow). This increase in ATF4 expression leads to increased GADD34 expression, which can then feedback and contribute to decreased phosphorylation of eIF2α.

As would be expected from increased ATF4 expression, *STC2*^{Tg} mice also exhibited an increased level of autophagy, a downstream consequence of elevated ATF4 levels. Autophagy is important for maintenance of cellular homeostasis through balancing synthesis and degradation or recycling of cellular components. Independent studies have indicated that either phosphorylation of eIF2a or expression of ATF4 is required for induction of autophagy *in vitro* (Kouroku et al., 2007; Milani et al., 2009; Rzymski et al., 2010).

Figure 2.12. Schematic Pathway Showing a Possible Role for STC2 in Affecting the PERK Signaling Pathway. The increased accumulation of ATF4 leads to increased expression of GADD34, ATF3 and STC2. Elevated levels of STC2 can alter both PERK phosphorylation and ATF4 levels through as yet undetermined mechanisms (dashed arrows), as well as promote reduced damage during pancreatic injury. Whether this protective effect of STC2 is a normal function of the protein needs to be clarified.

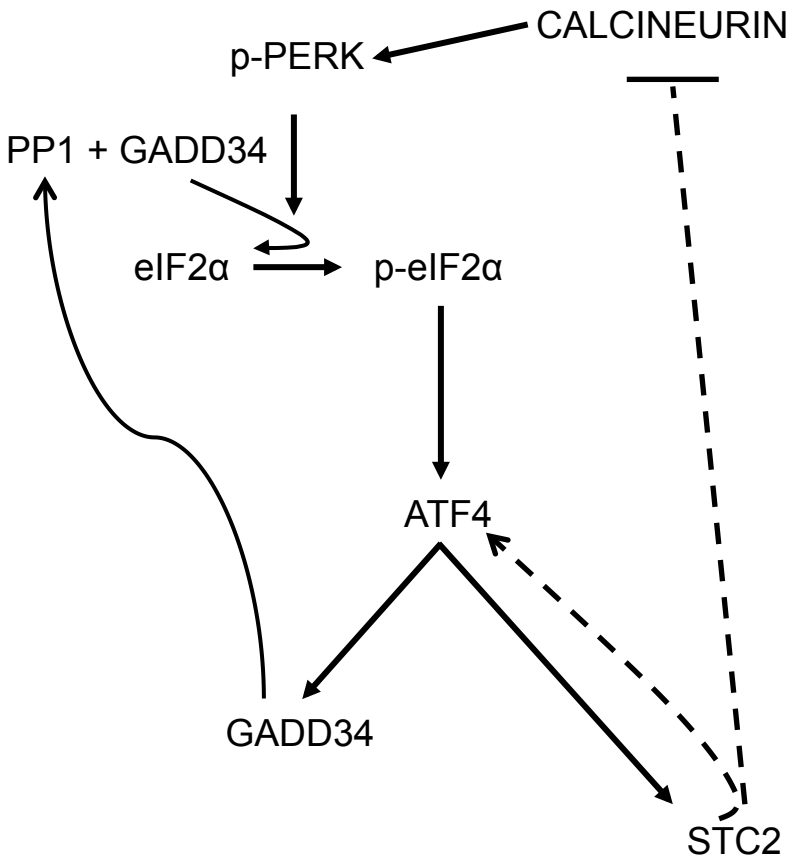

Figure 2.12. Schematic Pathway Showing a Possible Role for STC2 in Altering the PERK Signaling Pathway.

The increased expression of ATF4 in *STC2*^{Tg} pancreatic tissue may be the cause of increased autophagy. Interestingly, we did not observe increased acinar cell apoptosis (data not shown), which is another downstream result of increased UPR. Therefore, it appears that only certain parts of the UPR have been activated in *STC2*^{Tg} mice.

Whether STC2 is protective in nature is still unclear since studies have shown it has both protective (Raulic et al., 2008) and detrimental roles (Law and Wong, 2009, 2010) in cancer progression *in vitro*. Our results suggest a protective advantage following exocrine pancreatic injury *in vivo*. *STC2*^{Tg} mice exhibit a decreased proportional increase in serum amylase levels, increased maintenance of cellular junctions, decreased apoptosis and necrosis and decreased activation of CPA in exocrine pancreatic tissue, all suggestive of decreased pancreatitis severity. In addition, the enhanced autophagy observed in *STC2*^{Tg} acinar tissue would facilitate more rapid degradation of resident digestive enzymes upon injury, thereby limiting damage to cellular contents. This would account for increased maintenance of cellular junctions. However, to truly understand the role of STC2 in pancreatic injury, further experiments in mice lacking *Stc2* mice should be performed.

In conclusion, this is the first study to illustrate a link between the PERK signaling and STC2 *in vivo*, and suggests two novel roles for STC2, as a downstream effector of PERK signaling and possible protective factor during pancreatic injury. This is also the first time that STC2 has been shown to affect proteins that regulate Ca^{2+}-mediated response in the cell.

Chapter 3

3 « Stanniocalcin 2 affects endocrine pancreas structure and function »

The experiments in Chapter 2 revealed a role for STC2 in the exocrine pancreas. While the exocrine and endocrine pancreatic compartments perform distinct functions, they are inextricably linked to one another, where dysregulation of one compartment can affect the other (Angelopoulos et al., 2005; Czako et al., 2009; Frier et al., 1976; Hardt and Ewald, 2011). Since there was an observed alteration in exocrine pancreas function in *STC2*^{Tg} mice, I sought to determine whether there was also an effect in the endocrine pancreas. Additionally, STC2 is a member of the PERK pathway which is important for endocrine pancreas development and function. This chapter contains work to be submitted as a manuscript. All experimental work in this chapter was performed by E. Fazio. G. DiMattia and C. Pin conceived experiments and provided theoretical input.

3.1 « Introduction »

STC2 is transcriptionally regulated by ATF4 and part of the PERK pathway within the UPR (Figure 1.2; (Ito et al., 2004)). PERK signaling is activated to alleviate protein folding overload in a cell and is largely associated with translational control and is important in cell types that

respond to stimuli associated with increased protein production and secretion, including pancreatic acinar and β-cells. PERK acts as a Ca^{2+} sensor in the ER of pancreatic β-cells, since it is activated under conditions that deplete ER Ca^{2+} stores (Cnop et al., 2007; Gomez et al., 2008; Zhang et al., 2002). PERK has been implicated in the maintenance and function of the endocrine pancreas, in that various mouse models lacking PERK expression (*Perk*$^{-/-}$) exhibit symptoms congruent with Wolcott-Rallison syndrome (WRS) in humans. Mice exhibit deterioration of endocrine pancreas structure and function and hyperglycemia with decreased levels of serum insulin (Harding et al., 2001). Pancreatic islets in these mice degenerated over time, where insulin-producing β-cells underwent apoptosis and the normally peripheral glucagon expressing α-cells began to populate the islet core (Harding et al., 2001; Zhang et al., 2006).

Recent work suggests that osteoblast specific factors can affect endocrine pancreas function (Lee et al., 2007; Yoshizawa et al., 2009) and that ablation of ATF4 in osteoblasts (*Atf4*$_{osb}^{-/-}$) results in improved glucose tolerance, increased islet insulin content, increased β-cell area and increased β-cell mass (Yoshizawa et al., 2009). ATF4 also transcriptionally regulates *Stc2*, and mice over-expressing STC2 (*STC2*^{Tg}) exhibit dwarf phenotypes (Gagliardi et al., 2005; Johnston et al., 2010) related to negative effects on bone development (41). The fact that STC2 regulates bone growth, and is a target of ATF4 transcriptional regulation

make it an attractive factor to examine in elucidating the effect of the PERK pathway on endocrine structure and function.

Systemic over-expression of STC2 results in alterations to UPR signaling in the exocrine pancreas (Chapter 2). However, the primary site of *STC2* mRNA production in humans is the pancreas (DiMattia et al., 1998; Moore et al., 1999) with STC2 protein specifically detected in alpha cells of pancreatic islets (Moore et al., 1999). In addition, alterations in the UPR have adverse consequences in endocrine pancreas function that can lead to diabetes. Therefore, it is likely that STC2's effects would not be limited to the exocrine compartment of the pancreas.

The goal of this study was to determine if over-expression of STC2 affects endocrine pancreas structure and function. While $Stc2^{Tg}$ mice do not exhibit hyperglycemia under resting conditions, glucose stimulated insulin secretion revealed decreased glucose tolerance in these animals. Morphological analysis revealed increased islet number and a decreased proportion of β-cells in $STC2^{Tg}$ pancreata.

3.2 « Methodology»

3.2.1 « Mouse Handling »

$STC2^{Tg}$ and wild type mice were used as described in Section 2.2.1.

3.2.2 « Glucose Tolerance »

Two to four month-old female mice were fasted overnight to determine resting blood glucose levels. Following intraperitoneal administration of 2 g/kg D-glucose (t=0), blood glucose levels were monitored at t=10, 20, 40, 60, 90 and 120 minutes post-injection using tail blood with a Fast-Take Glucosemeter (Lifescan, Burnaby BC). Mice were sacrificed using 95% CO_2 and systemic blood collected via cardiac puncture. Pancreata were dissected and processed for immunohistochemistry or protein extraction. Area under the curve (AUC) represents absolute glucose tolerance and was calculated for the glucose tolerance profile of each mouse using the trapezoidal method (Allison et al., 1995).

3.2.3 « Morphological Analysis »

Dual IF was performed with antibodies specific for insulin (Sigma, Oakville ON) and glucagon (Sigma, Oakville, ON). Quantitative evaluation was performed using computer assisted image analysis with OpenLab 4.0.3 Modular Software for Scientific Imaging (Improvision; Lexington, MA). Under low magnification the area of the pancreas was manually traced using Openlab software. At a higher magnification, individual islets identified by insulin/glucagon staining were manually traced. In total, three sections were chosen per animal with at least 10 islets counted. Analysis parameters included total number of islets per unit area of pancreas, total

amount of islet area and number of insulin and glucagon positive cells (Fazio et al., 2005). .

3.2.4 « Statistical Analyses»

Data are expressed as mean ± standard error. All statistical analyses were performed using Graphpad Prism 4.02 for Windows (GraphPad Software, San Diego CA). For comparison between two groups, the paired, Mann-Whitney test was used, where significance was obtained if $p < 0.05$. The glucose tolerance time course was statistically analysed using two-way repeated measures analysis of variance (ANOVA) and a Bonferroni post-hoc test.

3.3 « Results»

3.3.1 « STC2 Expression Pattern»

Since STC2 is a secreted protein, pancreatic accumulation was assessed through IF analysis, which revealed STC2 localization to islets in wild type tissue (Figure 3.1A). Higher magnification revealed that STC2 protein was cytoplasmic (Figure 3.1B). IF revealed increased accumulation of STC2 protein in the pancreatic islets of *STC2*^{Tg} mice (Figure 3.1C) suggesting that the endocrine portion of the pancreas was a target for STC2 function. Co-IF with insulin revealed STC2 expression in a subset

of β-cells in *STC2*^{Tg} tissue (Figure 3.1D). Surprisingly, only low levels of STC2 were detected in the exocrine tissue in either situation.

3.3.2 « Analysis of Endocrine Function»

To assess whether exposure to high levels of STC2 affects endocrine function, the response of *STC2*^{Tg} mice to increased glucose challenge was examined. No significant difference in resting blood glucose levels was observed between *STC2*^{Tg} and WT mice (Figure 3.2A, t = 0). Following IP injection of a 2 g/kg bolus of 50% glucose, *STC2*^{Tg} mice showed a significantly different response in their ability to clear glucose. Blood glucose levels of WT and *STC2*^{Tg} mice were similar 10 minutes after injection (t = 10). However, by 20 minutes post- stimulation (t = 20), blood glucose levels of *STC2*^{Tg} mice (29.0 +/- 2.7 mmol/L) were significantly elevated compared to WT counterparts (21.4 +/- 2.3 mmol/L). At 40 (WT: 18.1 +/- 3.3 mmol/L; *STC2*^{Tg}: 28.0 +/- 4.1 mmol/L) and 60 minutes post injection (WT: 13.0 +/- 2.1 mmol/L; *STC2*^{Tg}: 21.7 +/- 3.4 mmol/L) (t = 40, 60) the blood glucose levels of *STC2*^{Tg} remained significantly higher than WT counterparts (*, $p < 0.01$; WT: n= 24, *STC2*^{Tg}: n= 21). By 120 minutes, blood glucose levels of WT and *STC2*^{Tg} mice returned to baseline levels. Area under the curve (Figure 3.2B), which represents absolute glucose clearance, was significantly higher in *STC2*^{Tg} mice (*, $p < 0.05$; WT: n= 24, *STC2*^{Tg}: n= 21) indicating a decreased efficiency in clearing glucose from the blood.

Figure 3.1. STC2 is Expressed in Pancreatic Islets. (A) STC2 is expressed in the islets of WT pancreata. (B) Magnification of boxed area in A illustrates that STC2 is cytosolic. Magnification bar = 5 μM. (C) STC2 expression is increased in the islets of $STC2^{Tg}$ mice. (D) STC colocalized with insulin (red) in $STC2^{Tg}$ islets. DAPI stain was used to identify nuclei. Magnification bar for A,C,D = 16 μM. Islet is outlined in A.

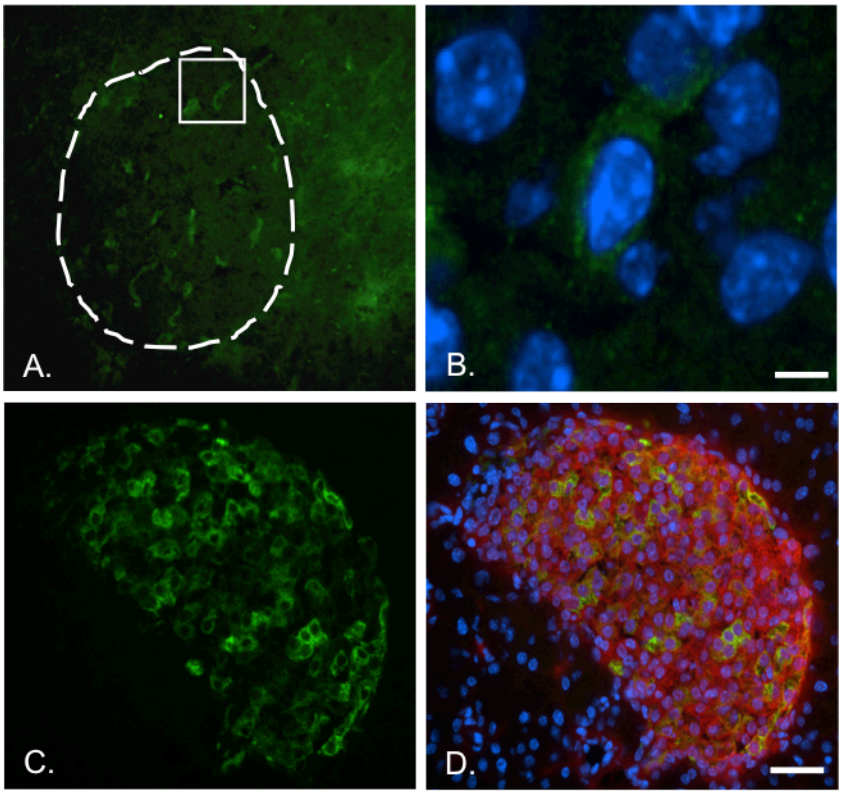

Figure 3.1. STC2 is Expressed in Pancreatic Islets.

Figure 3.2. Glucose Tolerance is Decreased in *STC2^{Tg}* Mice. *STC2^{Tg}* mice exhibit significantly decreased glucose tolerance at 40 and 60 minutes post administration of glucose load (A; □ = wild type, ▲ = *STC2^{Tg}*). (B) Area under the curve reveals overall significantly higher blood glucose levels in *STC2^{Tg}* mice illustrating glucose intolerance. Bars represent mean ± standard error.

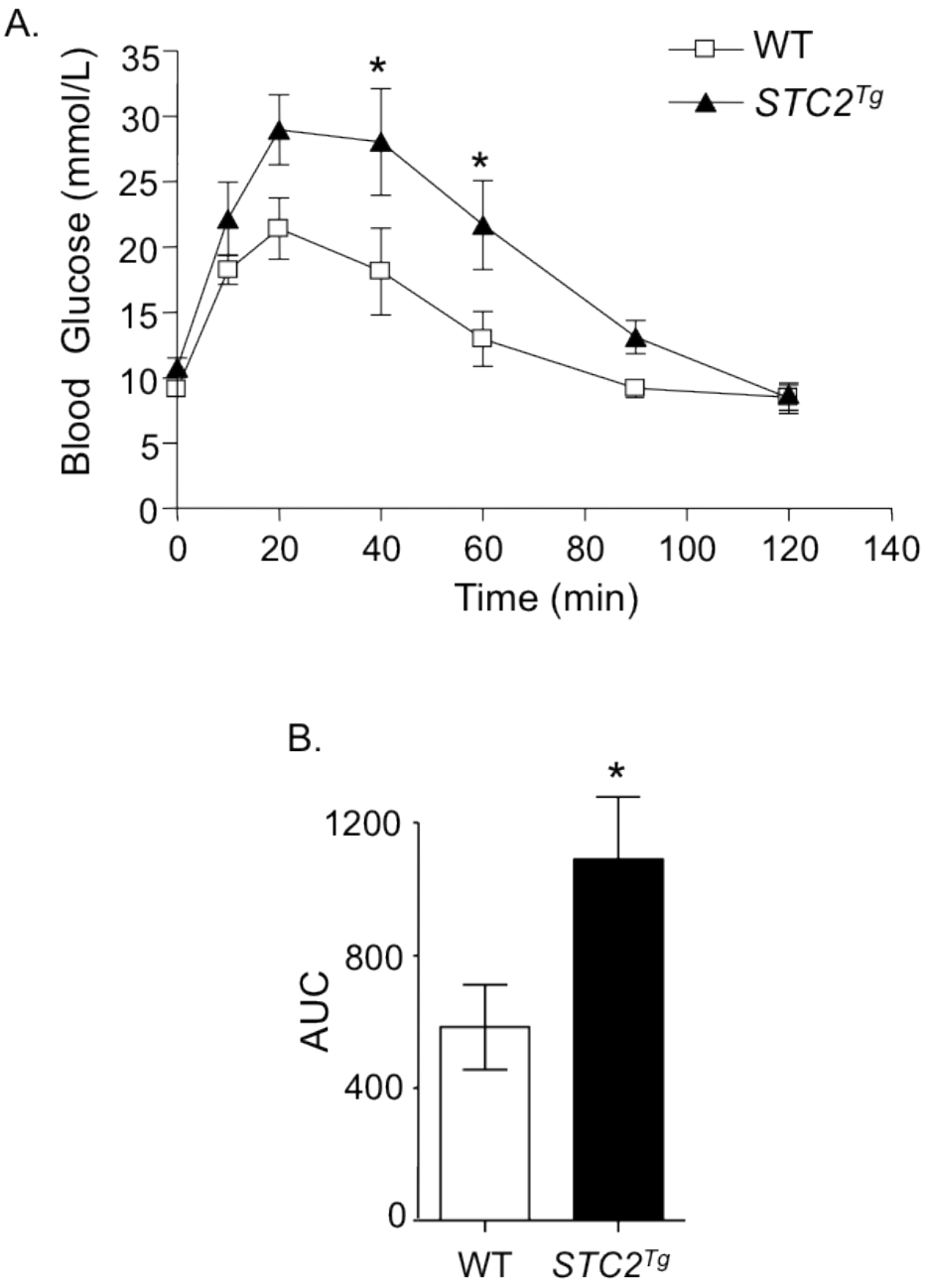

Figure 3.2. Glucose Tolerance is Decreased in *STC2^{Tg}* Mice.

3.3.3 « Analysis of Endocrine Pancreas Morphology»

To determine whether decreased glucose tolerance was due to endocrine tissue defects, pancreatic morphology in *STC2*^{Tg} mice was compared to that in WT mice. No overt morphological differences were observed and *STC2*^{Tg} acinar tissue showed no overt differences in morphology compared to WT mice (see Figure 2.3). However, morphometric analysis indicated that *STC2*^{Tg} mice had significantly more islets per unit section area ($1.55x10^{-4}$ +/- $1.27x10^{-5;}$) compared to WT counterparts ($1.06x10^{-4}$ +/- $8.92x10^{-6}$) (Figure 3.3A; *, $p < 0.05$; WT; n = 5, *STC2*^{Tg}: n= 5). This difference was accompanied by a general trend in decreased islet size (WT: 7976 +/- 688 μm^2; *STC2*^{Tg}: 6939 +/- 922.5 μm^2; Figure 3.3B) resulting in an overall increase in the percentage of endocrine area (WT: 0.86 +/- 0.13 %; *STC2*^{Tg}: 1.07 +/- 0.23 %; Figure 3.3C). Co-IF for glucagon (Figure 3.4A, B) and insulin (Figure 3.4C, D) revealed a similar localization pattern for both genotypes with glucagon positive α cells localized to the periphery of the islet. However, IF revealed a wider mantle of glucagon positive cells in *STC2*^{Tg} mice (Figure 3.4A,B). Quantification of the number of glucagon and insulin cells confirmed a significant increase in the number of glucagon expressing cells in *STC2*^{Tg} mice compared to WT counterparts with a 69% increase in glucagon-expressing cells, concomitant with a 20% decrease in insulin-secreting cells (Figure 3.4E, F; *, $p < 0.01$; WT; n = 5, *STC2*^{Tg}: n= 5; summarized in

Figure 3.3. Islet Morphology is Altered in *STC2*^{Tg} Pancreata. There is an increase in islet number (A), with no change in islet size (B) resulting in an overall increase in percent islet area (C) in *STC2*^{Tg} pancreatic tissue.

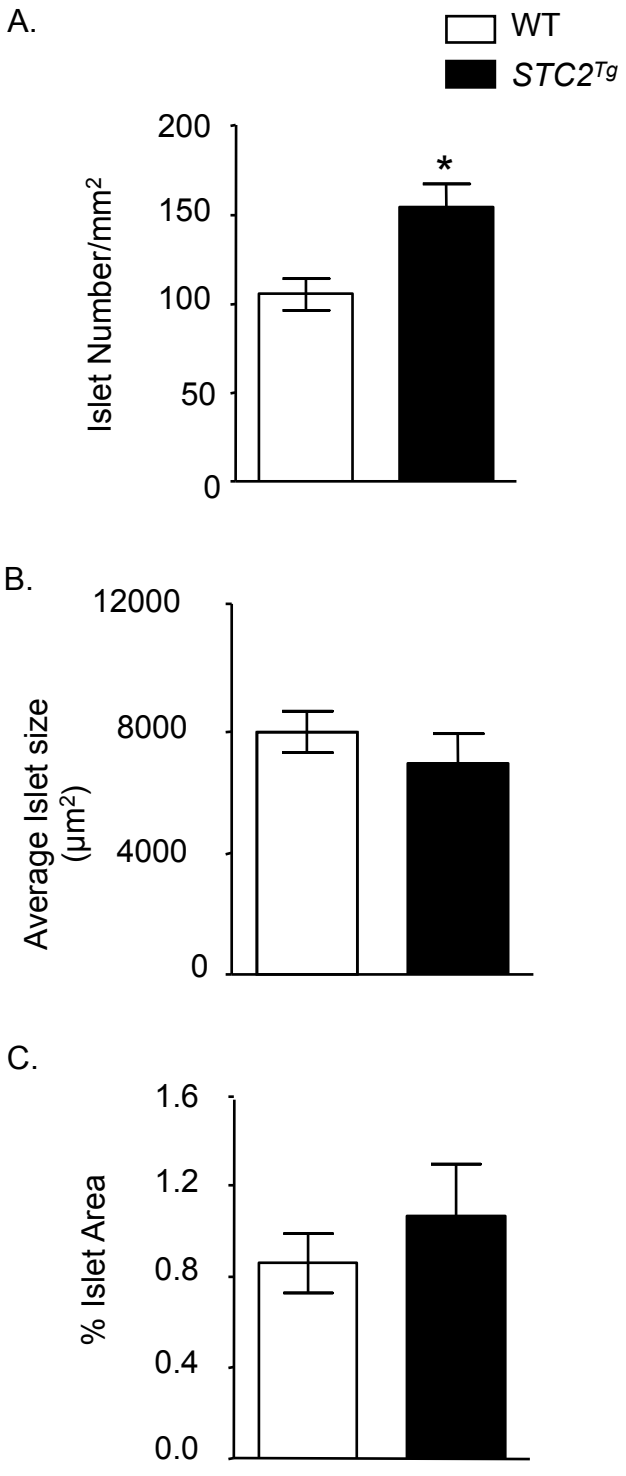

Figure 3.3. Islet Morphology is Altered in *STC2^{Tg}* Pancreata.

Figure 3.4. Islet Composition is Altered in *STC2^{Tg}* Mice. Glucagon expression is limited to the islet periphery in both WT (A) and *STC2^{Tg}* (B) tissue. Insulin is properly localized in both WT (C) and *STC2^{Tg}* (D) tissue. Cell counting revealed a significant increase in glucagon expressing cells (E) and a significant decrease in insulin positive cells (F) when compared to WT. Magnification bar = 35 μM. Bars represent mean ± standard error.

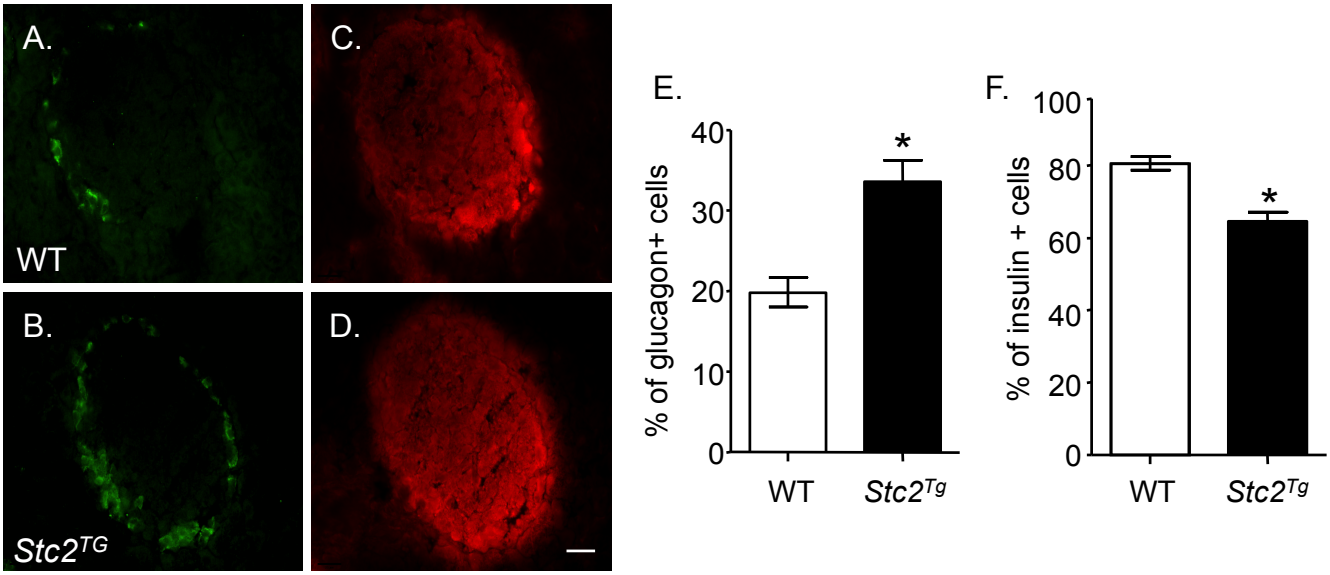

Figure 3.4. Islet Composition is Altered in *STC2^{Tg}* Mice.

Table 3.1). Therefore, exposure to constitutively higher levels of STC2 leads to altered endocrine function and morphology.

3.4 « Discussion and Future Directions»

Previous work identified alterations in the exocrine pancreas of mice overexpressing STC2. In the study, analysis of the endocrine pancreas of *STC2*^{Tg} mice revealed pancreas was also affected since the UPR has been shown to be required for differentiation and development of the tissue. Thus, *STC2*^{Tg} mice exhibit a bone (Johnston et al., 2010) and endocrine pancreas defect which have been previously linked in mice overexpressing ATF4 in osteoblasts (*α1(I)collagen-ATF4*). These mice exhibit decreased glucose tolerance, decreased islet insulin content, decreased islet size and decreased β-cell mass, decreased insulin sensitivity and decreased insulin secretion (Yoshizawa et al., 2009), revealing a strong link between osteoblast specific ATF4 expression and endocrine pancreas function. Assessment of endocrine function in *STC2*^{Tg} mice revealed several of the same outcomes, which indicates that STC2 may be a mediator of the endocrine effects exhibited in the *α1(I)collagen-ATF4* mice. which is similar to the phenotype characterized in *STC2*^{Tg} mice in this study. Assessment of insulin secretion and sensitivity in *α1(I)collagen-ATF4* mice revealed that both are decreased. The link between ATF4 and STC2, and the fact that STC2 is a secreted glycoprotein lead to a theory that ATF4 expression in bone can lead to

increased STC2 production that is then secreted and may act in a paracrine or endocrine manner. Thus, a potential mechanism is that ATF4 activates synthesis and secretion of STC2 in order to inhibit insulin secretion once blood glucose homeostasis is achieved. To validate this theory, insulin secretion and sensitivity should be measured in *STC2*^{Tg} mice, and STC2 expression should be assessed in *α1(I)collagen-ATF4* and *Atf4*$_{osb}^{-/-}$ mice. In addition, the endocrine compartment should be assessed in *Stc2*$^{-/-}$ mice.

This work illustrates that within the pancreas, STC2 accumulates in islets. However, it is still unclear whether STC2 is produced in islets and acts locally, or whether the STC2 associates with islets via an endocrine mechanism. Additionally, the mechanism by which STC2 alters the structure and function of pancreatic islets is still unclear. While downstream signaling mechanisms of STC2 are unknown, exposure of islets to STC2 could result in an altered transcriptional program. The *STC2* transgene is detected as early as embryonic day 10.5 in *STC2*^{Tg} mice (Gagliardi et al., 2005), which precedes the stage of pancreas development where endocrine cells begin to cluster into islet like aggregates. Exposure of endocrine tissue to STC2 during development could account for the decreased number of β-cells, increased number of α-cells and overall decreased islet size observed in these mice. The

Table 1. Summary of Islet Morphometric Analysis

Islet Parameter Examined	WT	*STC2*^{Tg}	Significance
Islet Number/total section area	1.06x10-4 ± 8.92x10-6	1.55x10-4 ± 1.27x10-5*	Yes, p<0.05
Islet Size	7976 ± 688 μm^2	6939 ± 922.5 μm^2	No
% Islet Area	0.86 ± 0.13	1.07 ± 0.23	No
% Glucagon Positive Cells	19.87 ± 1.81	33.63 ± 2.62*	Yes, p < 0.005
% Insulin Positive Cells	80.54 ±1.91	64.56 ± 2.50*	Yes, p < 0.001

alteration in islet cell proportion and size may result in decreased exocrine function observed in these mice, however, since STC2 plays a role in Ca^{2+} homeostasis, it's possible that STC2 inhibits Ca^{2+} influx required for release of insulin from β-cells.

The accumulation of STC2 in pancreatic islets also raises the question of how STC2 over-expression affects the exocrine pancreas. Previous work (Chapter 2) outlined altered PERK pathway signaling in the exocrine pancreas, and a decrease in severity of pancreatitis in *STC2*^{Tg} mice. While STC2 localization to the exocrine pancreas of *STC2*^{Tg} mice was not detectable using immunofluorescence, immunohistochemistry revealed small pockets of STC2 localization to the exocrine pancreas that can account for the altered UPR and response to injury in exocrine pancreatic tissue in these mice. However, the robust localization of STC2 to endocrine tissue suggests that cross-talk between the endocrine and exocrine compartments may be involved in altered exocrine pancreas responses in *STC2*^{Tg} mice. The influence of the endocrine component on the exocrine pancreas has been previously illustrated by the development of exocrine insufficiency during diabetes (reviewed in (Frier et al., 1976; Hardt and Ewald, 2011)). For example, in the Cohen diabetic rat, nutritionally induced diabetes results in the accumulation of exocrine lesions and macrophage infiltration, lipid accumulation and acinar atrophy (Weksler-Zangen et al., 2008). To determine whether exocrine effects are cell autonomous, primary cultures of acinar cells from *STC2*^{Tg} mice can be

used to determine whether the levels of PERK activity decrease to levels consistent with normal, wild type, levels. These cultures can also be used to determine whether the *STC2*^{Tg} acinar cell response to hyperstimulation with CCK mirrors that which is observed in CIP-treated animals. Alternatively, islets from *STC2*^{Tg} pancreatic tissue can be stimulated with glucose in culture to observe their glucose stimulated insulin secretion and address the possibility that primary effects in the exocrine pancreas affect endocrine pancreas function (Angelopoulos et al., 2005; Czako et al., 2009).

In conclusion, this study highlights a role for STC2 in endocrine pancreas structure and function, and suggests that STC2 is an endocrine mediator of the PERK pathway.

Chapter 4

4 « Chromatin Immunoprecipitation (ChIP) from pancreatic acinar cells and whole pancreatic tissue »

The first two results chapters delineated the outcomes of over-expressing a PERK mediator, STC2, in mice and the effects on pancreatic physiology and pathology. While over-expression models may uncover important functions of a protein, they do not mimic the in vivo situation and may be misleading regarding the physiological relevance. An alternative approach is to perform loss of function experiments with mediators of PERK signaling. We have chosen to study ATF3, a transcription factor that can bind and affect gene expression. To appropriately assess ATF3 function, it was necessary to develop a protocol for chromatin immunoprecipitation (ChIP) from whole pancreatic tissue. It was essential that I performed ChIP from whole pancreatic tissue since previous work from our lab indicated that the UPR is activated upon isolation of pancreatic acini. This characteristic was not desirable for the proposed studies since isolation-related activation of the UPR could mask in vivo physiological events mediated by the UPR during pancreatitis. The following is an excerpt from an article published in Pancreapedia (Fazio, 2011) an online database for researchers studying the exocrine pancreas. E. Fazio designed ChIP from tissue experiments and wrote >80% of the manuscript. R. Mehmood performed ChIP

from isolated cells and contributed to manuscript writing (not included here). C. Pin provided theoretical input and revised the manuscript.

4.1 « Introduction »

Over the past decade, chromatin immunoprecipitation (ChIP) has emerged as an important technique for determining the binding of proteins to specific DNA sequences. In particular, ChIP has been used to confirm whether transcription factors (TFs) work directly on target genes to promote gene activation or repression (reviewed in (Kuo and Allis, 1999)). ChIP has advantages over other techniques that examine the role of TFs in regulating gene expression. Promoter assays that use reporter genes such as *luciferase* or green fluorescent protein (GFP) can determine whether a TF stimulates the expression of a certain promoter, but do not assess DNA binding to determine whether the effects on expression are direct. Electrophoretic mobility shift assays (EMSA) can be used to determine TF binding but are relatively insensitive when compared to ChIP and require the ability of an antibody to supershift a protein/DNA complex to determine true interactions (Im et al., 2004).

ChIP protocols have been adapted to study epigenetic modifications that affect gene expression and can be combined with Next-Generation sequencing (ChIP-Seq) as a data output revealing previously unknown binding targets of proteins or epigenetic marks of interest (reviewed in (Park, 2009)). The ability to obtain good quality starting material for ChIP analysis is crucial if scientists want to

apply changes in gene transcription and epigenetic modifications to the study of human disease.

ChIP has become such a valuable tool that many companies have recognized a niche for ready-made ChIP kits, such as Millipore, Active Motif, Abcam and Pierce. While these kits are useful for some tissue or cell types, they are not especially cost-effective and have proven to be insufficient for use with adult pancreatic tissue or isolated acinar cells. After examining the efficiency and yield provided by a variety of ready-made ChIP kits, our laboratory has developed our own ChIP protocols for use with isolated acinar cells or whole pancreatic tissue.

One of the benefits for using isolated cells for ChIP is that the acinar cells are purified from other pancreatic cell populations (Williams et al., 1978), thereby reducing any background that may be occurring with DNA targets of interest in non-acinar cells. However, the use of isolated acinar cells for ChIP can affect downstream analyses as a number of stress signaling pathways are activated upon isolation (Blinman et al., 2000; Johnson et al., 2009), and may obscure relevant endogenous mechanisms. This becomes even more important if one is examining the transcriptional profile the tissue following the induction of cellular injury (i.e. pancreatitis). Therefore, acinar cell isolation may mask the effects of actual disease mechanisms on the disease process.

The following protocol was developed for ChIP analysis from whole pancreatic tissue. While protocols exist for ChIP from various other tissues, none were adequate for use in the pancreas. The pancreas presents a unique challenge

due to the high protein content, with the majority being proteases that may act to degrade TFs. Therefore, a methodology for performing ChIP on pancreatic tissue either from untreated or pancreatitis models was established.

4.2 « Preparation of Chromatin from Whole Pancreas »

4.2.1 « Preparation of Nuclei from Whole Tissue»

CIP was initiated as described in Section 2 and is a variation of the CIP model previously described (Niederau et al., 1990). The pancreas was dissected and finely minced. Fine mincing is crucial for proper processing as a rougher mince proved to be unsuccessful for crosslinking and subsequent ChIP. To cross-link protein to DNA, the minced pancreatic tissue was incubated in 40 mL of freshly made 1% formaldehyde in DMEM for 10 minutes at room temperature with rocking. To quench the formaldehyde, glycine was added to a final concentration of 0.125 M and tissue was incubated for 5 minutes with rocking. The tissue was pelleted by centrifugation at 95 x g for three minutes and washed with ice cold PBS containing aprotinin (5 µg/mL), leupeptin (5 µg/mL), pepstatin (5 µg/mL), and PMSF (75 µg/mL). The pellet was resuspended in 1 mL of cold cytoplasmic lysis buffer (10 mM HEPES, 60 mM KCl, 1 mM EDTA, 0.075% (v/v) NP40, 1 mM DTT, 1 mM PMSF and protease inhibitors, the final pH was adjusted to 7.6) and homogenized with a loose pestle in a 7 mL glass Dounce homogenizer (Wheaton, Millville, NJ) until uniform. The resulting lysate was centrifuged at 95 x g at 4°C for 3 minutes to pellet nuclei. The cytoplasmic supernatant was

removed, and the nuclear pellet resuspended in SDS lysis buffer (1% SDS, 10 mM EDTA, 50 mM Tris, pH 8.1, and protease inhibitors) and incubated on ice for a minimum of 30 minutes. The lysate was further homogenized using the tight pestle of the Dounce homogenizer and placed in a 1.5 mL centrifuge tube.

4.2.2 « Preparation of Chromatin for IP »

Sodium sarcosine was added to increase sonication efficiency (Acosta-Alvear et al., 2007) and was added to a final concentration of 0.5% (w/v) and the lysate split into 250 µL fractions. Suboptimal volumes for sonication can result in excessive sample frothing, which decreases sonication efficiency, or sample loss. To shear DNA into 200-600 base pair fragments, samples were sonicated on ice once at level 4 for 20 seconds and four times at level 4 for 10 seconds using the Sonic Dismembrator 100. Efficient sonication parameters must be empirically determined for individual sonic dismembrators. Our sonicator has a metal probe with a 3 mm tip and is optimal for shearing small volumes (0.1 to 50 mL). Between sonication, samples were left to incubate on ice. The resulting lysates were centrifuged at 4°C at 14,000 rpm for 10 minutes to remove debris. Sheared DNA samples should be stored at -80°C until use.

It is best to assess shearing efficiency prior to immunoprecipitation. To do so, 20 µl of the sonicated chromatin was combined with 6 µl of 5 M NaCl and incubated overnight at 65^{o}C, to reverse the cross-linking. 1 µl of proteinase K (5 mg/ml) was added to the reaction and incubated at 45^{o}C for 1-2 hours. Following phenol chloroform extraction and ethanol precipitation, the DNA was resuspended in 20

Figure 4.1. Chromatin Shearing Efficiency. Efficient shearing of chromatin from whole pancreatic tissue following cerulein (C) or saline (S) injection. Chromatin was sheared, crosslinks reversed and DNA resolved on a 1.5% agarose gel. Proper shearing was indicated by a smear with highest intensity in the region of 200-600 bp.

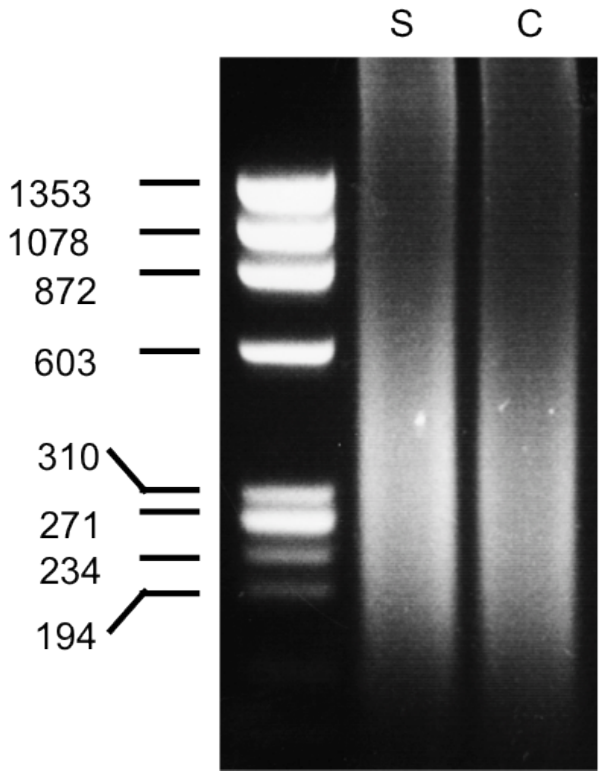

Figure 4.1. Chromatin Shearing Efficiency.

µl H_2O and 1 µl of RNase A (1 mg/ml). Following resolution on a 1.5% agarose gel, a DNA smear running from 200-600 bp was observed representing chromatin fragments (**Figure 4.1**).

4.3 « Chromatin Immunoprecipitation (ChIP) »

Each ChIP reaction requires approximately 50 µg of chromatin, but can be varied based on target protein abundance. The appropriate amount of chromatin was combined with dilution buffer (20 mM Tris pH8.1, 1% Triton X-100, 1 mM EDTA, 167 mM NaCl, protease inhibitors) to dilute chromatin 6-fold. The diluted chromatin was pre-cleared by incubating with protein A agarose (Millipore, Billerica, MA) for 1.5 hours at 4°C with rotating. Beads were pelleted at 95 x g at 4°C and the supernatant placed in a clean tube. At this point, 12% of total chromatin used per IP was set aside as an input control. Input samples are not required for each individual IP (per antibody) but are required per biological treatment or genotype (i.e. saline vs. cerulein). One to 5 µg of antibody was added and IP reactions incubated overnight at 4°C with rotating. As a negative control, an IP reaction using either similar IgG or an irrelevant antibody was used. Inclusion of a positive ChIP control is beneficial in preliminary experiments to determine if the protocol is working. The amount of antibody required for each IP varies depending on antibody quality and specificity. We have successfully used rabbit anti ATF3 (Santa Cruz Biotechnology, Santa Cruz, CA) and rabbit anti-spliced XBP1 (Biolegend, San Diego, CA) for ChIP from whole tissue. Rabbit anti-AcH3 (Millipore, Billerica, MA) has been used as a positive ChIP

control and Normal rabbit IgG (Millipore) as a negative control in both preparations (Figure 4.2). After antibody incubation, protein A agarose beads were added and the reaction incubated for another two hours at 4°C while rotating to capture antibody:protein complexes. Reactions were centrifuged at 95 x g at 4°C for 3 minutes to pellet beads and the supernatant was removed using thin bore pipet tips. Beads were run through successive washes for 10 minute intervals at 4°C with rotating, using the following buffers containing protease inhibitors: a low salt wash (20 mM Tris pH 8.1, 0.1% SDS, 1% Triton X-100, 2 mM EDTA, 150 mM NaCl), a high salt wash (20 mM Tris pH 8.1, 0.1% SDS, 1% Triton X-100, 2 mM EDTA, 500 mM NaCl), a LiCl wash (10 mM Tris pH 8.1, 0.25M LiCl, 1% NP40, 1% Na deoxycholate, 1 mM EDTA), and, finally, two washes in Tris-EDTA (TE). The resulting beads were incubated in 75 µl of elution buffer (1% SDS, 100 mM $NaHCO_3$) with rotating at room temperature for 15 minutes. Beads were pelleted and the eluent transferred to a new tube before repeating the elution procedure. The two eluents were pooled together and prepared for reversal of crosslinks. To the corresponding input samples, 150 µl of elution buffer was added and reversal of crosslinks carried out by adding 6 µl of 5 M NaCl at 65^{o}C for 4 hours to overnight. 1 µl RNase was added to the reaction at 37^{o}C for 30 minutes, and the mix was incubated with 3 µl of 0.5 M EDTA, 6 µl of 1 M Tris-HCl (pH 6.5), and 1 µl of Proteinase K (5 mg/ml) at 45^{o}C for 1-2 hours.

Figure 4.2. PCR of ChIP Results. Antibodies against acetylated histone 3 (AcH3) or rabbit IgG (negative control) were used to determine the fidelity of the ChIP protocol on whole tissue. PCR was performed using primers specific for the *Gapdh* promoter. S = saline, C = cerulein induced pancreatitis.

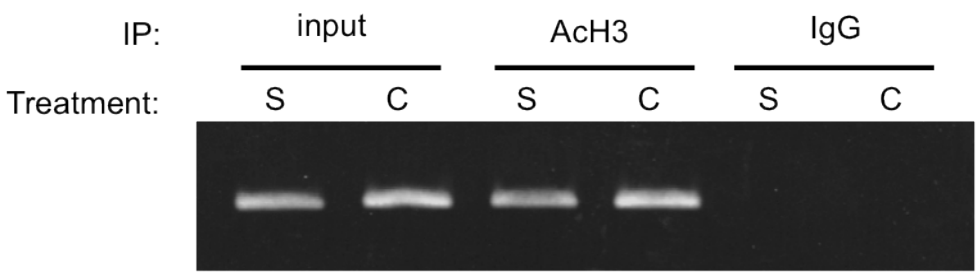

Figure 4.2. PCR of ChIP Results.

The DNA can be recovered by using either a PCR purification kit or by using phenol/chloroform extraction. We have successfully used Promega GenElute PCR purification columns (Fisher Scientific, Ottawa, ON) as per manufacturer specifications. After purification, chromatin was eluted to 80 µL for use in downstream applications. If the preferred method of DNA extraction is phenol/chloroform, precipitate using ethanol and 10 µl of glycogen (5 mg/ml). Glycogen is required as a carrier since there may be only a small amount of DNA recovered. Resuspend the DNA in 80 µl of H_2O.

The isolated DNA now can be used for ChIP-PCR or ChIP-qPCR. Depending on the recovery rate, the purified DNA is sufficient for library construction for Next generation sequencing and ChIP-on-chip or ChIP-seq. If not being immediately used, isolated DNA can be stored at -20°C.

4.4 « Analysis of DNA isolated from ChIP »

ChIP DNA was also assayed using the GoTaq PCR Mastermix system (Promega, Madison WI). Briefly, Glyceraldehyde 3-phosphate dehydrogenase (GAPDH) promoter primers (Fwd: 5' – CCCACACTTCTCCATTTCCC-3' and Rvs: 5'- CCTCTCTTTGGACCCGCC-3').were added to the GoTaq mastermix followed by addition of 2 µL of eluted DNA. Using similar cycling conditions as listed above, samples were evaluated using an ABI Prism 7900HT Sequence Detection System and corresponding SDS 2.2.1 software (Applied Biosystems,

Foster City, CA). Average Ct values for individual IPs and IgG controls are expressed as a percent of input (Mukhopadhyay et al., 2008). The formula for quantification was adapted (Kernohan et al., 2010; Mukhopadhyay et al., 2008) as percent input = $100*((2^{(\Delta Ct_{input}-\Delta Ct_{antibody})})/\text{input fraction})$, where input fraction represents the amount of chromatin taken for input as a proportion of chromatin used for an individual IP. For these experiments, the input fraction was 25, where the amount of input chromatin was $1/25^{th}$ of that used for an IP.

Chapter 5

5 « Activating Transcription Factor 3 promotes the loss of the acinar cell phenotype by repressing *Mist1* gene expression »

While chapters 2 and 3 examined the role of the PERK signaling molecule STC2 in the pancreas, development of a protocol for ChIP from whole pancreatic tissue allowed for analysis of PERK pathway transcriptional regulation in the pancreas. The PERK pathway contains multiple transcription factors, including ATF4, ATF3 and CHOP. ATF3 is unique in that it is not expressed under normal physiologic conditions on the exocrine pancreas, but is upregulated during exocrine pancreas stresses, identifying it as a purely stress response gene in this tissue. This chapter investigates the transcriptional role of ATF3 in the exocrine pancreas during pancreatitis. This work is being prepared for a manuscript. E. Fazio performed all experiments except for the immunohistochemistry on human pancreatitis samples, which was performed by C. Johnson.

5.1 « Introduction»

Pancreatitis is an inflammatory disease of the exocrine pancreas with significant morbidity and mortality associated with chronic conditions. More than 50,000 Americans suffer from chronic pancreatitis (CP) each year, and

individuals with CP are 53-fold more likely to be diagnosed with pancreatic adenocarcinoma (PDAC) (Lowenfels et al., 1997). Recently, we have shown that loss of MIST1 expression is correlated with both CP and PDAC. MIST1 is a transcription factor required for complete acinar cell maturation (Pin et al., 2001) and an absence of MIST1 leads to increased acinar-duct-transdifferentiation, a process that may provide a link between CP and PDAC (Johnson et al., 2012). Therefore, it is critical to identify the factors that affect *MIST1* expression.

The unfolded protein response (UPR) is a series of molecular cascades associated with the endoplasmic reticulum (ER) activated by cell stress. The UPR is triggered when protein-folding load within the ER exceeds folding capacity, leading to accumulation of unfolded or misfolded proteins. Three distinct, yet complimentary pathways comprise the UPR, and are mediated by Protein kinase RNA (PKR)-like ER kinase (PERK); Activating Transcription Factor 6 (ATF6) and inositol-requiring protein-1 (IRE1).

Activation of PERK results in phosphorylation of elongation initiation factor 2α (eIF2α), leading to attenuation of translation for most proteins (Harding et al., 1999). When active, ATF6 translocates to the Golgi, where it is cleaved and subsequently shuttled to the nucleus where it activates genes associated with ER quality control (Haze et al., 1999; Yoshida et al., 2000). Active IRE1 targets the *X-box binding protein 1* (*Xbp1*) transcript, splicing out a 26 bp sequence that results in translation of an efficient transcriptional activator, spliced XBP1 (XBP1s) (Yoshida et al., 2001), that targets genes responsible for protein folding

and degradation. The combined effects of UPR signaling reduce protein load in the cell.

Abnormal activation of the UPR has been linked to a number of pathologies including Alzheimer's disease, Parkinson's disease, and various cancers (Bellucci et al., 2011; Hoozemans et al., 2007; Katayama et al., 1999; Kudo et al., 2002; Mahadevan and Zanetti, 2011; Sato et al., 2010; Sato et al., 2000). In the pancreas, the UPR has important roles in normal physiology and pathology, and is necessary for β-cell (Harding et al., 2001; Zhang et al., 2006), and acinar cell (Harding et al., 2001; Lee et al., 2005) function. Exocrine specific ablation of *Perk* results in tissue atrophy due to oncosis (Iida et al., 2007), while targeted deletion of *Xbp1* leads to loss of acinar cells (Lee et al., 2005). Under conditions that induce exocrine pancreatic injury, the UPR activity is markedly enhanced (Kowalik et al., 2007; Kubisch et al., 2006). Similarly, chronic exposure to factors that increase susceptibility to pancreatitis, such as alcohol and high fat (Alahari et al., 2011; Lugea et al., 2011), leads to increased activity of the UPR. However, it is unclear what molecular role the UPR has in the context of pancreatitis.

Effects of the UPR are mediated by a number of transcription factors including ATF6, ATF4, ATF3, and XBP1s. Molecular analysis of the pancreas during cerulein-induced pancreatitis (CIP) revealed increased expression of genes involved in pancreatic development (Jensen et al., 2005), suggesting a loss of acinar cell differentiation characteristics. Previous studies have shown that XBP1s can regulate differentiation in both gastric zymogenic cells (Huh et

al., 2010) and cultured myoblasts (Acosta-Alvear et al., 2007), identifying a role for the UPR in cell differentiation. However, XBP1s is expressed in mature acinar cells under normal physiological conditions, indicating it has roles outside of response to cell injury.

An alternative stress response candidate is ATF3, a member of the ATF/CREB family of basic leucine zipper (bZIP) transcription factors, which binds to the unfolded protein response element (UPRE; (Deutsch et al., 1988)). While many members of the ATF/CRE family are transcriptional activators, ATF3 functions mainly as a repressor (Chen et al., 1994) and is expressed to negligible levels in mature acinar cells (Fazio et al., 2011). Following multiple forms of pancreatic injury, including partial pancreatectomy, taurocholate induced pancreatitis, and CIP, ATF3 is rapidly and specifically upregulated in acinar cells (Allen-Jennings et al., 2001; Ji et al., 2003; Kowalik et al., 2007; Kubisch et al., 2006).

The goal of this study was to determine the relationship between ATF3 and *Mist1* during pancreatic injury. Through chromatin immunoprecipitation (ChIP) and characterization of mice carrying a targeted ablation of *Atf3 (Atf3*$^{-/-}$*)*, we have uncovered a novel role for ATF3 in repressing *Mist1* leading to loss of acinar cell differentiation. ATF3 directly repressed *Mist1* by recruiting Histone Deacetylase (HDAC) 5 to the *Mist1* promoter. Importantly, increased ATF3 accumulation was observed in samples from CP patients suggesting similar events contribute to the disease in humans.

5.2 « Methodology»

5.2.1 « Mice and the induction of pancreatitis»

Wild type (WT) and *Atf3*$^{-/-}$ mice were maintained on a C57/Bl6 background. Mice carrying a targeted ablation of the *Atf3* gene (*Atf3*$^{-/-}$) have been described (Hartman et al., 2004). All experiments were approved by the Animal Care Committee at the University of Western Ontario (Protocol #116-2008) and mice handled according to regulations stipulated by the Canadian Council on Animal Care. To induce CIP, 2-4 month-old mice were given four hourly intraperitoneal injections of cerulein (50 µg/kg body weight; Sigma-Aldrich). As a control, mice were injected with 0.9% saline. To induce CP, mice received eight cerulein injections over a seven-hour span and this was repeated five times over 12 days. Mice were sacrificed either four hours after the initial cerulein injection, one hour after the final injection in the CP regime, or 3, 7 or 28 days following the last set of cerulein injections. Pancreatic tissue was processed for RNA, protein, tissue histology and chromatin from acute pancreatitis experiments or for tissue histology from CP experiments.

5.2.2 « Tissue preparation and histology»

Pancreatic tissue was directly embedded in OCT. Immunofluorescent (IF) analysis was performed on fresh frozen sections as described (Fazio and Pin, 2007). Following primary antibody incubation, sections were incubated for one

hour in anti-rabbit FITC or anti-mouse TRITC secondary antibodies (1:250; Sigma-Aldrich). Sections were washed, stained with DAPI (1:1000) and mounted with Vectashield (Vector Laboratories, Burlingame CA, USA). Staining was visualized with a Leica DMIOS upright microscope and images captured using OpenLab 4.0.3 Software (PerkinElmer, Waltham, MA, USA). Human tissue was obtained following guidelines established by the University of Western Ontario and the Lawson Health Research Institute, and processed as described in REB #17012. Paraffin sections were obtained from patients diagnosed with CP or a non-related disease and immunohistochemistry (IHC) performed as described (Alahari et al., 2011). An antibody specific for ATF3 was used (1:100; Santa Cruz Biotechnology, Santa Cruz, CA, USA).

5.2.3 « RNA isolation, Northern blotting and Real-Time RT-PCR»

RNA was isolated from the pancreas and processed using TRIzol (Invitrogen, Burlington, ON, Canada) as described (Kowalik et al., 2007). For RT-PCR, two µg of RNA was reverse transcribed using Improm-II reverse transcriptase and random primers (Promega, Madison WI). qRT-PCR for *Mist1*, *Atf3 and 18S* was performed using the GoTaq PCR Mastermix system (Promega). Reactions were performed using the BioRad CFX96 Touch Real-time PCR Detection System (BioRad Laboratories, Mississauga, ON, Canada) and data analyzed using CFX Manager (BioRad Laboratories, Mississauga, ON, Canada).

5.2.4 « Protein isolation and immunoblot analysis»

Protein extraction, electrophoresis and immunoblotting were carried out as previously described (Johnson et al., 2004). For immunoblot analysis, 40 to 60 µg of pancreatic protein was resolved by SDS/PAGE and transferred to PVDF membrane (Biorad, Mississauga, ON, Canada). Blots were probed with antibodies specific for MIST1 (ProSci Inc, Poway, CA, USA), ATF3 (Santa Cruz Biotechnology, Santa Cruz, CA, USA), and HES1 (Millipore, Billerica, MA, USA) followed by incubation with anti-rabbit or anti-mouse HRP-conjugated secondary antibodies (1:10,000 or 1:2000, Jackson Labs, Bar Harbor, ME, USA). Blots were processed with Western Lightning chemiluminescence substrate (Perkin Elmer, Waltham MA, USA), and visualized using the VersaDoc Imager and Quantity One Software (BioRad, Mississauga, ON, Canada).

5.2.5 « Chromatin Immunoprecipitation»

Pancreatic tissue was dissected from CIP or saline-treated WT and *Atf3*$^{-/-}$ mice, chromatin isolated, and chromatin immunoprecipitation (ChIP) was performed as described in Chapter 4. Following chromatin isolation, antibodies specific for ATF3 (Santa Cruz Biotechnology, Santa Cruz CA, USA), HDAC1 (Active Motif, Carlsbad, CA, USA) and HDAC5 (Active Motif, Carlsbad, CA, USA), or rabbit IgG (Millipore, Billerica, MA, USA) as a control, were used to IP protein/DNA complexes. DNA was recovered using Promega GenElute PCR purification

columns (Fisher Scientific, Ottawa, ON, Canada) as per manufacturer specifications. After purification, chromatin was used for PCR and qPCR.

5.2.6 « Statistical Analyses»

All statistical analyses were performed using Graphpad Prism 4.02 (Graphpad Software, San Diego CA, USA). Analysis of *Mist1* and *Atf3* expression in WT pancreatic tissue following CIP was performed using an unpaired t-test. Comparisons of apoptosis, ChIP occupancy and *Mist1* and *Atf3* expression between CIP or saline-treated WT and *Atf3*$^{-/-}$ mice was performed using a two-way ANOVA with a Bonferroni post-hoc test.

5.3 « Results»

5.3.1 « Acinar Cell Differentiation During Pancreatitis»

To determine the effects on cerulein-induced pancreatitis (CIP) on the maturation state of acinar cells, cell junctions were assessed by IF analysis (Figure 5.1). Within four hours of initial cerulein injections, Zona occludens 1 (ZO1), a component of tight junctions, was completely lost from the apical borders of acinar cells (Figure 5.1A,B). Disruptions in β-catenin (adherens junctions) and connexin 32 (Cx32; gap junctions) accumulation were also observed (Figure 5.1C,D and E,F respectively). Disruptions of cell junctions

suggested effects on polarity (Adamo et al., 2001). Therefore, the localization of atypical protein kinase C ζ (PKCζ), which interacts with partitioning proteins (PAR) 3 and 6 to establish cell polarity (Izumi et al., 1998), was assessed. Similar to β-catenin, PKCζ localization was disrupted within four hours of initiating CIP. The normal apical localization of PKCζ was replaced by diffuse basal localization indicative of aberrant cell polarity (Figure 5.1G,H). Western blots of whole pancreatic extracts (Figure 5.2) confirmed decreased expression of Cx32 and β-catenin, and not simply a redistribution of protein within the cell.

The loss of cell polarity, on its own, does not indicate a loss of acinar cell differentiation. Therefore, the expression of transcription factors that affect acinar cell differentiation was examined. Hairy and Enhancer of Split (HES) 1 is part of the Notch signaling pathway that defines exocrine precursor cells, and HES1 re-expression in acinar cell explants induces dedifferentiation (Miyamoto et al., 2003). Western blot analysis of whole pancreatic protein revealed increased HES1 expression one and four hours into CIP relative to saline controls (Figure 5.2A) indicating acinar cells reactivated developmental genes during pancreatitis. Conversely, the expression of MIST1 was dramatically reduced in acinar cells concomitantly. IF confirmed a loss of nuclear MIST1 accumulation 4 hours into CIP (Figure 5.2B,C). The decreased expression of MIST1 was due to reduced transcription as qRT-PCR verified a 75% decrease in *Mist1* mRNA levels (Figure

Figure 5.1. Acinar Cell Differentiation Characterisitcs are Disrupted During CIP. IF for zona occludens (A, B; ZO1), β-catenin (C, D), Connexin32 (E, F; Cx32) or PKCζ (G, H) in saline (SAL) or cerulein (CIP) treated pancreatic tissue. Individual acini are outlined and the apical lumen indicated with *. Punctate staining representing Cx32 is indicated with an arrow. Nuclei are identified with DAPI counterstain. Magnification bar = 14 μm.

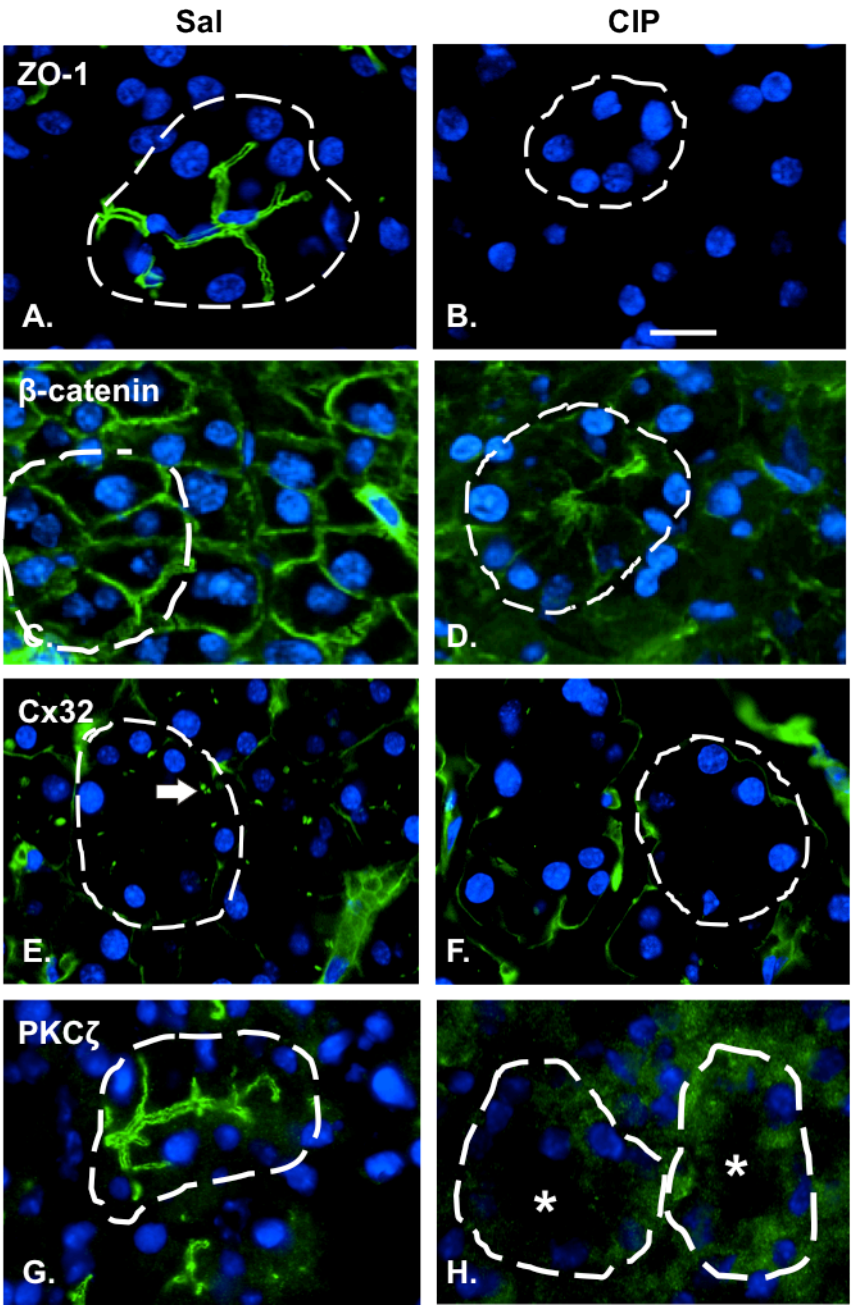

Figure 5.1. Acinar Cell Differentiation Characteristics are Disrupted During CIP.

Figure 5.2. Cell Differentiation is Lost During Pancreatitis. (A) Western blot analysis for β-catenin, Cx32, HES1 and MIST1 one, four and eight hours after initial saline (SAL) or cerulein (CIP) injection. GLUT2 was used as a loading control. IF for MIST1 four hours into saline (B) or cerulein (C) treatment. * indicates an islet. Magnification bar = 35 μm. (D) qRT-PCR for *Mist1* four hours into saline or cerulein treatment. *Mist1* RNA levels were normalized to β-actin. Error bars indicate mean±standard error. * $p<0.05$; n=3.

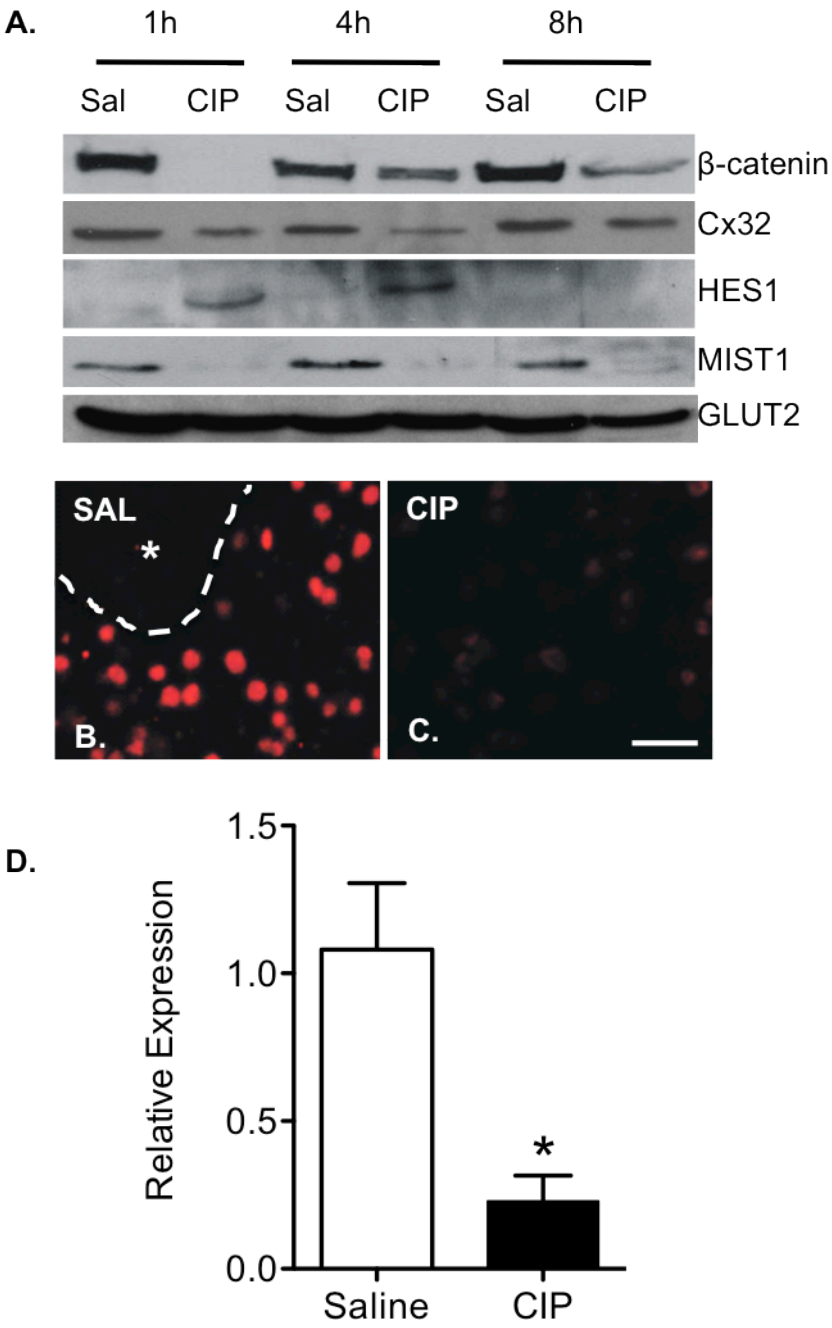

Figure 5.2. Cell Differentiation is Lost During Pancreatitis.

5.2D). These results support a model in which acinar cell differentiation characteristics are repressed early in CIP. However, the actual mechanism of how this occurs is unknown.

5.3.2 « Activation of UPR Transcription Factors During CIP»

We next examined the accumulation of transcriptional regulators involved in the UPR. Western blot and IF confirmed increased accumulation of XBP1s, a known transcriptional activator of *Mist1*, one to eight hours into CIP (Figure 5.3A-E). In addition, analysis of ATF3, a known transcriptional repressors in the UPR, revealed a dramatic increase 4 hours into CIP at both protein (Figure 5.3A) and mRNA levels (Figure 5.3F) relative to saline conditions where ATF3 was not detected. Since many pathways are activated during CIP, to determine the effect of UPR activation alone in MIST1 expression, mice were treated with the direct UPR inducer, tunicamycin (Zinszner et al., 1998). Activation of the UPR alone resulted in decreased MIST1 expression (Figure 5.4), specifying a role for the UPR in MIST1 regulation during CIP.

Figure 5.3. UPR Transcription Factors are Upregulated During CIP. (A) Representative western blots for XBP1 and ATF3 pancreatic protein extracts one, four and eight hours after induction of pancreatitis. Total (t) eIF2α was used as a loading control. Immunofluorescence reveals that nuclear expression of XBP1 is increased as early as 1h into CIP (C) and persists at up to 8h after CIP (D, E**).** Magnification bar = 30 μM. (F) QRT-PCR analysis for *Atf3* mRNA normalized to β-actin four hours after initial saline or cerulein (black bar) injection. n = 3; * $p < 0.001$. Bars represent mean ± standard error.

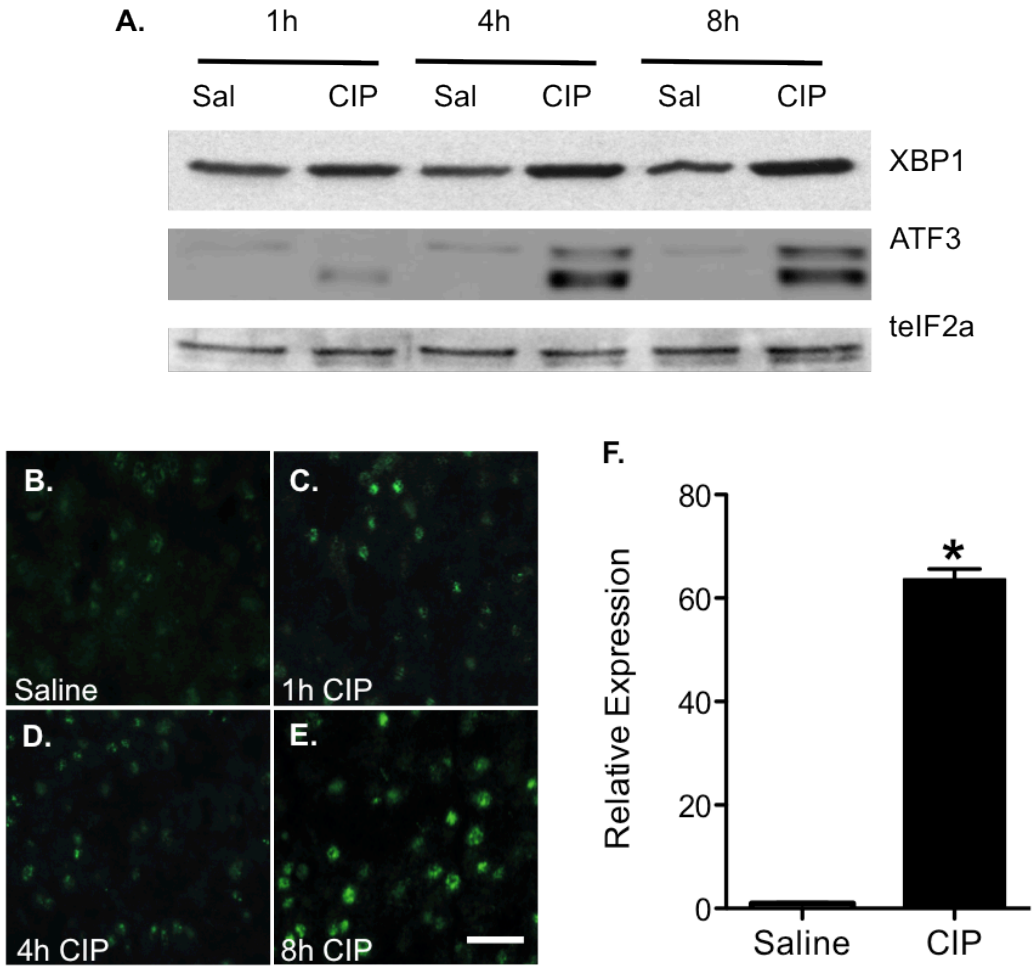

Figure 5.3. UPR Transcription Factors are Upregulated During CIP.

Figure 5.4. Direct Activation of the UPR Results in Decreased MIST1 Expression. Mice were sacrificed 8 hours after a single injection of tunicamycin or a dextrose control. Phosphorylation of PERK (p-PERK) and expression of XBP1 were both increased after tunicamycin treatment, indicative of activation of the UPR. Expression of MIST1 was decreased after injection of tunicamycin, indicating that the UPR is sufficient for decreased MIST1 expression. Amylase was used as a loading control.

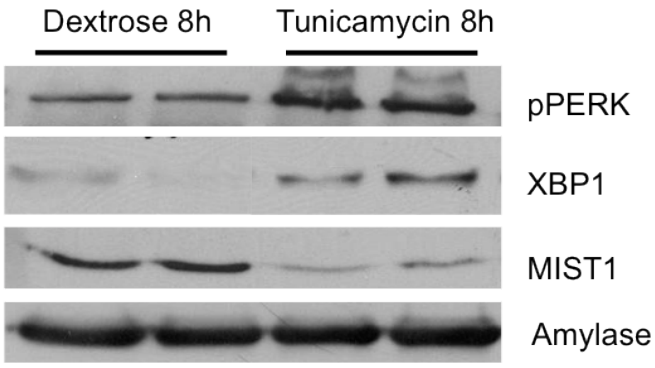

Figure 5.4. Direct Activation of the UPR Results in Decreased MIST1 Expression.

5.3.3 « ATF3 Expression During Chronic Pancreatitis»

Recently, we identified a loss of MIST1 accumulation in acinar cells of CP patients (Johnson et al., 2012). To determine if the relationship between MIST1 and ATF3 extended to CP, we first examined expression of these factors in a mouse model of CP that involves repeated induction of acute CIP, by extending cerulein injections over a period of two weeks. IF confirmed an inverse correlation between ATF3 and MIST1 accumulation. By Day 28 after the final cerulein injection, ATF3 was limited to focal pockets within the acinar tissue. Interestingly, these same regions showed limited MIST1 accumulation (Figure 5.5). We next examined tissue samples from patients diagnosed with CP. IHC for ATF3 revealed limited staining above background in non-pancreatitis samples (Figure 5.6A-C) while CP samples showed extensive nuclear ATF3 localization in acinar cells (Figure 5.6D-F). Taken together, these findings suggest ATF3 promotes loss of MIST1 expression and acinar cell differentiation during pancreatitis.

5.3.4 « ATF3 Represses Mist1 Expression During CIP»

To determine if the *Mist1* gene was a direct transcriptional target of ATF3 repression, ChIP-qPCR was performed to assess ATF3 occupancy of the *Mist1* promoter during CIP. Analysis of multiple regions upstream of the *Mist1* transcriptional start site (TSS; Figure 5.7A) revealed no ATF3 enrichment along the *Mist1* promoter under saline control conditions (Figure 5.7B,C), including

regions as far as 5 kb upstream of the TSS. Within four hours of inducing pancreatitis, peak enrichment for ATF3 was observed in a region spanning -2593 to -2424 relative to the *Mist1* TSS (Figure 5.7B,C). Interestingly, XBP1s also appeared to associate with this same region of the *Mist1* gene only after CIP (Appendix Figure A2). Examination of the 5 kb genomic region upstream of the *Mist1* promoter with PATCH (Pattern Search for Transcription Factor Binding Sites; www.biobase.com) identified three putative ATF/CRE consensus sites, two of which are on the reverse strand, at -2541 (TTACGTCA) and -2428 (TTGCGTCA) relative to the *Mist1* TSS (Figure 5.8). Both sites were contained within the region identified as enriched for ATF3 by ChIP analysis. Sequence alignment with ClustalW2 (www.ebi.ac.uk/Tools/msa/clustalw2/) determined that the ATF/CRE sites are conserved between *mus musculus*, *canis lupus familiaris* and *homo sapiens* sequences. The ATF/CRE site located at -2541 exhibited 50% sequence homology between the three species, whereas the ATF/CRE site at -2428 exhibited 62.5% sequence homology.

Next, the requirement of ATF3 for repression of *Mist1* expression during CIP was examined in *Atf3*$^{-/-}$ mice. *Atf3*$^{-/-}$ mice express MIST1 within the pancreas to comparable levels relative to genetically-matched WT tissue. Four hours into the induction of pancreatitis, IF revealed maintenance of MIST1 nuclear accumulation in *Atf3*$^{-/-}$ pancreata that is not observed in WT tissue (Figure 5.9A-

Figure 5.5. ATF3 is Localized to Areas Where MIST1 is not Expressed During Recovery from CP. Serial sections of pancreatic tissue from mice with chronic pancreatitis were examined for MIST1 (A,B) and ATF3 (C,D) expression. By day 28, ATF3 expression was limited to focal pockets (C) that do not express MIST1 (A). B and D are magnified regions of boxed areas in A and B. Magnification bar = 70 μM (A,B); 35 μM (C,D).

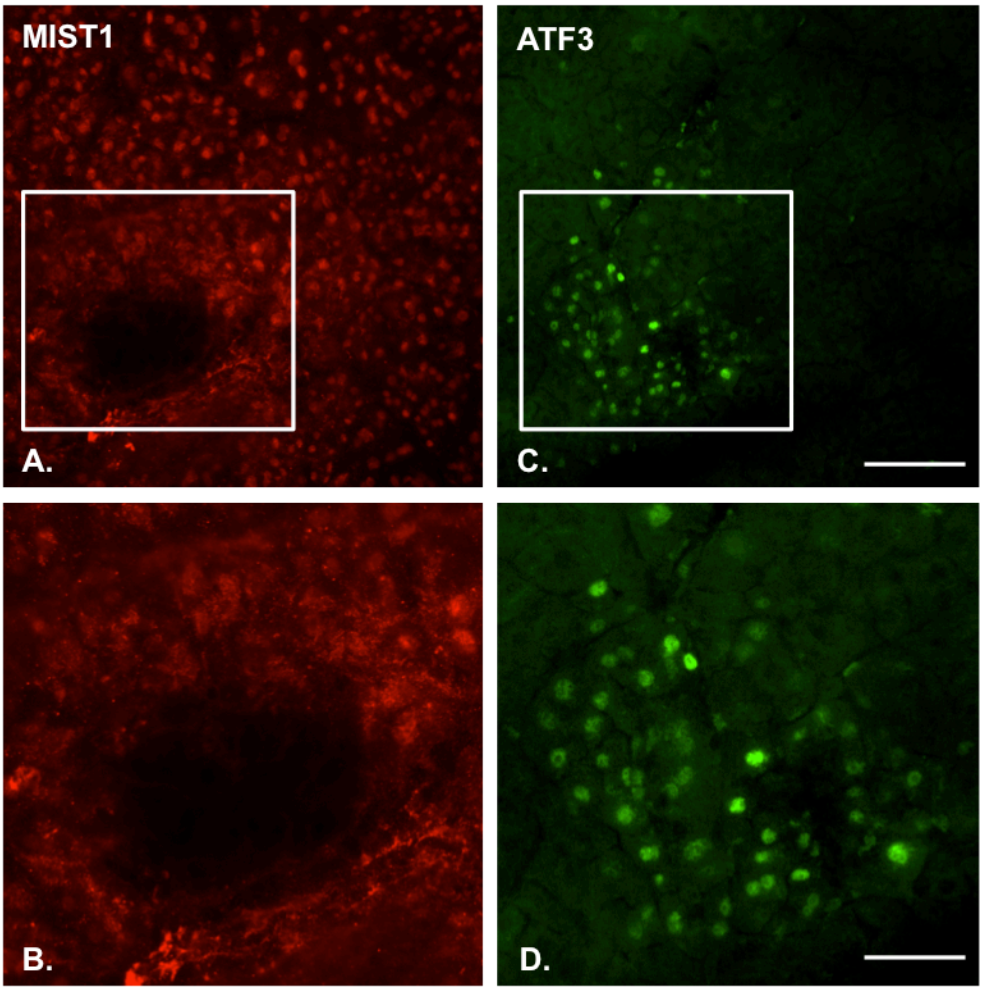

Figure 5.5. ATF3 is Localized tp Areas Where MIST1 is not Expressed During Recovery From CP.

Figure 5.6. ATF3 is Expressed in the Pancreatic Tissue of Chronic Pancreatitis Patients. Immunohistochemical analysis for ATF3 in pancreatic tissue from (A-C) patients with no pancreatic disease or (D-F) patients suffering from chronic pancreatitis. Boxed areas are magnified to illustrate individual acini, where there is no nuclear expression of ATF3 observed (dotted line outlines an acinus). Note that pancreatic tissue from chronic pancreatitis patients reveals much less acinar tissue. Magnification: A,D = 27 μm, B,C,E,F = 18 μm.

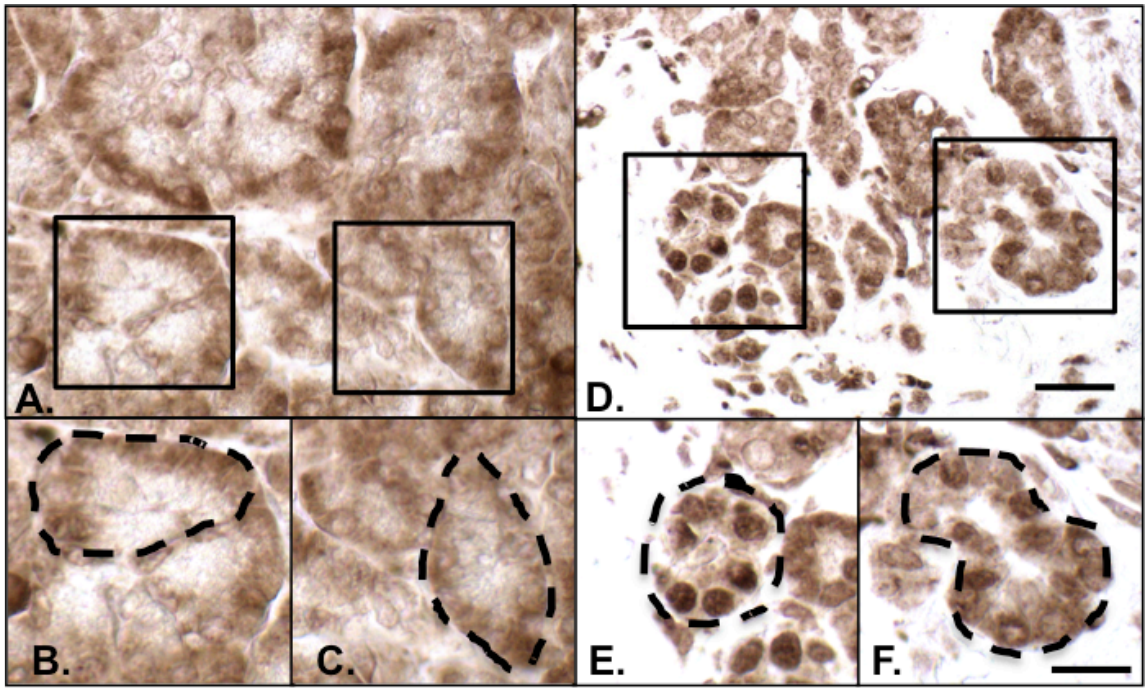

Figure 5.6. ATF3 is Expressed in the Pancreatic Tissue of Chronic Pancreatitis Patients.

Figure 5.7. ATF3 Occupies the *Mist1* Promoter During CIP. (A) Schematic representation of the *Mist1* gene denoting the transcription start site (TSS) and consensus ATF/CRE binding sites (filled ovals). Scale bar = 1 kB. (**C)** ChIP-PCR or **(D)** ChIP-qPCR analysis of ATF3 occupancy for areas designated in A along the *Mist1* promoter 4 hours after initial saline or cerulein (CIP) injections. White bars represent ATF3 ChIP and black bars represent ChIP with a normal rabbit IgG as a negative control. N = 3; * $p < 0.001$). For qRT-PCR, *Mist1* mRNA expression was normalized to β-actin. N = 3; *$p < 0.001$).

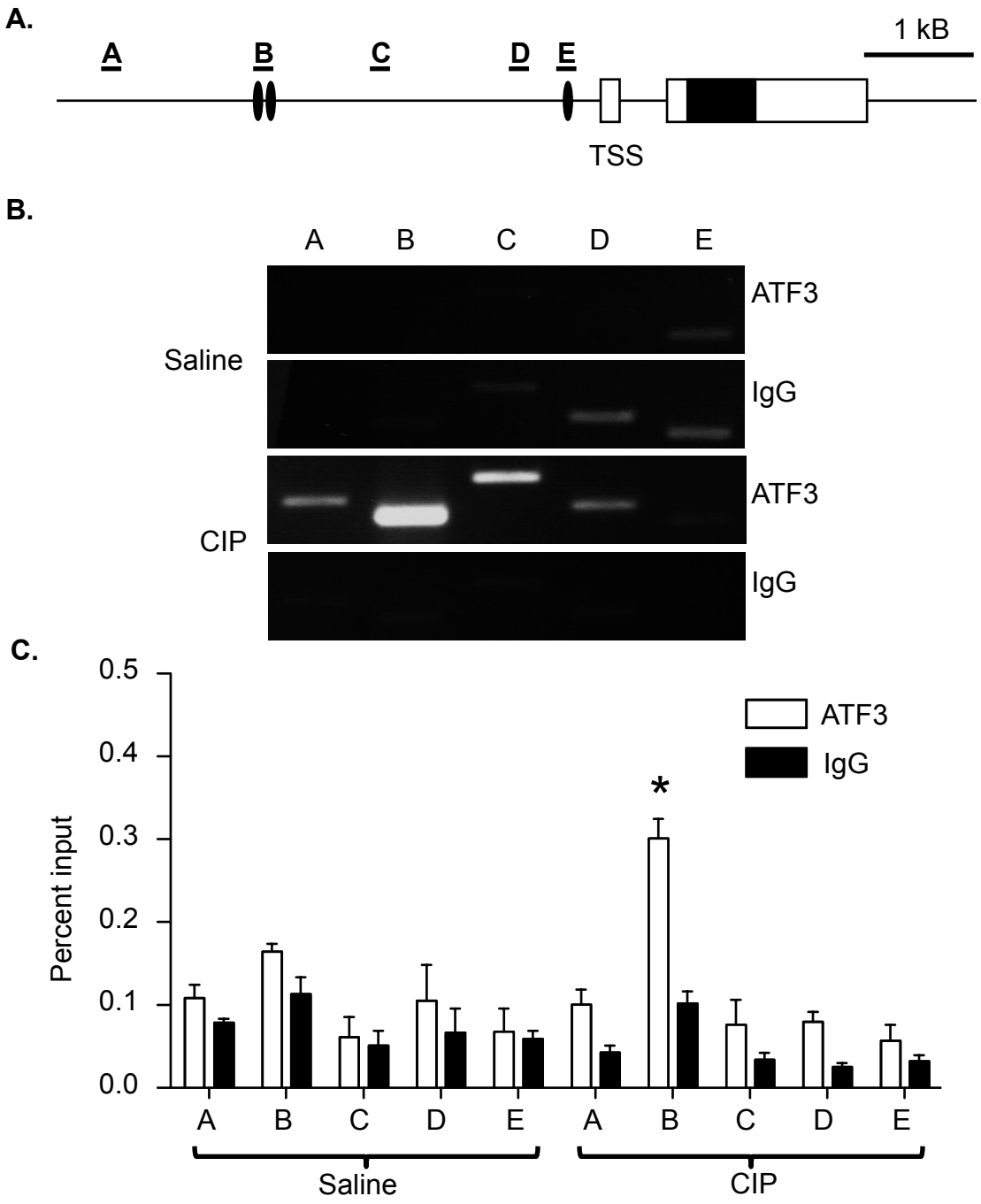

Figure 5.7. ATF3 Occupies the *Mist1* Promoter During CIP.

Figure 5.8. Sequence Alignment of the *Mist1* Promoter Region. Sequence analysis of the region spanned by primer set B (-2533 to -2317)**.** Alignment was carried out between *mus musculus*, *canus lupus familiaris* and *homo sapiens* sequences. Areas outlined in red are ATF/CRE binding sites.

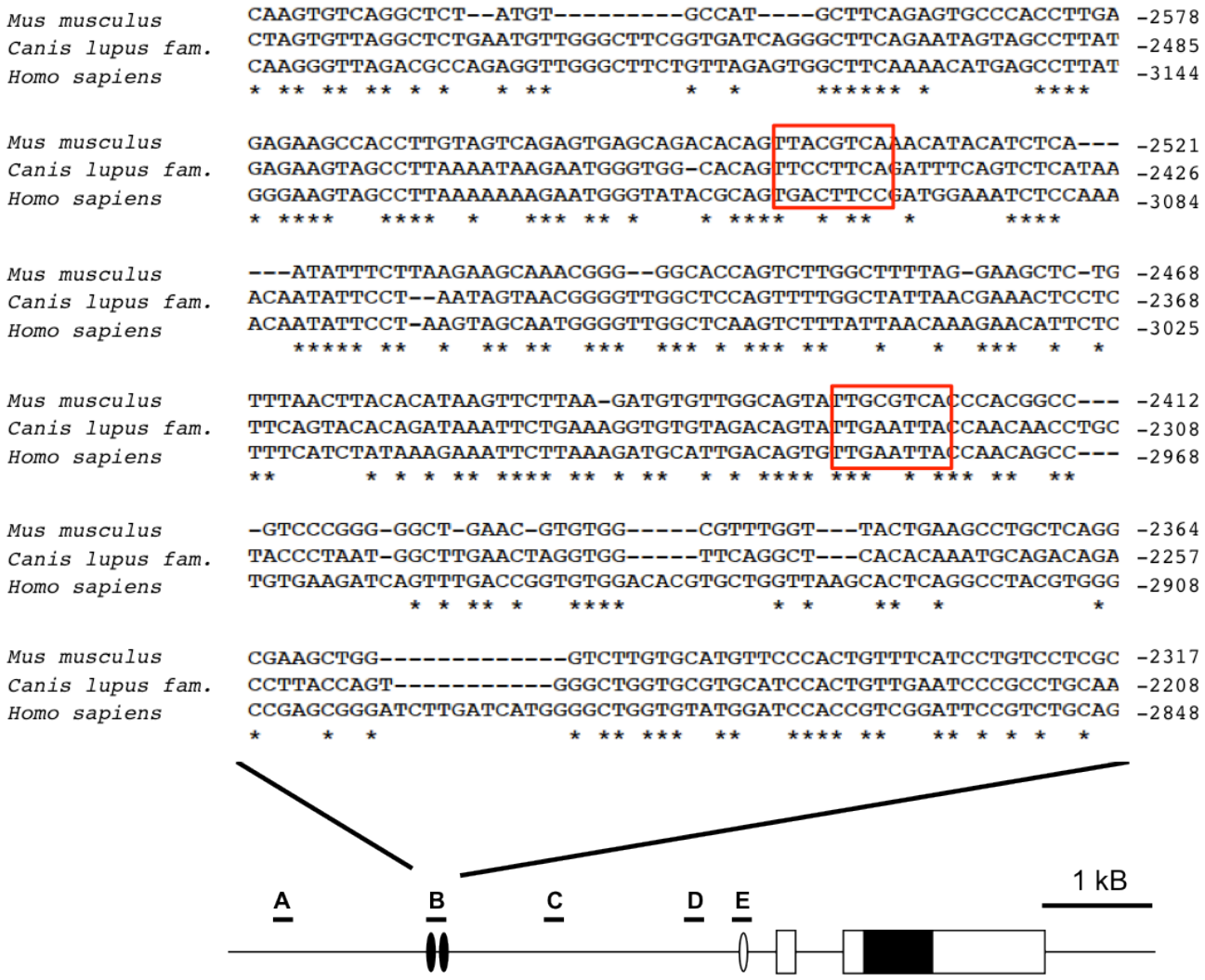

Figure 5.8. Sequence Alignment of the *Mist1* Promoter Region.

Figure 5.9. *Mist1* Expression is Maintained in *Atf3*$^{-/-}$ Mice During CIP. IF for MIST1 in WT (A,B) and *Atf3*$^{-/-}$ (C,D) pancreatic tissue following four hours of cerulein or saline treatment. (E) Magnification bar = 26 μm. Sal = saline, CIP = cerulein induced pancreatitis**.** qRT-PCR for MIST1 in WT and *Atf3*$^{-/-}$ pancreatic tissue following four hours of cerulein or saline treatment. *Mist1* mRNA expression was normalized to β-actin. n = 3; *p < 0.001).

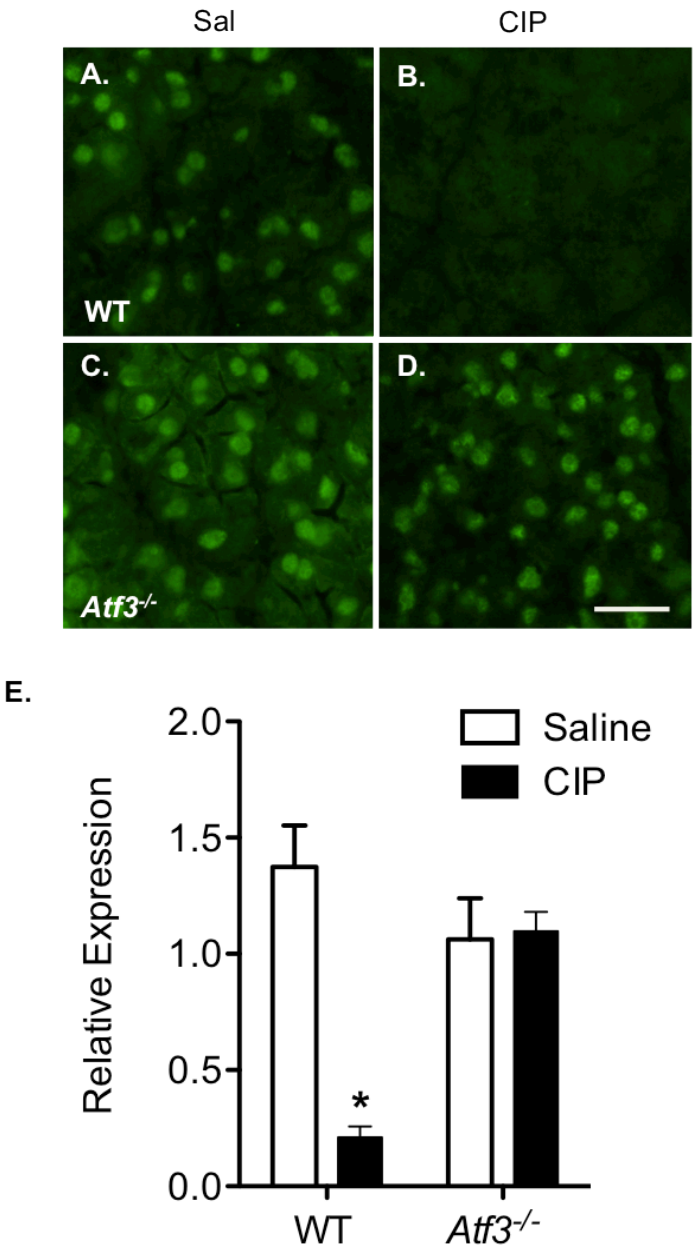

Figure 5.9. *Mist1* Expression is Maintained in *Atf3*$^{-/-}$ Mice During CIP.

D**).** QRT-PCR analysis showed that *Mist1* mRNA was not reduced in CIP-treated *Atf3*$^{-/-}$ pancreatic tissue indicating that ATF3 is required for repression.

To determine the mechanism by which ATF3 represses *Mist1* expression and whether the role of ATF3 was only to promote the loss of the acinar cell phenotype during pancreatitis. To do this, another target of ATF3 binding was identified. *Growth arrested and DNA damage inducible* (*Gadd*) *34* gene, which contains an ATF/CRE binding site in its promoter region (Ma and Hendershot, 2003), is upregulated during CIP (Kowalik et al., 2007) and activated by ATF3 over-expression independent of PERK activation (Jiang et al., 2004). ChIP-PCR and qPCR analysis spanning 5 kb upstream of the *Gadd34* TSS **(**Figure 5.11B,C**)** revealed no significant occupancy of ATF3 until initiation of CIP (Figure 5.11B,C). Significant enrichment of ATF3 was observed within 250 bp of the *Gadd34* TSS where the ATF/CRE consensus sequence is located (Figure 5.11B,C**)**. Interestingly, *Gadd34* expression was still increased in CIP-treated *Atf3*$^{-/-}$ pancreata indicating ATF3 is not required for *Gadd34* expression (Appendix Figure A3). However, this still provided an alternative target for ATF3 binding.

Figure 5.10. Differentiation Characteristics are Maintained in *Atf3*$^{-/-}$ Pancreatic Tissue During CIP. IF analysis for expression of PKCζ (A-D), β-catenin (E –H), zona occludens 1 (ZO-1; I-L) or connexin 32 (Cx32; M-P) **in** wild type (WT) and *Atf3*$^{-/-}$ animals treated with either saline (SAL) or cerulein (CIP) to induce pancreatitis for 4 hours. Magnification bar = 15 μM. Individual acini have been outlined.

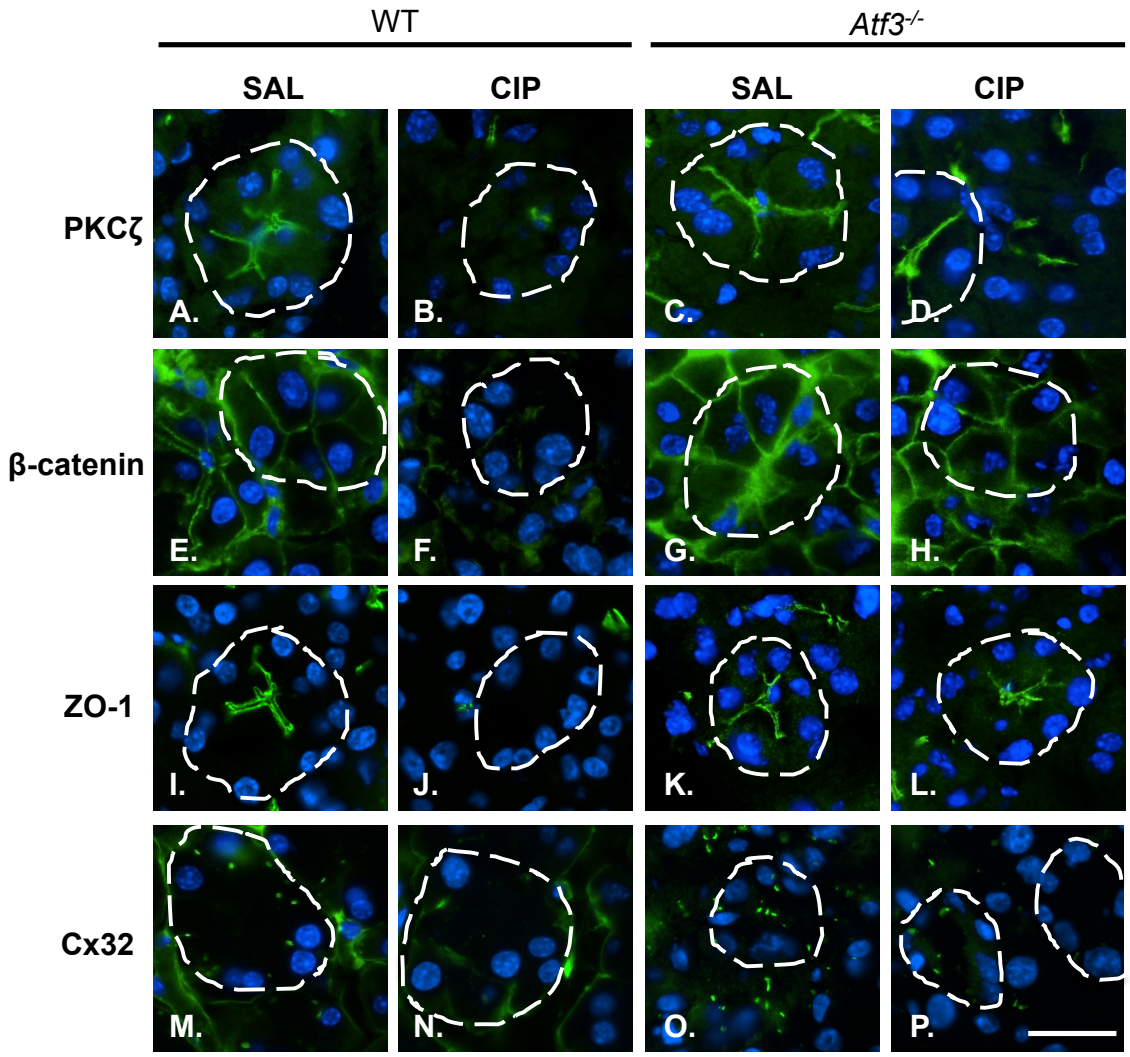

Figure 5.10. Differentiation Characteristics are Maintained in *Atf3*$^{-/-}$ Pancreatic Tissue During CIP.

Figure 5.11. ATF3 Binds the *Gadd34* Promoter During CIP. (A) Schematic of the mouse *Gadd34* gene with exons (boxes) and coding sequence (black box) indicated. A previously identified ATF binding site is located in primer set E (filled oval) transcriptional start site (TSS). Scale bar = 1kB. (B) ChIP-PCR or (C) ChIP-qPCR analysis of ATF3 occupancy at each region of the *Gadd34* promoter during control (saline) conditions or 4 hours into CIP. White bars represent ATF3 ChIP and black bars represent ChIP with a normal rabbit IgG negative control. N = 3; * $p < 0.001$.

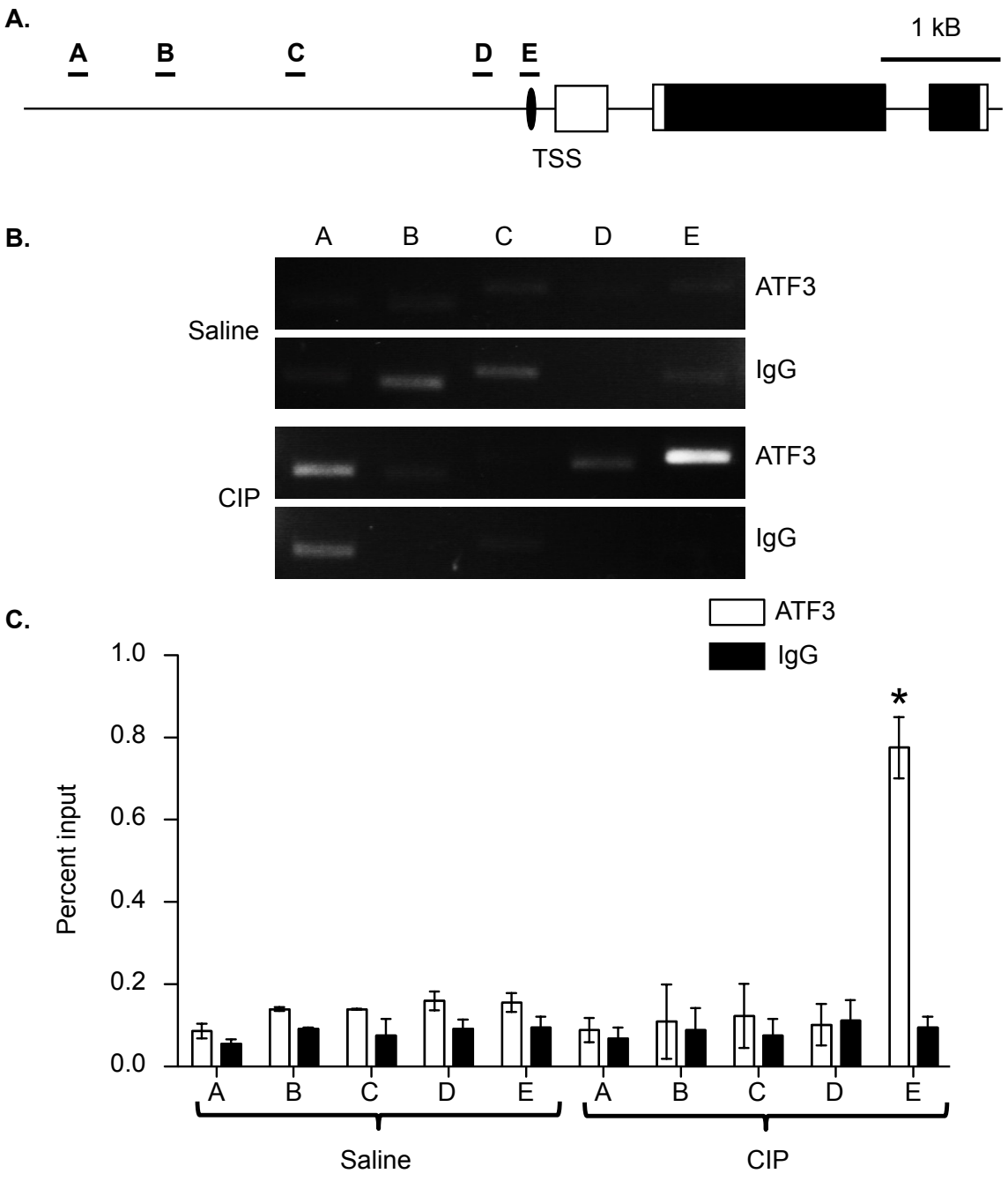

Figure 5.11. ATF3 binds the *Gadd34* Promoter During CIP.

5.3.5 « ATF3 Recruits HDAC5 during Repression of *Mist1*»

ATF3 can bind and recruit HDAC1 to gene promoters in the kidney (Li et al., 2010). Previous microarray analysis of pancreatic gene expression following saline or cerulein treatment suggested that HDACs 1, 3, 5, 6 and 7A were all expressed in pancreatic tissue (Kowalik et al., 2007), but only HDAC5 showed any increase in expression during CIP. ChIP-qPCR analysis revealed HDAC5 recruitment to the same region of the *Mist1* promoter enriched for ATF3 during CIP (Figure 5.12A,B). HDAC5 was not recruited to the ATF3-bound region of the *Gadd34* promoter during CIP (Figure 5.12C), illustrating a dual mechanism where ATF3 recruits HDAC5 during gene repression but not during gene activation. This recruitment was specific to HDAC5, as HDAC1 was not recruited to the *Mist1* promoter during CIP (Figure 5.12B). ChIP-PCR and ChIP-qPCR revealed no HDAC5 recruitment to the *Mist1* promoter following cerulein treatment in *Atf3*$^{-/-}$ pancreata (**Figure 5,12 A,B**) indicating that ATF3 is required for HDAC5 recruitment to the *Mist1* promoter.

5.4 « Discussion»

Defining the early molecular events that occur during pancreatic injury is important for understanding the mechanisms that dictate pancreatitis severity. This is particularly important as individuals hospitalized for pancreatitis have a 25% mortality rate and patients with CP are 53-fold more likely to develop pancreatic adenocarcinoma (PDAC). Previous work from a number of

Figure 5.12. ATF3 Recruits HDAC5 During Transcriptional Repression.

(A) qPCR analysis for HDAC occupancy at regions A, B and D of the *Mist1* promoter revealed significant occupancy of HDAC5 at region B of the *Mist1* promoter in pancreatic tissue during CIP (n = 3 (* $p < 0.01$). (B) ChIP-PCR analysis revealed HDAC occupancy at region B of the *Mist1* promoter only after CIP, and requires expression of ATF3 (*Atf3*$^{-/-}$ CIP; n = 3). HDAC1 is not recruited to region B of the *Mist1* promoter under any conditions. (C) ChIP-qPCR analysis revealed no occupancy of HDAC5 at region A of the *Gadd34* promoter (n = 3). IgG was used as a negative antibody control. Bars represent mean ± standard error.

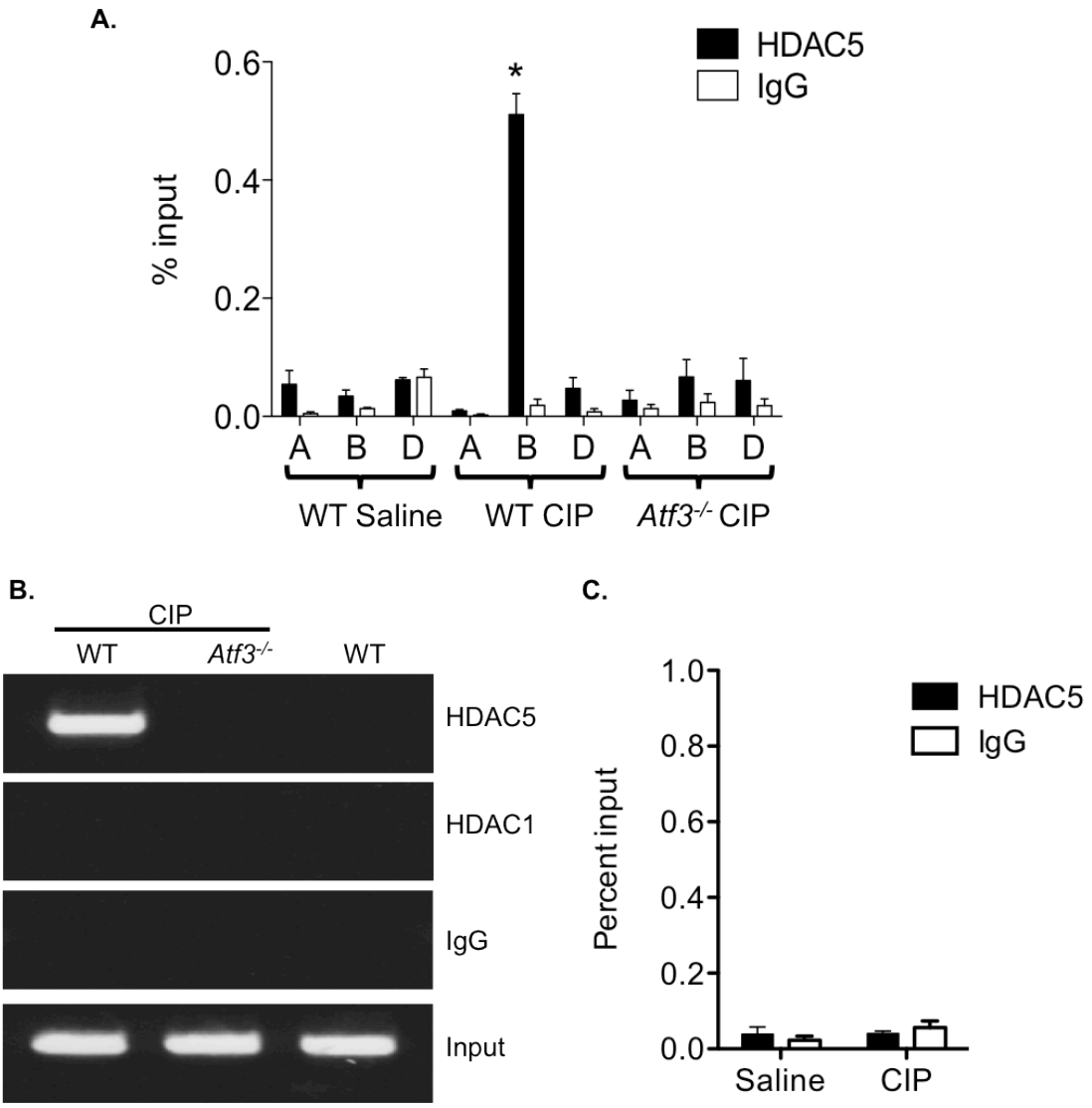

Figure 5.12. ATF3 Recruits HDAC5 During Transcriptional Repression.

laboratories have shown that the UPR is activated within hours of initiating injury, as well as by a number of conditions that predispose an individual for pancreatitis, most notably chronic ethanol consumption or a diet high in fat (Alahari et al., 2011; Kowalik et al., 2007; Kubisch et al., 2006; Lugea et al., 2011). However, the effects of the UPR on acinar cell biology and tissue damage in the context of injury have not been elucidated. In this study, we have identified a novel relationship between the UPR and *Mist1* that affects acinar cell differentiation. ATF3, a mediator of the UPR, recruits HDAC5 to the *Mist1* promoter leading to repression of transcription. MIST1 is required for complete acinar cell maturation and its expression is dramatically decreased in acinar tissue of patients with CP. Since ATF3 expression is enhanced in both animal models and patient samples for CP, the identification of ATF3 repression of *Mist1* provides important mechanistic insight into the initiating molecular events of exocrine pancreas injury, and into mechanisms by which MIST1 expression can be compromised.

While other studies have identified a role for ATF3 in promoting cell differentiation (Filen et al., 2010; James et al., 2006; Xu et al., 2011), this is the first study to link ATF3 to repression of cell differentiation status. Surprisingly, ATF3 targets the *Mist1* gene, which has been identified as a target of XBP1s. XBP1s binds to the *Mist1* promoter approximately 60 bp upstream of the TSS and activates expression in both myoblast (Acosta-Alvear et al., 2007) and gastric zymogenic cells (Huh et al., 2010). The XBP1s mediated activation of

Mist1 promotes differentiation in zymogenic cells, but promotes loss of the myogenic phenotype upon activation of the UPR. We have shown that, in the pancreas, XBP1s did not bind the *Mist1* promoter under physiologic conditions but was recruited upon CIP treatment. In fact, both ATF3 and XBP1s bind a region approximately 2.5 kb upstream of the *Mist1* TSS. Whether XBP1 is part of the repressive complex bound to this region of the *Mist1* promoter is unclear, but it suggests an interesting possibility in which XBP1s binding is altered along the same promoter to change its role from activating to repressive. It is likely that differences in the transcriptional network between myoblasts and acinar cells account for the unique outcomes. What is clear is that ATF3 is required for HDAC5 recruitment to the -2500 bp ATF/CREB site within the *Mist1* promoter and that repression overrides any inductive effects XBP1s would have.

The specificity of HDAC5 for ATF3-induced repression was supported by our findings that ATF3 was recruited to genes with increased expression during CIP, such as *Gadd34*. In this situation, HDAC5 was not recruited and gene transcription proceeded, indicating that HDAC recruitment is a mechanism of ATF3-regulated gene repression. The role of ATF3 at the *Gadd34* promoter is less clear. ATF3 splice variants lacking a leucine zipper domain are thought to act as transcriptional activators by sequestering repressive factors from gene promoters (Chen et al., 1994). However, we observed that ATF3 is bound to the *Gadd34* promoter. It is possible that ATF3 does not directly interact with the *Gadd34* promoter since ATF/CREB family members can dimerize (Hai and Hartman, 2001), and perhaps ATF3 was dimerized with ATF4, a known

transcriptional activator of *Gadd34* (Ma and Hendershot, 2003). This notion is supported by the fact that *Gadd34* upregulation during CIP is not altered in *Atf3*$^{-/-}$ pancreatic tissue (Appendix Figure A3), indicating that ATF3 is not absolutely required for its expression.

Our work shows that ATF3 was required for the observed loss of differentiated cell characteristics including cell polarity and cellular junctions, but does not resolve whether ATF3 plays a transcriptional role at each promoter. What is clear is that ATF3 binds to the *Mist1* promoter to induce its repression during CIP. This singular transcriptional event may be a trigger for subsequent loss of polarity and junctional markers since MIST1 is a transcriptional regulator required for proper acinar cell maturation. Thus, the loss of Mist1 may be resulting in the loss of transcriptional activation at these polarity and junctional promoters. Further evidence to support this is illustrated in *Mist1*$^{-/-}$ mice where *Cx32* expressions is absent. The finding that *Mist1* expression was maintained during CIP in *Atf3*$^{-/-}$ tissue, along with expression of junctional and polarity genes, supports a model including MIST1.

What is still unclear is whether the loss of acinar cell differentiation characteristics during pancreatitis is a protective mechanism, or if it is a measure of cell damage. The theory that loss of acinar cell differentiation is protective may be counterintuitive at first, but it is possible that the cell is more capable of dealing with insult in a less differentiated state. In this work, the experimental CIP time point is too early to assess longer-term pancreatitis severity measures like serum amylase and tissue necrosis, which would clarify whether the

maintenance of acinar cell differentiation is protective or damaging. However, the persistence of ATF3 expression and concomitant absence of MIST1 expression (Johnson et al., 2012) in pancreatic tissue from patients with CP indicates that ATF3 accumulation an loss of MIST1 are not early response protective mechanisms. Furthermore, the increased expression of ATF3 in CP coinciding with decreased expression of MIST1, suggests that ATF3-mediated repression of *Mist1* expression may be a contributing factor for pancreatitis in humans.

In conclusion, this study uncovers a molecular role for ATF3 and the UPR during pancreatitis, and gives insight into how acinar cell differentiation and *Mist1* expression are regulated during injury. The study also provides a mechanism by which environmental factors that enhance the UPR can promote pancreatitis and presents another link between CP and PDAC.

Chapter 6

6 « Summary and Discussion »

The purpose of this study was to determine whether the PERK pathway contributes to exocrine pancreas pathology at both a transcriptional and molecular level. To determine the molecular role of the PERK pathway, the effect of STC2 overexpression on exocrine pancreas injury was assessed following repeated doses of cerulein to initiate pancreatitis. Assessment of pancreatitis severity parameters revealed a muted elevation in serum amylase, decreased necrosis, and increased maintenance of cellular junctions, indicative of a role for STC2 in reducing the severity of exocrine pancreas injury.

To uncover a transcriptional role for the PERK pathway, a protocol for chromatin immunoprecipitation from whole pancreatic tissue was designed. This allowed for analysis of the contribution of the transcription factors ATF3 in pancreatitis. ATF3 occupied the *Mist1* promoter during pancreatitis, and studies with *Atf3*$^{-/-}$ mice revealed that ATF3 was required for the downregulation of *Mist1* expression during CIP. Furthermore, this regulation was conferred through recruitment of HDAC5 by ATF3. Thus, this work illustrates a dual role for the PERK pathway in exocrine pancreas injury.

6.1 « STC2 »

STC2 has been previously associated with the PERK pathway in vitro. This is the first study to link STC2 to the PERK pathway in vivo through overexpression and subsequent alteration in PERK pathway activation. Furthermore, this study illustrates that STC2 expression was upregulated during pancreatitis, illustrating that it is part of a pathological response mechanism. Upregulation of STC2 during pancreatitis is not observed in a mouse model of increased pancreatitis severity (*Mist1*$^{-/-}$), indicative of a protective role. Additionally, *STC2*^{Tg} mice exhibit decreased severity of pancreatitis based on numerous parameters, including decreased cellular necrosis, increased maintenance of cell junctions and a muted increased in serum amylase.

Furthermore, *STC2*^{Tg} mice exhibit altered development and function of the endocrine pancreas. While islet composition and glucose tolerance are altered in these mice, further studies are required to solidify an endocrine defect. Assessment of insulin secretion during GSIS would indicate whether *STC2*^{Tg} exocrine pancreata are deficient in sensing glucose or producing insulin. To deterime whether these mice are insulin resistant, insulin stimulated insulin release could be performed, where decreased secretion of insulin after stimulation would indicated insulin resistance.

In terms of the exocrine pancreas, PERK pathway activation in *STC2*^{Tg} pancreata during pancreatitis was aberrant, where PERK and eIF2α both exhibit increased phosphorylation and ATF4 expression is increased. However, it is

important to consider that eIF2α can be phosphorylated via mechanisms other than PERK, indicating that the observed alteration in PERK phosphorylation may be secondary to a peIF2α driven mechanism in these mice.

The dysregulation of these molecules indicates that pancreatic tissue overexpressing STC2 was more sensitive to pancreatic insult, and that this tissue may be primed to respond to lower levels of injury. This priming effect results in more efficient induction of the UPR during injury, resulting in earlier presence of protective effects and decreased pancreatitis severity, as observed in $STC2^{Tg}$ tissue. Interestingly, ATF3 was not involved in this priming phenomenon, where it was only expressed in $STC2^{Tg}$ tissue after induction of pancreatitis. However, its expression was more robust than that seen in WT tissue under the same conditions. This observation might indicate that other factors are required for expression of ATF3. Additionally, ATF3 may be required for the acinar cell response that is present in only pancreatitis and not after saline treatment, including loss of acinar cell differentiation.

6.2 « ATF3 »

Unlike other members of the PERK pathway, ATF3 was not expressed at detectable levels in pancreatic exocrine tissue under normal physiologic conditions. This indicates that, while other PERK pathway members have a role in normal physiology of the cell, the role of ATF3 was strictly as a stress response gene. Since ATF3 is a transcription factor, further elucidation of its role during pancreatitis required identification of its transcriptional targets. ATF3 had

been previously implicated in cell differentiation (Filen et al., 2010; James et al., 2006; Xu et al., 2011), suggesting that MIST1, a regulator of acinar cell differentiation, may be a potential target. *Mist1* expression was decreased during pancreatitis, in addition to loss of cell polarity and junctional complexes, indicative of a loss of acinar cell differentiation. ATF3 binds to the *Mist1* promoter only after induction of pancreatitis, to a region that contains two ATF/CRE consensus sequences. When bound to the *Mist1* promoter during pancreatitis, ATF3 recruits HDAC5, which is known to act as a repressor of transcription (Lemercier et al., 2000). ATF3 was required for HDAC5 recruitment under these conditions since assessment of the *Mist1* promoter in *Atf3*$^{-/-}$ mice revealed no HDAC5 recruitment. Additionally, *Mist1* expression was not decreased in *Atf3*$^{-/-}$ during pancreatitis, indicating that ATF3 and HDAC5 are critical to this process. These observations are novel, outline a mechanism of ATF3-mediated gene repression, and identify important transcriptional regulators of *Mist1*.

While ATF3 and HDAC5 are important for transcriptional downregulation of *Mist1*, the observation that MIST1 protein expression decreases as early as one hour after the induction of pancreatitis inidicates that another mechanism is at play since one hour is likely too soon to be a wholly ATF3-based transcriptional mechanism. Thus, the early downregulation of MIST1 protein might occur via enhanced protein degradation through either decreased protein stability or increased activation of degradation mechansims.

The specificity of the ATF3/HDAC5 repressive complex is illustrated by analysis of the *Gadd34* promoter. GADD34 is a PERK pathway member that is

upregulated during pancreatitis and serves as a negative feedback mechanism to dephosphorylate peIF2α (Ma and Hendershot, 2003). ATF4 regulates *Gadd34* expression, and there is an identified ATF/CRE consensus site in the *Gadd34* promoter (Ma and Hendershot, 2003). This study shows a novel occupancy of the *Gadd34* promoter by ATF3 in the absence of HDAC5, occurring during pancreatitis, when *Gadd34* expression is increased. Thus, ATF3 binds to promoters of both active and repressed genes, with HDAC5 recruited only in the repressive situation. This duality is in keeping with a previously postulated mechanism where full length ATF3 acts as a repressor and ATF3 splice variants lacking leucine zipper motifs act as transcriptional activators by sequestering inhibitory factors from gene promoters (Figure 1.4B). The work presented here extends this hypothesis, and shows that ATF3 acts as a repressor and activator by binding DNA in both circumstances, and the differentiating factor between activation and repression is other members of the transcriptional complex, including HDAC5. However, *Gadd34* expression during pancreatitis is not reliant on expression of ATF3, since *Atf3*$^{-/-}$ pancreata exhibit similar levels of *Gadd34* upregulation during pancreatitis (Appendix Figure A3).

6.3 « A dual role for PERK Pathway Activation »

Analysis of the onset of mRNA expression reveals robust upregulation of *Atf3* one hour after the induction of pancreatitis, with *Stc2* expression following by 4 hours (Figure 2.2). These observations suggest a model where ATF3 promotes *Stc2* expression, and the two work in a linear pathway following PERK/ATF4

activation. If ATF3 and STC2 are involved in the same processes following CIP, then *Atf3*$^{-/-}$ and *STC2*^{Tg} lines should exhibit opposite responses to induction of pancreatitis. However, this study revealed similar protective response in both mouse models following induction of pancreatitis. This reveals a non-linear relationship between ATF3 and STC2, and indicates that activation of the PERK pathway may have two opposing outcomes with STC2 serving as a protective molecule and ATF3 promoting damage during pancreatitis.

It is counterintuitive for a singular pathway to promote opposing cellular responses, especially via two molecules regulated by the same transcription factor, ATF4, indicating that the timing of each event might be of importance. *Atf3* is rapidly upregulated on hour after the induction of pancreatitis, and contributes to loss of acinar cell differentiation and polarity. Thus, the loss of acinar cell differentiation and polarity is an immediate response. *Stc2* expression is first seen at 4 hours after the induction of pancreatitis, indicating that the cellular events it mediates follow those instigated by ATF3. Since STC2 serves to downregulate phosphorylation of PERK and eIF2α and potentially dampen the activity of the PERK pathway, its role could be to counteract the outcome of ATF3 activity and for example, initiate restoration of cell polarity (Figure 6.1). One caveat to consider is that the observations are based on assessment of a model of STC2 overexpression, which may not be reflective of physiological or pathological STC2 levels in the pancreas. Endogenous STC2 expression in the pancreas after induction of pancreatitis is virtually undetectable (data not shown) and while protein content visualized by IF cannot be compared between STC2

and ATF3, and is also not indicative of the individual protein potency, this observation could illustrate that the amount of STC2 present at the assessed time point is not required to completely counteract the activation of PERK pathway activation, but to modulate its activity in a rheostat-like fashion.

Another point to consider is whether the loss of polarity and cell differentiation is actually detrimental or advantageous. It is possible that acinar cells revert to a less differentiated phenotype that may be better equipped to deal with tissue injury. However, the classical measures of pancreatitis severity, measurement

Figure 6.1. Proposed Mechanism of PERK Activity. Activation of the PERK pathway leads to ATF4-mediated expression of STC2 and ATF3. This study illustrates a role for ATF3 in repressing *Mist1* expression, that is a key acinar cell differentiation molecule (red line 1), and that XBP1 may contribute to this process (red dotted line, ?). Additionally, STC2 acts a feedback mechanism to decreased phosphorylation of PERK and eIF2α (red line 2).

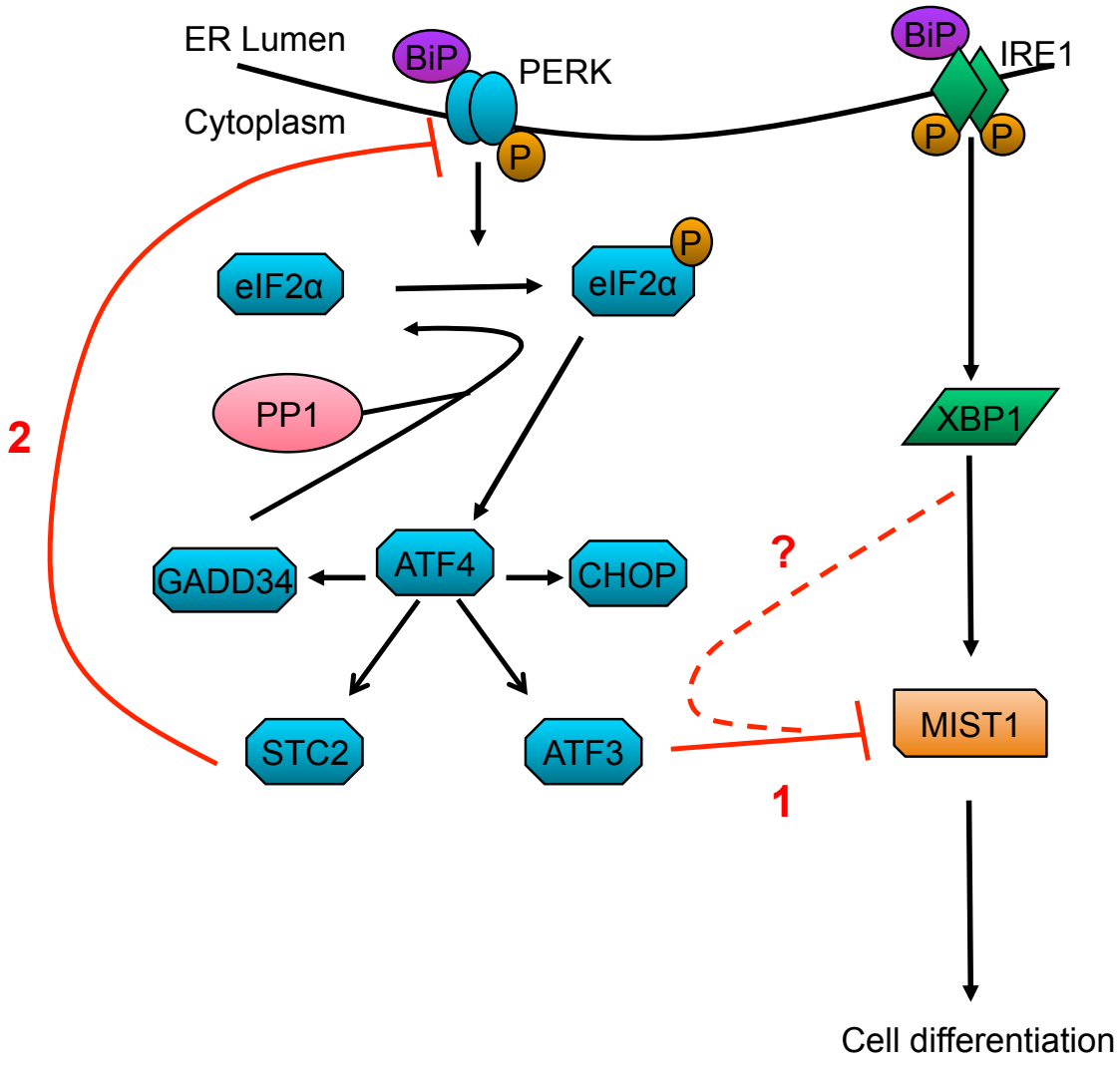

Figure 6.1. Proposed Mechanism of PERK Activity.

of serum amylase and exocrine tissue fibrosis are based on amylase and other digestive enzymes leaking between cells and into the tissue and vasculature. This process is facilitated by the loss of cellular junctions, namely tight junctions, which normally form a barrier to such events. Examination of CIP responses at four after initial injections allowed for assessment of early events in pancreatitis, including induction of transcriptional cascades that contribute to cellular response to stress. However, assessment of tissue fibrosis and serum amylase at this early timepoint does not give a full representation of disease severity since peak serum amylase levels, apoptosis and necrosis occur several hours later after initiating pancreatitis. Therefore, ongoing studies include assessment of pancreatitis severity at later timepoints in *Atf3*$^{-/-}$ mice in order to determine the contribution of ATF3 to disease severity.

6.4 « Cross-talk Between UPR Pathways »

This work also uncovers a unique interaction between the PERK and IRE signaling pathways. Both XBP1 and ATF3 are recruited to the *Mist1* promoter during CIP. Little is known about *Mist1* transcriptional regulation, other than activation by XBP1 during cultured myoblast differentiation (Acosta-Alvear et al., 2007) and during gastric zymogenic cell differentiation (Huh et al., 2010). The potential presence of XBP1 at the *Mist1* promoter during a time of repression would be a novel finding since previous work showed that XBP1 activates *Mist1* expression during cell differentiation. However, the present work indicates that XBP1 may be enriched at a region further upstream from the *Mist1* TSS (Acosta-

Alvear et al., 2007). While I have not been able to show a direct interaction between XBP1 and ATF3 due to limitations of the antibodies, such an interaction is possible since both are bZIP proteins that can heterodimerize (Hai et al., 1989; Ono et al., 1991). A contribution of XBP1 in this process is appealing for numerous reasons. First, this would reveal a novel interaction between ATF3 and XBP1, and would be indicative of cross-talk between two distinct UPR pathways. Second, it would reveal a dual role for XBP1 in the regulation of *Mist1* that is context dependent, where it is activating during cell differentiation and repressive during cell injury. XBP1 is consistently expressed in the adult exocrine pancreas indicating it has a role outside of cell differentiation, and that the role of XBP1 in the pancreas is context dependent, just as it may be during pancreatic injury.

6.5 « Future Directions »

Since the this study presents only preliminary evidence that XBP1 participates in the ATF3 driven repressive complex, further analysis of XBP1 occupancy at the Mist1 promoter during CIP should be carried out. Additionally, co-immunoprecipitation studies should be carried out to determine if XBP1 and ATF3 do, in fact bind to each other, or are located within the same complex. Similarly, ChIP re-ChIP should be carried out to determine if they are both, in fact, occupying the same region of the *Mist1* promoter at the same time. Further analysis by inducing CIP in mice lacking Xbp1 in the exocrine pancreas ($Xbp1^{\Delta Ex2}$) may be carried out.

Clear evidence has been presented that ATF3 recruits HDAC5 to form a repressive complex at the *Mist1* promoter. To extend this analysis, CIP experiments can be carried out in mice lacking *Hdac5* (*Hdac5*$^{-/-}$) (Chang et al., 2004) to observe whether these mice exhibit a response to pancreatitis similar to that seen in *Atf3*$^{-/-}$ mice. Additionally, determining whether ATF3 occupies the *Mist1* promoter in the absence of HDAC5 will strengthen the conclusion that ATF3 recruits HDAC5 in this process.

To further elucidate whether ATF3 is protective or deleterious during pancreatitis, *Atf3*$^{-/-}$ mice should be examined over a longer time period of CIP exposure and assessed for severity parameters including serum amylase, edema and fibrosis. Additionally, the exocrine pancreas of mice overexpressing ATF3 (*ATF3*^{Tg}) can be examined to observe whether cells exhibit similar characteristics seen during pancreatitis. Additionally, generating ChIP material suitable for ChIP-Seq would confirm the ChIP results presented here, and uncover novel ATF3 transcriptional targets.

6.6 « Conclusion »

This work illustrates that the PERK pathway is responsive during pancreatitis. In both a transcriptional (ATF3) and a molecular (STC2) fashion, and that activation of these molecules elicit opposing responses, illustrating a dual role for this pathway. Furthermore, the expression of ATF3 in human pancreatitis samples reveals a potential clinical role for ATF3 in exocrine pancreas pathology.

7 « References »

Acosta-Alvear, D., Zhou, Y., Blais, A., Tsikitis, M., Lents, N.H., Arias, C., Lennon, C.J., Kluger, Y., and Dynlacht, B.D. (2007). XBP1 controls diverse cell type- and condition-specific transcriptional regulatory networks. Mol Cell *27*, 53-66.

Adamo, J.E., Moskow, J.J., Gladfelter, A.S., Viterbo, D., Lew, D.J., and Brennwald, P.J. (2001). Yeast Cdc42 functions at a late step in exocytosis, specifically during polarized growth of the emerging bud. J Cell Biol *155*, 581-592.

Ais, G., Lopez-Farre, A., Gomez-Garre, D.N., Novo, C., Romeo, J.M., Braquet, P., and Lopez-Novoa, J.M. (1992). Role of platelet-activating factor in hemodynamic derangements in an acute rodent pancreatic model. Gastroenterology *102*, 181-187.

Alahari, S., Mehmood, R., Johnson, C.L., and Pin, C.L. (2011). The Absence of MIST1 Leads to Increased Ethanol Sensitivity and Decreased Activity of the Unfolded Protein Response in Mouse Pancreatic Acinar Cells. PLoS One *6*, e28863.

Allen-Jennings, A.E., Hartman, M.G., Kociba, G.J., and Hai, T. (2001). The roles of ATF3 in glucose homeostasis. A transgenic mouse model with liver dysfunction and defects in endocrine pancreas. J Biol Chem *276*, 29507-29514.

Allen-Jennings, A.E., Hartman, M.G., Kociba, G.J., and Hai, T. (2002). The roles of ATF3 in liver dysfunction and the regulation of phosphoenolpyruvate carboxykinase gene expression. J Biol Chem *277*, 20020-20025.

Allison, D.B., Paultre, F., Maggio, C., Mezzitis, N., and Pi-Sunyer, F.X. (1995). The use of areas under curves in diabetes research. Diabetes Care *18*, 245-250.

Angelopoulos, N., Dervenis, C., Goula, A., Rombopoulos, G., Livadas, S., Kaltsas, D., Kaltzidou, V., and Tolis, G. (2005). Endocrine pancreatic insufficiency in chronic pancreatitis. Pancreatology *5*, 122-131.

Annis, M.G., Zamzami, N., Zhu, W., Penn, L.Z., Kroemer, G., Leber, B., and Andrews, D.W. (2001). Endoplasmic reticulum localized Bcl-2 prevents apoptosis when redistribution of cytochrome c is a late event. Oncogene *20*, 1939-1952.

Anthony, T.G., McDaniel, B.J., Byerley, R.L., McGrath, B.C., Cavener, D.R., McNurlan, M.A., and Wek, R.C. (2004). Preservation of liver protein synthesis during dietary leucine deprivation occurs at the expense of skeletal muscle mass in mice deleted for eIF2 kinase GCN2. J Biol Chem *279*, 36553-36561.

Badger, T.M., Ronis, M.J., Seitz, H.K., Albano, E., Ingelman-Sundberg, M., and Lieber, C.S. (2003). Alcohol metabolism: role in toxicity and carcinogenesis. Alcohol Clin Exp Res *27*, 336-347.

Bank, S., Singh, P., Pooran, N., and Stark, B. (2002). Evaluation of factors that have reduced mortality from acute pancreatitis over the past 20 years. J Clin Gastroenterol *35*, 50-60.

Bardeesy, N., and DePinho, R.A. (2002). Pancreatic cancer biology and genetics. Nat Rev Cancer *2*, 897-909.

Bell, A.C., and Felsenfeld, G. (1999). Stopped at the border: boundaries and insulators. Curr Opin Genet Dev *9*, 191-198.

Bellucci, A., Navarria, L., Zaltieri, M., Falarti, E., Bodei, S., Sigala, S., Battistin, L., Spillantini, M., Missale, C., and Spano, P. (2011). Induction of the unfolded protein response by alpha-synuclein in experimental models of Parkinson's disease. J Neurochem *116*, 588-605.

Bertolotti, A., Zhang, Y., Hendershot, L.M., Harding, H.P., and Ron, D. (2000). Dynamic interaction of BiP and ER stress transducers in the unfolded-protein response. Nature cell biology *2*, 326-332.

Bhatia, M., Saluja, A.K., Hofbauer, B., Frossard, J.L., Lee, H.S., Castagliuolo, I., Wang, C.C., Gerard, N., Pothoulakis, C., and Steer, M.L. (1998). Role of substance P and the neurokinin 1 receptor in acute pancreatitis and pancreatitis-associated lung injury. Proc Natl Acad Sci U S A *95*, 4760-4765.

Blinman, T.A., Gukovsky, I., Mouria, M., Zaninovic, V., Livingston, E., Pandol, S.J., and Gukovskaya, A.S. (2000). Activation of pancreatic acinar cells on isolation from tissue: cytokine upregulation via p38 MAP kinase. Am J Physiol Cell Physiol *279*, C1993-2003.

Bollo, M., Paredes, R.M., Holstein, D., Zheleznova, N., Camacho, P., and Lechleiter, J.D. (2010). Calcineurin interacts with PERK and dephosphorylates calnexin to relieve ER stress in mammals and frogs. PLoS One *5*, e11925.

Bowden, J.J., Garland, A.M., Baluk, P., Lefevre, P., Grady, E.F., Vigna, S.R., Bunnett, N.W., and McDonald, D.M. (1994). Direct observation of substance P-induced internalization of neurokinin 1 (NK1) receptors at sites of inflammation. Proc Natl Acad Sci U S A *91*, 8964-8968.

Brostrom, C.O., and Brostrom, M.A. (1998). Regulation of translational initiation during cellular responses to stress. Prog Nucleic Acid Res Mol Biol *58*, 79-125.

Bruhat, A., Jousse, C., Carraro, V., Reimold, A.M., Ferrara, M., and Fafournoux, P. (2000). Amino acids control mammalian gene transcription: activating

transcription factor 2 is essential for the amino acid responsiveness of the CHOP promoter. Mol Cell Biol *20*, 7192-7204.

Calfon, M., Zeng, H., Urano, F., Till, J.H., Hubbard, S.R., Harding, H.P., Clark, S.G., and Ron, D. (2002). IRE1 couples endoplasmic reticulum load to secretory capacity by processing the XBP-1 mRNA. Nature *415*, 92-96.

Chang, A.C., Hook, J., Lemckert, F.A., McDonald, M.M., Nguyen, M.A., Hardeman, E.C., Little, D.G., Gunning, P.W., and Reddel, R.R. (2008). The murine stanniocalcin 2 gene is a negative regulator of postnatal growth. Endocrinology *149*, 2403-2410.

Chang, S., McKinsey, T.A., Zhang, C.L., Richardson, J.A., Hill, J.A., and Olson, E.N. (2004). Histone deacetylases 5 and 9 govern responsiveness of the heart to a subset of stress signals and play redundant roles in heart development. Mol Cell Biol *24*, 8467-8476.

Chen, B.P., Liang, G., Whelan, J., and Hai, T. (1994). ATF3 and ATF3 delta Zip. Transcriptional repression versus activation by alternatively spliced isoforms. J Biol Chem *269*, 15819-15826.

Chen, B.P., Wolfgang, C.D., and Hai, T. (1996). Analysis of ATF3, a transcription factor induced by physiological stresses and modulated by gadd153/Chop10. Mol Cell Biol *16*, 1157-1168.

Cherasse, Y., Maurin, A.C., Chaveroux, C., Jousse, C., Carraro, V., Parry, L., Deval, C., Chambon, C., Fafournoux, P., and Bruhat, A. (2007). The p300/CBP-associated factor (PCAF) is a cofactor of ATF4 for amino acid-regulated transcription of CHOP. Nucleic Acids Res *35*, 5954-5965.

Clauss, I.M., Gravallese, E.M., Darling, J.M., Shapiro, F., Glimcher, M.J., and Glimcher, L.H. (1993). In situ hybridization studies suggest a role for the basic region-leucine zipper protein hXBP-1 in exocrine gland and skeletal development during mouse embryogenesis. Dev Dyn *197*, 146-156.

Cnop, M., Ladriere, L., Hekerman, P., Ortis, F., Cardozo, A.K., Dogusan, Z., Flamez, D., Boyce, M., Yuan, J., and Eizirik, D.L. (2007). Selective inhibition of eukaryotic translation initiation factor 2 alpha dephosphorylation potentiates fatty acid-induced endoplasmic reticulum stress and causes pancreatic beta-cell dysfunction and apoptosis. J Biol Chem *282*, 3989-3997.

Cox, J.S., Chapman, R.E., and Walter, P. (1997). The unfolded protein response coordinates the production of endoplasmic reticulum protein and endoplasmic reticulum membrane. Mol Biol Cell *8*, 1805-1814.

Credle, J.J., Finer-Moore, J.S., Papa, F.R., Stroud, R.M., and Walter, P. (2005). On the mechanism of sensing unfolded protein in the endoplasmic reticulum. Proc Natl Acad Sci U S A *102*, 18773-18784.

Czako, L., Hegyi, P., Rakonczay, Z., Jr., Wittmann, T., and Otsuki, M. (2009). Interactions between the endocrine and exocrine pancreas and their clinical relevance. Pancreatology *9*, 351-359.

Davis, R.J. (2000). Signal transduction by the JNK group of MAP kinases. Cell *103*, 239-252.

Desilva, M.G., Lu, J., Donadel, G., Modi, W.S., Xie, H., Notkins, A.L., and Lan, M.S. (1996). Characterization and chromosomal localization of a new protein disulfide isomerase, PDIp, highly expressed in human pancreas. DNA Cell Biol *15*, 9-16.

Deutsch, P.J., Hoeffler, J.P., Jameson, J.L., Lin, J.C., and Habener, J.F. (1988). Structural determinants for transcriptional activation by cAMP-responsive DNA elements. J Biol Chem *263*, 18466-18472.

DiMattia, G.E., Varghese, R., and Wagner, G.F. (1998). Molecular cloning and characterization of stanniocalcin-related protein. Mol Cell Endocrinol *146*, 137-140.

Ekholm, R., Zelander, T., and Edlund, Y. (1962). The ultrastructural organization of the rat exocrine pancreas. I. Acinar cells. Journal of Ultrastructural Research *7*, 61-72.

Falkowski, M.A., Thomas, D.D., Messenger, S.W., Martin, T.F., and Groblewski, G.E. (2011). Expression, localization, and functional role for synaptotagmins in pancreatic acinar cells. Am J Physiol Gastrointest Liver Physiol *301*, G306-316.

Fazio, E.N., Dimattia, G.E., Chadi, S.A., Kernohan, K.D., and Pin, C.L. (2011). Stanniocalcin 2 alters PERK signalling and reduces cellular injury during cerulein induced pancreatitis in mice. BMC Cell Biol *12*, 17.

Fazio, E.N., Everest, M., Colman, R., Wang, R., and Pin, C.L. (2005). Altered Glut-2 accumulation and beta-cell function in mice lacking the exocrine-specific transcription factor, Mist1. J Endocrinol *187*, 407-418.

Fazio, E.N., Mehmood, R., Pin, C.L. (2011). Chromatin Immunoprecipitation (ChIP) from pancreatic acinar cells and whole pancreatic tissue. In The Pancreapedia: Exocrine Pancreas Knowledge Base http://wwwpancreapediaorg/?q=node/765.

Fazio, E.N., and Pin, C.L. (2007). Mist1-null mice are resistant to streptozotocin-induced beta cell damage. Biochem Biophys Res Commun *353*, 823-828.

Filen, S., Ylikoski, E., Tripathi, S., West, A., Bjorkman, M., Nystrom, J., Ahlfors, H., Coffey, E., Rao, K.V., Rasool, O.*, et al.* (2010). Activating transcription factor 3 is a positive regulator of human IFNG gene expression. J Immunol *184*, 4990-4999.

Filippin, L., Magalhaes, P.J., Di Benedetto, G., Colella, M., and Pozzan, T. (2003). Stable interactions between mitochondria and endoplasmic reticulum allow rapid accumulation of calcium in a subpopulation of mitochondria. J Biol Chem *278*, 39224-39234.

Flik, G., Labedz, T., Neelissen, J.A., Hanssen, R.G., Wendelaar Bonga, S.E., and Pang, P.K. (1990). Rainbow trout corpuscles of Stannius: stanniocalcin synthesis in vitro. Am J Physiol *258*, R1157-1164.

Freiden, P.J., Gaut, J.R., and Hendershot, L.M. (1992). Interconversion of three differentially modified and assembled forms of BiP. Embo J *11*, 63-70.

Friend, D.S., and Gilula, N.B. (1972). Variations in tight and gap junctions in mammalian tissues. J Cell Biol *53*, 758-776.

Frier, B.M., Saunders, J.H., Wormsley, K.G., and Bouchier, I.A. (1976). Exocrine pancreatic function in juvenile-onset diabetes mellitus. Gut *17*, 685-691.

Gagliardi, A.D., Kuo, E.Y., Raulic, S., Wagner, G.F., and DiMattia, G.E. (2005). Human stanniocalcin-2 exhibits potent growth-suppressive properties in transgenic mice independently of growth hormone and IGFs. Am J Physiol Endocrinol Metab *288*, E92-105.

Gaisano, H.Y. (2000). A hypothesis: SNARE-ing the mechanisms of regulated exocytosis and pathologic membrane fusions in the pancreatic acinar cell. Pancreas *20*, 217-226.

Gaisano, H.Y., Sheu, L., Foskett, J.K., and Trimble, W.S. (1994). Tetanus toxin light chain cleaves a vesicle-associated membrane protein (VAMP) isoform 2 in rat pancreatic zymogen granules and inhibits enzyme secretion. J Biol Chem *269*, 17062-17066.

Galli, P., Brenna, A., Camilli de, P., and Meldolesi, J. (1976). Extracellular calcium and the organization of tight junctions in pancreatic acinar cells. Experimental cell research *99*, 178-183.

Gardner, B.M., and Walter, P. (2011). Unfolded proteins are Ire1-activating ligands that directly induce the unfolded protein response. Science *333*, 1891-1894.

Gomez, E., Powell, M.L., Bevington, A., and Herbert, T.P. (2008). A decrease in cellular energy status stimulates PERK-dependent eIF2alpha phosphorylation and regulates protein synthesis in pancreatic beta-cells. Biochem J *410*, 485-493.

Gorry, M.C., Gabbaizedeh, D., Furey, W., Gates, L.K., Jr., Preston, R.A., Aston, C.E., Zhang, Y., Ulrich, C., Ehrlich, G.D., and Whitcomb, D.C. (1997). Mutations

in the cationic trypsinogen gene are associated with recurrent acute and chronic pancreatitis. Gastroenterology *113*, 1063-1068.

Grady, T., Liang, P., Ernst, S.A., and Logsdon, C.D. (1997). Chemokine gene expression in rat pancreatic acinar cells is an early event associated with acute pancreatitis. Gastroenterology *113*, 1966-1975.

Grady, T., Saluja, A., Kaiser, A., and Steer, M. (1996). Edema and intrapancreatic trypsinogen activation precede glutathione depletion during caerulein pancreatitis. Am J Physiol *271*, G20-26.

Grunstein, M. (1998). Yeast heterochromatin: regulation of its assembly and inheritance by histones. Cell *93*, 325-328.

Gukovskaya, A.S., Vaquero, E., Zaninovic, V., Gorelick, F.S., Lusis, A.J., Brennan, M.L., Holland, S., and Pandol, S.J. (2002). Neutrophils and NADPH oxidase mediate intrapancreatic trypsin activation in murine experimental acute pancreatitis. Gastroenterology *122*, 974-984.

Guy-Crotte, O., Carrere, J., and Figarella, C. (1996). Exocrine pancreatic function in cystic fibrosis. Eur J Gastroenterol Hepatol *8*, 755-759.

Haber, P.S., Apte, M.V., Moran, C., Applegate, T.L., Pirola, R.C., Korsten, M.A., McCaughan, G.W., and Wilson, J.S. (2004). Non-oxidative metabolism of ethanol by rat pancreatic acini. Pancreatology *4*, 82-89.

Hacki, J., Egger, L., Monney, L., Conus, S., Rosse, T., Fellay, I., and Borner, C. (2000). Apoptotic crosstalk between the endoplasmic reticulum and mitochondria controlled by Bcl-2. Oncogene *19*, 2286-2295.

Hai, T., and Hartman, M.G. (2001). The molecular biology and nomenclature of the activating transcription factor/cAMP responsive element binding family of transcription factors: activating transcription factor proteins and homeostasis. Gene *273*, 1-11.

Hai, T.W., Liu, F., Coukos, W.J., and Green, M.R. (1989). Transcription factor ATF cDNA clones: an extensive family of leucine zipper proteins able to selectively form DNA-binding heterodimers. Genes Dev *3*, 2083-2090.

Halangk, W., Lerch, M.M., Brandt-Nedelev, B., Roth, W., Ruthenbuerger, M., Reinheckel, T., Domschke, W., Lippert, H., Peters, C., and Deussing, J. (2000). Role of cathepsin B in intracellular trypsinogen activation and the onset of acute pancreatitis. J Clin Invest *106*, 773-781.

Hansen, N.J., Antonin, W., and Edwardson, J.M. (1999). Identification of SNAREs involved in regulated exocytosis in the pancreatic acinar cell. J Biol Chem *274*, 22871-22876.

Harding, H.P., Novoa, I., Zhang, Y., Zeng, H., Wek, R., Schapira, M., and Ron, D. (2000). Regulated translation initiation controls stress-induced gene expression in mammalian cells. Mol Cell *6*, 1099-1108.

Harding, H.P., Zeng, H., Zhang, Y., Jungries, R., Chung, P., Plesken, H., Sabatini, D.D., and Ron, D. (2001). Diabetes mellitus and exocrine pancreatic dysfunction in perk-/- mice reveals a role for translational control in secretory cell survival. Mol Cell *7*, 1153-1163.

Harding, H.P., Zhang, Y., and Ron, D. (1999). Protein translation and folding are coupled by an endoplasmic-reticulum-resident kinase. Nature *397*, 271-274.

Hardt, P.D., and Ewald, N. (2011). Exocrine pancreatic insufficiency in diabetes mellitus: a complication of diabetic neuropathy or a different type of diabetes? Exp Diabetes Res *2011*, 761950.

Hargreaves, D.C., and Crabtree, G.R. (2011). ATP-dependent chromatin remodeling: genetics, genomics and mechanisms. Cell Res *21*, 396-420.

Hartman, M.G., Lu, D., Kim, M.L., Kociba, G.J., Shukri, T., Buteau, J., Wang, X., Frankel, W.L., Guttridge, D., Prentki, M.*, et al.* (2004). Role for activating transcription factor 3 in stress-induced beta-cell apoptosis. Mol Cell Biol *24*, 5721-5732.

Hashimoto, Y., Zhang, C., Kawauchi, J., Imoto, I., Adachi, M.T., Inazawa, J., Amagasa, T., Hai, T., and Kitajima, S. (2002). An alternatively spliced isoform of transcriptional repressor ATF3 and its induction by stress stimuli. Nucleic Acids Res *30*, 2398-2406.

Haze, K., Okada, T., Yoshida, H., Yanagi, H., Yura, T., Negishi, M., and Mori, K. (2001). Identification of the G13 (cAMP-response-element-binding protein-related protein) gene product related to activating transcription factor 6 as a transcriptional activator of the mammalian unfolded protein response. Biochem J *355*, 19-28.

Haze, K., Yoshida, H., Yanagi, H., Yura, T., and Mori, K. (1999). Mammalian transcription factor ATF6 is synthesized as a transmembrane protein and activated by proteolysis in response to endoplasmic reticulum stress. Mol Biol Cell *10*, 3787-3799.

He, B., Chou, J., Liebermann, D.A., Hoffman, B., and Roizman, B. (1996). The carboxyl terminus of the murine MyD116 gene substitutes for the corresponding domain of the gamma(1)34.5 gene of herpes simplex virus to preclude the premature shutoff of total protein synthesis in infected human cells. J Virol *70*, 84-90.

Hess, D.A., Humphrey, S.E., Ishibashi, J., Damsz, B., Lee, A.H., Glimcher, L.H., and Konieczny, S.F. (2011). Extensive pancreas regeneration following acinar-specific disruption of Xbp1 in mice. Gastroenterology *141*, 1463-1472.

Hettmann, T., Barton, K., and Leiden, J.M. (2000). Microphthalmia due to p53-mediated apoptosis of anterior lens epithelial cells in mice lacking the CREB-2 transcription factor. Dev Biol *222*, 110-123.

Hinnebusch, A.G. (1997). Translational regulation of yeast GCN4. A window on factors that control initiator-trna binding to the ribosome. J Biol Chem *272*, 21661-21664.

Hofbauer, B., Saluja, A.K., Bhatia, M., Frossard, J.L., Lee, H.S., Bhagat, L., and Steer, M.L. (1998). Effect of recombinant platelet-activating factor acetylhydrolase on two models of experimental acute pancreatitis. Gastroenterology *115*, 1238-1247.

Hong, L., Schroth, G.P., Matthews, H.R., Yau, P., and Bradbury, E.M. (1993). Studies of the DNA binding properties of histone H4 amino terminus. Thermal denaturation studies reveal that acetylation markedly reduces the binding constant of the H4 "tail" to DNA. J Biol Chem *268*, 305-314.

Hoozemans, J.J., van Haastert, E.S., Eikelenboom, P., de Vos, R.A., Rozemuller, J.M., and Scheper, W. (2007). Activation of the unfolded protein response in Parkinson's disease. Biochem Biophys Res Commun *354*, 707-711.

Hosokawa, N., Wada, I., Hasegawa, K., Yorihuzi, T., Tremblay, L.O., Herscovics, A., and Nagata, K. (2001). A novel ER alpha-mannosidase-like protein accelerates ER-associated degradation. EMBO Rep *2*, 415-422.

Hu, P., Han, Z., Couvillon, A.D., Kaufman, R.J., and Exton, J.H. (2006). Autocrine tumor necrosis factor alpha links endoplasmic reticulum stress to the membrane death receptor pathway through IRE1alpha-mediated NF-kappaB activation and down-regulation of TRAF2 expression. Mol Cell Biol *26*, 3071-3084.

Huh, W.J., Esen, E., Geahlen, J.H., Bredemeyer, A.J., Lee, A.H., Shi, G., Konieczny, S.F., Glimcher, L.H., and Mills, J.C. (2010). XBP1 controls maturation of gastric zymogenic cells by induction of MIST1 and expansion of the rough endoplasmic reticulum. Gastroenterology *139*, 2038-2049.

Iida, K., Li, Y., McGrath, B.C., Frank, A., and Cavener, D.R. (2007). PERK eIF2 alpha kinase is required to regulate the viability of the exocrine pancreas in mice. BMC Cell Biol *8*, 38.

Im, H., Grass, J.A., Johnson, K.D., Boyer, M.E., Wu, J., and Bresnick, E.H. (2004). Measurement of protein-DNA interactions in vivo by chromatin immunoprecipitation. Methods Mol Biol *284*, 129-146.

Ishii, S., and Shimizu, T. (2000). Platelet-activating factor (PAF) receptor and genetically engineered PAF receptor mutant mice. Prog Lipid Res *39*, 41-82.

Ito, D., Walker, J.R., Thompson, C.S., Moroz, I., Lin, W., Veselits, M.L., Hakim, A.M., Fienberg, A.A., and Thinakaran, G. (2004). Characterization of stanniocalcin 2, a novel target of the mammalian unfolded protein response with cytoprotective properties. Mol Cell Biol *24*, 9456-9469.

Iwawaki, T., Akai, R., Kohno, K., and Miura, M. (2004). A transgenic mouse model for monitoring endoplasmic reticulum stress. Nat Med *10*, 98-102.

Izumi, Y., Hirose, T., Tamai, Y., Hirai, S., Nagashima, Y., Fujimoto, T., Tabuse, Y., Kemphues, K.J., and Ohno, S. (1998). An atypical PKC directly associates and colocalizes at the epithelial tight junction with ASIP, a mammalian homologue of Caenorhabditis elegans polarity protein PAR-3. J Cell Biol *143*, 95-106.

James, C.G., Woods, A., Underhill, T.M., and Beier, F. (2006). The transcription factor ATF3 is upregulated during chondrocyte differentiation and represses cyclin D1 and A gene transcription. BMC Mol Biol *7*, 30.

Jensen, J.N., Cameron, E., Garay, M.V., Starkey, T.W., Gianani, R., and Jensen, J. (2005). Recapitulation of elements of embryonic development in adult mouse pancreatic regeneration. Gastroenterology *128*, 728-741.

Ji, B., Chen, X.Q., Misek, D.E., Kuick, R., Hanash, S., Ernst, S., Najarian, R., and Logsdon, C.D. (2003). Pancreatic gene expression during the initiation of acute pancreatitis: identification of EGR-1 as a key regulator. Physiol Genomics *14*, 59-72.

Jiang, H.Y., Wek, S.A., McGrath, B.C., Lu, D., Hai, T., Harding, H.P., Wang, X., Ron, D., Cavener, D.R., and Wek, R.C. (2004). Activating transcription factor 3 is integral to the eukaryotic initiation factor 2 kinase stress response. Mol Cell Biol *24*, 1365-1377.

Johnson, C.L., Kowalik, A.S., Rajakumar, N., and Pin, C.L. (2004). Mist1 is necessary for the establishment of granule organization in serous exocrine cells of the gastrointestinal tract. Mechanisms of development *121*, 261-272.

Johnson, C.L., Peat, J.M., Volante, S.N., Wang, R., McLean, C.A., and Pin, C.L. (2012). Activation of Protein Kinase C delta leads to increased pancreatic acinar cell de-differentiation in the absence of MIST1. J Pathol.

Johnson, C.L., Weston, J.Y., Chadi, S.A., Fazio, E.N., Huff, M.W., Kharitonenkov, A., Koester, A., and Pin, C.L. (2009). Fibroblast growth factor 21 reduces the severity of cerulein-induced pancreatitis in mice. Gastroenterology *137*, 1795-1804.

Johnston, J., Ramos-Valdes, Y., Stanton, L.A., Ladhani, S., Beier, F., and Dimattia, G.E. (2010). Human stanniocalcin-1 or -2 expressed in mice reduces bone size and severely inhibits cranial intramembranous bone growth. Transgenic Res *19*, 1017-1039.

Kasai, H., and Augustine, G.J. (1990). Cytosolic Ca2+ gradients triggering unidirectional fluid secretion from exocrine pancreas. Nature *348*, 735-738.

Katayama, T., Imaizumi, K., Sato, N., Miyoshi, K., Kudo, T., Hitomi, J., Morihara, T., Yoneda, T., Gomi, F., Mori, Y*., et al.* (1999). Presenilin-1 mutations downregulate the signalling pathway of the unfolded-protein response. Nature cell biology *1*, 479-485.

Kaufman, R.J. (1999). Stress signaling from the lumen of the endoplasmic reticulum: coordination of gene transcriptional and translational controls. Genes Dev *13*, 1211-1233.

Kerem, B., Rommens, J.M., Buchanan, J.A., Markiewicz, D., Cox, T.K., Chakravarti, A., Buchwald, M., and Tsui, L.C. (1989). Identification of the cystic fibrosis gene: genetic analysis. Science *245*, 1073-1080.

Kernohan, K.D., Jiang, Y., Tremblay, D.C., Bonvissuto, A.C., Eubanks, J.H., Mann, M.R., and Berube, N.G. (2010). ATRX partners with cohesin and MeCP2 and contributes to developmental silencing of imprinted genes in the brain. Dev Cell *18*, 191-202.

Kimata, Y., Ishiwata-Kimata, Y., Ito, T., Hirata, A., Suzuki, T., Oikawa, D., Takeuchi, M., and Kohno, K. (2007). Two regulatory steps of ER-stress sensor Ire1 involving its cluster formation and interaction with unfolded proteins. J Cell Biol *179*, 75-86.

Kouroku, Y., Fujita, E., Tanida, I., Ueno, T., Isoai, A., Kumagai, H., Ogawa, S., Kaufman, R.J., Kominami, E., and Momoi, T. (2007). ER stress (PERK/eIF2alpha phosphorylation) mediates the polyglutamine-induced LC3 conversion, an essential step for autophagy formation. Cell death and differentiation *14*, 230-239.

Kowalik, A.S., Johnson, C.L., Chadi, S.A., Weston, J.Y., Fazio, E.N., and Pin, C.L. (2007). Mice lacking the transcription factor Mist1 exhibit an altered stress response and increased sensitivity to caerulein-induced pancreatitis. Am J Physiol Gastrointest Liver Physiol *292*, G1123-1132.

Kruger, B., Albrecht, E., and Lerch, M.M. (2000). The role of intracellular calcium signaling in premature protease activation and the onset of pancreatitis. Am J Pathol *157*, 43-50.

Kubisch, C.H., and Logsdon, C.D. (2007). Secretagogues differentially activate endoplasmic reticulum stress responses in pancreatic acinar cells. Am J Physiol Gastrointest Liver Physiol *292*, G1804-1812.

Kubisch, C.H., Sans, M.D., Arumugam, T., Ernst, S.A., Williams, J.A., and Logsdon, C.D. (2006). Early activation of endoplasmic reticulum stress is associated with arginine-induced acute pancreatitis. Am J Physiol Gastrointest Liver Physiol *291*, G238-245.

Kudo, T., Katayama, T., Imaizumi, K., Yasuda, Y., Yatera, M., Okochi, M., Tohyama, M., and Takeda, M. (2002). The unfolded protein response is involved in the pathology of Alzheimer's disease. Ann N Y Acad Sci *977*, 349-355.

Kukor, Z., Toth, M., Pal, G., and Sahin-Toth, M. (2002). Human cationic trypsinogen. Arg(117) is the reactive site of an inhibitory surface loop that controls spontaneous zymogen activation. J Biol Chem *277*, 6111-6117.

Kuo, M.H., and Allis, C.D. (1999). In vivo cross-linking and immunoprecipitation for studying dynamic Protein:DNA associations in a chromatin environment. Methods *19*, 425-433.

Kuwata, K., Hirota, M., Shimizu, H., Nakae, M., Nishihara, S., Takimoto, A., Mitsushima, K., Kikuchi, N., Endo, K., Inoue, M.*, et al.* (2002). Functional analysis of recombinant pancreatic secretory trypsin inhibitor protein with amino-acid substitution. J Gastroenterol *37*, 928-934.

Laitusis, A.L., Brostrom, M.A., and Brostrom, C.O. (1999). The dynamic role of GRP78/BiP in the coordination of mRNA translation with protein processing. J Biol Chem *274*, 486-493.

Lane, J.S., Todd, K.E., Gloor, B., Chandler, C.F., Kau, A.W., Ashley, S.W., Reber, H.A., and McFadden, D.W. (2001). Platelet activating factor antagonism reduces the systemic inflammatory response in a murine model of acute pancreatitis. J Surg Res *99*, 365-370.

Langerhans, P. (1869). Beiträge zur mikroskopischen Anatomie der Bauchspeicheldrüse. Quoted by EL Opie (1903) Disease of the Pancreas JB Lippincott, Philadelphia, 67.

Laposata, E.A., and Lange, L.G. (1986). Presence of nonoxidative ethanol metabolism in human organs commonly damaged by ethanol abuse. Science *231*, 497-499.

Lassot, I., Estrabaud, E., Emiliani, S., Benkirane, M., Benarous, R., and Margottin-Goguet, F. (2005). p300 modulates ATF4 stability and transcriptional activity independently of its acetyltransferase domain. J Biol Chem *280*, 41537-41545.

Law, A.Y., and Wong, C.K. (2009). Stanniocalcin-2 is a HIF-1 target gene that promotes cell proliferation in hypoxia. Experimental cell research *316*, 466-476.

Law, A.Y., and Wong, C.K. (2010). Stanniocalcin-2 promotes epithelial-mesenchymal transition and invasiveness in hypoxic human ovarian cancer cells. Experimental cell research *316*, 3425-3434.

Lee, A.H., Chu, G.C., Iwakoshi, N.N., and Glimcher, L.H. (2005). XBP-1 is required for biogenesis of cellular secretory machinery of exocrine glands. EMBO J *24*, 4368-4380.

Lee, K., Tirasophon, W., Shen, X., Michalak, M., Prywes, R., Okada, T., Yoshida, H., Mori, K., and Kaufman, R.J. (2002). IRE1-mediated unconventional mRNA splicing and S2P-mediated ATF6 cleavage merge to regulate XBP1 in signaling the unfolded protein response. Genes Dev *16*, 452-466.

Lee, N.K., Sowa, H., Hinoi, E., Ferron, M., Ahn, J.D., Confavreux, C., Dacquin, R., Mee, P.J., McKee, M.D., Jung, D.Y.*, et al.* (2007). Endocrine regulation of energy metabolism by the skeleton. Cell *130*, 456-469.

Lemercier, C., Verdel, A., Galloo, B., Curtet, S., Brocard, M.P., and Khochbin, S. (2000). mHDA1/HDAC5 histone deacetylase interacts with and represses MEF2A transcriptional activity. J Biol Chem *275*, 15594-15599.

Li, H.F., Cheng, C.F., Liao, W.J., Lin, H., and Yang, R.B. (2010). ATF3-mediated epigenetic regulation protects against acute kidney injury. J Am Soc Nephrol *21*, 1003-1013.

Lindkvist, B., Appelros, S., Manjer, J., Berglund, G., and Borgstrom, A. (2008). A prospective cohort study of smoking in acute pancreatitis. Pancreatology *8*, 63-70.

Liu, C.Y., and Kaufman, R.J. (2003). The unfolded protein response. Journal of cell science *116*, 1861-1862.

Liu, L.R., and Xia, S.H. (2006). Role of platelet-activating factor in the pathogenesis of acute pancreatitis. World J Gastroenterol *12*, 539-545.

Lowenfels, A.B., Maisonneuve, P., Cavallini, G., Ammann, R.W., Lankisch, P.G., Andersen, J.R., Dimagno, E.P., Andren-Sandberg, A., and Domellof, L. (1993). Pancreatitis and the risk of pancreatic cancer. International Pancreatitis Study Group. N Engl J Med *328*, 1433-1437.

Lowenfels, A.B., Maisonneuve, P., DiMagno, E.P., Elitsur, Y., Gates, L.K., Jr., Perrault, J., and Whitcomb, D.C. (1997). Hereditary pancreatitis and the risk of pancreatic cancer. International Hereditary Pancreatitis Study Group. J Natl Cancer Inst *89*, 442-446.

Lu, P.D., Harding, H.P., and Ron, D. (2004). Translation reinitiation at alternative open reading frames regulates gene expression in an integrated stress response. J Cell Biol *167*, 27-33.

Lugea, A., Tischler, D., Nguyen, J., Gong, J., Gukovsky, I., French, S.W., Gorelick, F.S., and Pandol, S.J. (2011). Adaptive unfolded protein response attenuates alcohol-induced pancreatic damage. Gastroenterology *140*, 987-997.

Ma, K., Vattem, K.M., and Wek, R.C. (2002a). Dimerization and release of molecular chaperone inhibition facilitate activation of eukaryotic initiation factor-2 kinase in response to endoplasmic reticulum stress. J Biol Chem *277*, 18728-18735.

Ma, Y., Brewer, J.W., Diehl, J.A., and Hendershot, L.M. (2002b). Two distinct stress signaling pathways converge upon the CHOP promoter during the mammalian unfolded protein response. J Mol Biol *318*, 1351-1365.

Ma, Y., and Hendershot, L.M. (2003). Delineation of a negative feedback regulatory loop that controls protein translation during endoplasmic reticulum stress. J Biol Chem *278*, 34864-34873.

Mahadevan, N.R., and Zanetti, M. (2011). Tumor stress inside out: cell-extrinsic effects of the unfolded protein response in tumor cells modulate the immunological landscape of the tumor microenvironment. J Immunol *187*, 4403-4409.

Makhija, R., and Kingsnorth, A.N. (2002). Cytokine storm in acute pancreatitis. J Hepatobiliary Pancreat Surg *9*, 401-410.

Maruyama, Y., and Petersen, O.H. (1994). Delay in granular fusion evoked by repetitive cytosolic Ca2+ spikes in mouse pancreatic acinar cells. Cell Calcium *16*, 419-430.

Masuoka, H.C., and Townes, T.M. (2002). Targeted disruption of the activating transcription factor 4 gene results in severe fetal anemia in mice. Blood *99*, 736-745.

Matozaki, T., and Williams, J.A. (1989). Multiple sources of 1,2-diacylglycerol in isolated rat pancreatic acini stimulated by cholecystokinin. Involvement of phosphatidylinositol bisphosphate and phosphatidylcholine hydrolysis. J Biol Chem *264*, 14729-14734.

Mayerle, J., Schnekenburger, J., Kruger, B., Kellermann, J., Ruthenburger, M., Weiss, F.U., Nalli, A., Domschke, W., and Lerch, M.M. (2005). Extracellular cleavage of E-cadherin by leukocyte elastase during acute experimental pancreatitis in rats. Gastroenterology *129*, 1251-1267.

McCullough, K.D., Martindale, J.L., Klotz, L.O., Aw, T.Y., and Holbrook, N.J. (2001). Gadd153 sensitizes cells to endoplasmic reticulum stress by down-regulating Bcl2 and perturbing the cellular redox state. Mol Cell Biol *21*, 1249-1259.

McCuskey, R.S., and Chapman, T.M. (1969). Microscopy of the living pancreas in situ. Am J Anat *126*, 395-407.

Milani, M., Rzymski, T., Mellor, H.R., Pike, L., Bottini, A., Generali, D., and Harris, A.L. (2009). The role of ATF4 stabilization and autophagy in resistance of breast cancer cells treated with Bortezomib. Cancer Res *69*, 4415-4423.

Mithofer, K., Fernandez-del Castillo, C., Rattner, D., and Warshaw, A.L. (1998). Subcellular kinetics of early trypsinogen activation in acute rodent pancreatitis. Am J Physiol *274*, G71-79.

Miyamoto, Y., Maitra, A., Ghosh, B., Zechner, U., Argani, P., Iacobuzio-Donahue, C.A., Sriuranpong, V., Iso, T., Meszoely, I.M., Wolfe, M.S.*, et al.* (2003). Notch mediates TGF alpha-induced changes in epithelial differentiation during pancreatic tumorigenesis. Cancer Cell *3*, 565-576.

Montminy, M.R., and Bilezikjian, L.M. (1987). Binding of a nuclear protein to the cyclic-AMP response element of the somatostatin gene. Nature *328*, 175-178.

Moore, E.E., Kuestner, R.E., Conklin, D.C., Whitmore, T.E., Downey, W., Buddle, M.M., Adams, R.L., Bell, L.A., Thompson, D.L., Wolf, A.*, et al.* (1999). Stanniocalcin 2: characterization of the protein and its localization to human pancreatic alpha cells. Horm Metab Res *31*, 406-414.

Motta, P.M., Macchiarelli, G., Nottola, S.A., and Correr, S. (1997). Histology of the exocrine pancreas. Microsc Res Tech *37*, 384-398.

Mukhopadhyay, A., Deplancke, B., Walhout, A.J., and Tissenbaum, H.A. (2008). Chromatin immunoprecipitation (ChIP) coupled to detection by quantitative real-time PCR to study transcription factor binding to DNA in Caenorhabditis elegans. Nat Protoc *3*, 698-709.

Nakagomi, S., Suzuki, Y., Namikawa, K., Kiryu-Seo, S., and Kiyama, H. (2003). Expression of the activating transcription factor 3 prevents c-Jun N-terminal kinase-induced neuronal death by promoting heat shock protein 27 expression and Akt activation. J Neurosci *23*, 5187-5196.

Nathanson, M.H., Padfield, P.J., O'Sullivan, A.J., Burgstahler, A.D., and Jamieson, J.D. (1992). Mechanism of Ca2+ wave propagation in pancreatic acinar cells. J Biol Chem *267*, 18118-18121.

Nicolis, E., Bonizzato, A., Assael, B.M., and Cipolli, M. (2005). Identification of novel mutations in patients with Shwachman-Diamond syndrome. Hum Mutat *25*, 410.

Niederau, C., Niederau, M., Luthen, R., Strohmeyer, G., Ferrell, L.D., and Grendell, J.H. (1990). Pancreatic exocrine secretion in acute experimental pancreatitis. Gastroenterology *99*, 1120-1127.

Nishitoh, H., Saitoh, M., Mochida, Y., Takeda, K., Nakano, H., Rothe, M., Miyazono, K., and Ichijo, H. (1998). ASK1 is essential for JNK/SAPK activation by TRAF2. Mol Cell *2*, 389-395.

Novoa, I., Zeng, H., Harding, H.P., and Ron, D. (2001). Feedback inhibition of the unfolded protein response by GADD34-mediated dephosphorylation of eIF2alpha. J Cell Biol *153*, 1011-1022.

Okada, T., Yoshida, H., Akazawa, R., Negishi, M., and Mori, K. (2002). Distinct roles of activating transcription factor 6 (ATF6) and double-stranded RNA-activated protein kinase-like endoplasmic reticulum kinase (PERK) in transcription during the mammalian unfolded protein response. Biochem J *366*, 585-594.

Okamura, K., Kimata, Y., Higashio, H., Tsuru, A., and Kohno, K. (2000). Dissociation of Kar2p/BiP from an ER sensory molecule, Ire1p, triggers the unfolded protein response in yeast. Biochem Biophys Res Commun *279*, 445-450.

Ono, S.J., Liou, H.C., Davidon, R., Strominger, J.L., and Glimcher, L.H. (1991). Human X-box-binding protein 1 is required for the transcription of a subset of human class II major histocompatibility genes and forms a heterodimer with c-fos. Proc Natl Acad Sci U S A *88*, 4309-4312.

Pan, Y., Chen, H., Siu, F., and Kilberg, M.S. (2003). Amino acid deprivation and endoplasmic reticulum stress induce expression of multiple activating transcription factor-3 mRNA species that, when overexpressed in HepG2 cells, modulate transcription by the human asparagine synthetase promoter. J Biol Chem *278*, 38402-38412.

Papa, F.R., Zhang, C., Shokat, K., and Walter, P. (2003). Bypassing a kinase activity with an ATP-competitive drug. Science *302*, 1533-1537.

Park, P.J. (2009). ChIP-seq: advantages and challenges of a maturing technology. Nat Rev Genet *10*, 669-680.

Pastor, C.M., Vonlaufen, A., Georgi, F., Hadengue, A., Morel, P., and Frossard, J.L. (2006). Neutrophil depletion--but not prevention of Kupffer cell activation--decreases the severity of cerulein-induced acute pancreatitis. World J Gastroenterol *12*, 1219-1224.

Pearson, A.G., Gray, C.W., Pearson, J.F., Greenwood, J.M., During, M.J., and Dragunow, M. (2003). ATF3 enhances c-Jun-mediated neurite sprouting. Brain Res Mol Brain Res *120*, 38-45.

Petersen, O.H., Gerasimenko, O.V., Gerasimenko, J.V., Mogami, H., and Tepikin, A.V. (1998). The calcium store in the nuclear envelope. Cell Calcium *23*, 87-90.

Pin, C.L., Rukstalis, J.M., Johnson, C., and Konieczny, S.F. (2001). The bHLH transcription factor Mist1 is required to maintain exocrine pancreas cell organization and acinar cell identity. J Cell Biol *155*, 519-530.

Pincus, D., Chevalier, M.W., Aragon, T., van Anken, E., Vidal, S.E., El-Samad, H., and Walter, P. (2010). BiP binding to the ER-stress sensor Ire1 tunes the homeostatic behavior of the unfolded protein response. PLoS Biol *8*, e1000415.

Qiu, R.G., Abo, A., and Steven Martin, G. (2000). A human homolog of the C. elegans polarity determinant Par-6 links Rac and Cdc42 to PKCzeta signaling and cell transformation. Curr Biol *10*, 697-707.

Ramakrishnan, V. (1997). Histone H1 and chromatin higher-order structure. Crit Rev Eukaryot Gene Expr *7*, 215-230.

Rapoport, T.A., Jungnickel, B., and Kutay, U. (1996). Protein transport across the eukaryotic endoplasmic reticulum and bacterial inner membranes. Annu Rev Biochem *65*, 271-303.

Raraty, M., Ward, J., Erdemli, G., Vaillant, C., Neoptolemos, J.P., Sutton, R., and Petersen, O.H. (2000). Calcium-dependent enzyme activation and vacuole formation in the apical granular region of pancreatic acinar cells. Proc Natl Acad Sci U S A *97*, 13126-13131.

Raulic, S., Ramos-Valdes, Y., and DiMattia, G.E. (2008). Stanniocalcin 2 expression is regulated by hormone signalling and negatively affects breast cancer cell viability in vitro. J Endocrinol *197*, 517-529.

Riordan, J.R., Rommens, J.M., Kerem, B., Alon, N., Rozmahel, R., Grzelczak, Z., Zielenski, J., Lok, S., Plavsic, N., Chou, J.L.*, et al.* (1989). Identification of the cystic fibrosis gene: cloning and characterization of complementary DNA. Science *245*, 1066-1073.

Rommens, J.M., Iannuzzi, M.C., Kerem, B., Drumm, M.L., Melmer, G., Dean, M., Rozmahel, R., Cole, J.L., Kennedy, D., Hidaka, N.*, et al.* (1989). Identification of the cystic fibrosis gene: chromosome walking and jumping. Science *245*, 1059-1065.

Rzymski, T., Milani, M., Pike, L., Buffa, F., Mellor, H.R., Winchester, L., Pires, I., Hammond, E., Ragoussis, I., and Harris, A.L. (2010). Regulation of autophagy by ATF4 in response to severe hypoxia. Oncogene *29*, 4424-4435.

Sahin-Toth, M., and Toth, M. (2000). Gain-of-function mutations associated with hereditary pancreatitis enhance autoactivation of human cationic trypsinogen. Biochem Biophys Res Commun *278*, 286-289.

Saluja, A., Hashimoto, S., Saluja, M., Powers, R.E., Meldolesi, J., and Steer, M.L. (1987). Subcellular redistribution of lysosomal enzymes during caerulein-induced pancreatitis. Am J Physiol *253*, G508-516.

Saluja, A.K., Bhagat, L., Lee, H.S., Bhatia, M., Frossard, J.L., and Steer, M.L. (1999). Secretagogue-induced digestive enzyme activation and cell injury in rat pancreatic acini. Am J Physiol *276*, G835-842.

Saluja, A.K., Donovan, E.A., Yamanaka, K., Yamaguchi, Y., Hofbauer, B., and Steer, M.L. (1997). Cerulein-induced in vitro activation of trypsinogen in rat pancreatic acini is mediated by cathepsin B. Gastroenterology *113*, 304-310.

Sandoval, D., Gukovskaya, A., Reavey, P., Gukovsky, S., Sisk, A., Braquet, P., Pandol, S.J., and Poucell-Hatton, S. (1996). The role of neutrophils and platelet-activating factor in mediating experimental pancreatitis. Gastroenterology *111*, 1081-1091.

Sato, M., Yao, V.J., Arap, W., and Pasqualini, R. (2010). GRP78 signaling hub a receptor for targeted tumor therapy. Adv Genet *69*, 97-114.

Sato, N., Urano, F., Yoon Leem, J., Kim, S.H., Li, M., Donoviel, D., Bernstein, A., Lee, A.S., Ron, D., Veselits, M.L.*, et al.* (2000). Upregulation of BiP and CHOP by the unfolded-protein response is independent of presenilin expression. Nature cell biology *2*, 863-870.

Scheuner, D., Song, B., McEwen, E., Liu, C., Laybutt, R., Gillespie, P., Saunders, T., Bonner-Weir, S., and Kaufman, R.J. (2001). Translational control is required for the unfolded protein response and in vivo glucose homeostasis. Mol Cell *7*, 1165-1176.

Schindler, A.J., and Schekman, R. (2009). In vitro reconstitution of ER-stress induced ATF6 transport in COPII vesicles. Proc Natl Acad Sci U S A *106*, 17775-17780.

Schroder, M., and Kaufman, R.J. (2005). ER stress and the unfolded protein response. Mutat Res *569*, 29-63.

Schwaller, M., Wilkinson, B., and Gilbert, H.F. (2003). Reduction-reoxidation cycles contribute to catalysis of disulfide isomerization by protein-disulfide isomerase. J Biol Chem *278*, 7154-7159.

Shamu, C.E., and Walter, P. (1996). Oligomerization and phosphorylation of the Ire1p kinase during intracellular signaling from the endoplasmic reticulum to the nucleus. EMBO J *15*, 3028-3039.

Shi, Y., Vattem, K.M., Sood, R., An, J., Liang, J., Stramm, L., and Wek, R.C. (1998). Identification and characterization of pancreatic eukaryotic initiation factor 2 alpha-subunit kinase, PEK, involved in translational control. Mol Cell Biol *18*, 7499-7509.

Shin, J., and Sohn, Y.C. (2009). cDNA cloning of Japanese flounder stanniocalcin 2 and its mRNA expression in a variety of tissues. Comp Biochem Physiol A Mol Integr Physiol *153*, 24-29.

Shwachman, H., Diamond, L.K., Oski, F.A., and Khaw, K.T. (1964). The Syndrome of Pancreatic Insufficiency and Bone Marrow Dysfunction. J Pediatr *65*, 645-663.

Sidrauski, C., Cox, J.S., and Walter, P. (1996). tRNA ligase is required for regulated mRNA splicing in the unfolded protein response. Cell *87*, 405-413.

Song, M., Zaninovic, V., Kim, D., Gukovsky, I., Gukovskaya, A., Kang, K., and Pandol, S. (1999). Amelioration of rat cerulein pancreatitis by guamerin-derived peptide, a novel elastase inhibitor. Pancreas *18*, 231-239.

Sood, R., Porter, A.C., Ma, K., Quilliam, L.A., and Wek, R.C. (2000). Pancreatic eukaryotic initiation factor-2alpha kinase (PEK) homologues in humans, Drosophila melanogaster and Caenorhabditis elegans that mediate translational control in response to endoplasmic reticulum stress. Biochem J *346 Pt 2*, 281-293.

Stafforini, D.M., McIntyre, T.M., Zimmerman, G.A., and Prescott, S.M. (2003). Platelet-activating factor, a pleiotrophic mediator of physiological and pathological processes. Crit Rev Clin Lab Sci *40*, 643-672.

Sundell, K., Bjornsson, B.T., Itoh, H., and Kawauchi, H. (1992). Chum salmon (Oncorhynchus keta) stanniocalcin inhibits in vitro intestinal calcium uptake in Atlantic cod (Gadus morhua). Journal of comparative physiology *162*, 489-495.

Suzuki, A., Yamanaka, T., Hirose, T., Manabe, N., Mizuno, K., Shimizu, M., Akimoto, K., Izumi, Y., Ohnishi, T., and Ohno, S. (2001). Atypical protein kinase C is involved in the evolutionarily conserved par protein complex and plays a critical role in establishing epithelia-specific junctional structures. J Cell Biol *152*, 1183-1196.

Suzuki, M., Isaji, S., Stanten, R., Frey, C.F., and Ruebner, B. (1992). Effect of protease inhibitor FUT-175 on acute hemorrhagic pancreatitis in mice. Int J Pancreatol *11*, 59-65.

Szilagyi, L., Kenesi, E., Katona, G., Kaslik, G., Juhasz, G., and Graf, L. (2001). Comparative in vitro studies on native and recombinant human cationic trypsins. Cathepsin B is a possible pathological activator of trypsinogen in pancreatitis. J Biol Chem *276*, 24574-24580.

Takahashi, H. (1984). Scanning electron microscopy of the rat exocrine pancreas. Arch Histol Jpn *47*, 387-404.

Tashiro, M., Schafer, C., Yao, H., Ernst, S.A., and Williams, J.A. (2001). Arginine induced acute pancreatitis alters the actin cytoskeleton and increases heat shock protein expression in rat pancreatic acinar cells. Gut *49*, 241-250.

Teich, N., Nemoda, Z., Kohler, H., Heinritz, W., Mossner, J., Keim, V., and Sahin-Toth, M. (2005). Gene conversion between functional trypsinogen genes PRSS1 and PRSS2 associated with chronic pancreatitis in a six-year-old girl. Hum Mutat *25*, 343-347.

Tolstrup, J.S., Kristiansen, L., Becker, U., and Gronbaek, M. (2009). Smoking and risk of acute and chronic pancreatitis among women and men: a population-based cohort study. Arch Intern Med *169*, 603-609.

Ubeda, M., and Habener, J.F. (2000). CHOP gene expression in response to endoplasmic-reticular stress requires NFY interaction with different domains of a conserved DNA-binding element. Nucleic Acids Res *28*, 4987-4997.

Urano, F., Wang, X., Bertolotti, A., Zhang, Y., Chung, P., Harding, H.P., and Ron, D. (2000). Coupling of stress in the ER to activation of JNK protein kinases by transmembrane protein kinase IRE1. Science *287*, 664-666.

Van Acker, G.J., Saluja, A.K., Bhagat, L., Singh, V.P., Song, A.M., and Steer, M.L. (2002). Cathepsin B inhibition prevents trypsinogen activation and reduces pancreatitis severity. Am J Physiol Gastrointest Liver Physiol *283*, G794-800.

Varallyay, E., Pal, G., Patthy, A., Szilagyi, L., and Graf, L. (1998). Two mutations in rat trypsin confer resistance against autolysis. Biochem Biophys Res Commun *243*, 56-60.

Vattem, K.M., and Wek, R.C. (2004). Reinitiation involving upstream ORFs regulates ATF4 mRNA translation in mammalian cells. Proc Natl Acad Sci U S A *101*, 11269-11274.

Volkmer, J., Guth, S., Nastainczyk, W., Knippel, P., Klappa, P., Gnau, V., and Zimmermann, R. (1997). Pancreas specific protein disulfide isomerase, PDIp, is in transient contact with secretory proteins during late stages of translocation. FEBS Lett *406*, 291-295.

Walter, P., and Ron, D. (2011). The unfolded protein response: from stress pathway to homeostatic regulation. Science *334*, 1081-1086.

Wang, A., Arantes, S., Conti, C., McArthur, M., Aldaz, C.M., and MacLeod, M.C. (2007). Epidermal hyperplasia and oral carcinoma in mice overexpressing the transcription factor ATF3 in basal epithelial cells. Mol Carcinog *46*, 476-487.

Wang, A., Arantes, S., Yan, L., Kiguchi, K., McArthur, M.J., Sahin, A., Thames, H.D., Aldaz, C.M., and Macleod, M.C. (2008). The transcription factor ATF3 acts as an oncogene in mouse mammary tumorigenesis. BMC Cancer *8*, 268.

Wang, C.C., Ng, C.P., Lu, L., Atlashkin, V., Zhang, W., Seet, L.F., and Hong, W. (2004). A role of VAMP8/endobrevin in regulated exocytosis of pancreatic acinar cells. Dev Cell *7*, 359-371.

Watanabe, O., Baccino, F.M., Steer, M.L., and Meldolesi, J. (1984). Supramaximal caerulein stimulation and ultrastructure of rat pancreatic acinar cell: early morphological changes during development of experimental pancreatitis. Am J Physiol *246*, G457-467.

Weksler-Zangen, S., Raz, I., Lenzen, S., Jorns, A., Ehrenfeld, S., Amir, G., Oprescu, A., Yagil, Y., Yagil, C., Zangen, D.H.*, et al.* (2008). Impaired glucose-stimulated insulin secretion is coupled with exocrine pancreatic lesions in the Cohen diabetic rat. Diabetes *57*, 279-287.

Werner, J., Saghir, M., Warshaw, A.L., Lewandrowski, K.B., Laposata, M., Iozzo, R.V., Carter, E.A., Schatz, R.J., and Fernandez-Del Castillo, C. (2002). Alcoholic pancreatitis in rats: injury from nonoxidative metabolites of ethanol. Am J Physiol Gastrointest Liver Physiol *283*, G65-73.

Whitcomb, D.C., Gorry, M.C., Preston, R.A., Furey, W., Sossenheimer, M.J., Ulrich, C.D., Martin, S.P., Gates, L.K., Jr., Amann, S.T., Toskes, P.P.*, et al.* (1996). Hereditary pancreatitis is caused by a mutation in the cationic trypsinogen gene. Nat Genet *14*, 141-145.

Williams, J.A., Korc, M., and Dormer, R.L. (1978). Action of secretagogues on a new preparation of functionally intact, isolated pancreatic acini. Am J Physiol *235*, 517-524.

Witt, H., Luck, W., Hennies, H.C., Classen, M., Kage, A., Lass, U., Landt, O., and Becker, M. (2000). Mutations in the gene encoding the serine protease inhibitor, Kazal type 1 are associated with chronic pancreatitis. Nat Genet *25*, 213-216.

Wittel, U.A., Pandey, K.K., Andrianifahanana, M., Johansson, S.L., Cullen, D.M., Akhter, M.P., Brand, R.E., Prokopczyk, B., and Batra, S.K. (2006). Chronic pancreatic inflammation induced by environmental tobacco smoke inhalation in rats. Am J Gastroenterol *101*, 148-159.

Workman, J.L., and Kingston, R.E. (1998). Alteration of nucleosome structure as a mechanism of transcriptional regulation. Annu Rev Biochem *67*, 545-579.

Xu, Y.Z., Thuraisingam, T., Marino, R., and Radzioch, D. (2011). Recruitment of SWI/SNF complex is required for transcriptional activation of the SLC11A1 gene during macrophage differentiation of HL-60 cells. J Biol Chem *286*, 12839-12849.

Yadav, D., Hawes, R.H., Brand, R.E., Anderson, M.A., Money, M.E., Banks, P.A., Bishop, M.D., Baillie, J., Sherman, S., DiSario, J.*, et al.* (2009). Alcohol consumption, cigarette smoking, and the risk of recurrent acute and chronic pancreatitis. Arch Intern Med *169*, 1035-1045.

Yadav, D., and Lowenfels, A.B. (2006). Trends in the epidemiology of the first attack of acute pancreatitis: a systematic review. Pancreas *33*, 323-330.

Ye, J., Rawson, R.B., Komuro, R., Chen, X., Dave, U.P., Prywes, R., Brown, M.S., and Goldstein, J.L. (2000). ER stress induces cleavage of membrane-bound ATF6 by the same proteases that process SREBPs. Mol Cell *6*, 1355-1364.

Yoshida, H., Matsui, T., Hosokawa, N., Kaufman, R.J., Nagata, K., and Mori, K. (2003). A time-dependent phase shift in the mammalian unfolded protein response. Dev Cell *4*, 265-271.

Yoshida, H., Matsui, T., Yamamoto, A., Okada, T., and Mori, K. (2001). XBP1 mRNA is induced by ATF6 and spliced by IRE1 in response to ER stress to produce a highly active transcription factor. Cell *107*, 881-891.

Yoshida, H., Okada, T., Haze, K., Yanagi, H., Yura, T., Negishi, M., and Mori, K. (2000). ATF6 activated by proteolysis binds in the presence of NF-Y (CBF) directly to the cis-acting element responsible for the mammalian unfolded protein response. Mol Cell Biol *20*, 6755-6767.

Yoshida, H., Oku, M., Suzuki, M., and Mori, K. (2006). pXBP1(U) encoded in XBP1 pre-mRNA negatively regulates unfolded protein response activator pXBP1(S) in mammalian ER stress response. J Cell Biol *172*, 565-575.

Yoshizawa, T., Hinoi, E., Jung, D.Y., Kajimura, D., Ferron, M., Seo, J., Graff, J.M., Kim, J.K., and Karsenty, G. (2009). The transcription factor ATF4 regulates glucose metabolism in mice through its expression in osteoblasts. J Clin Invest *119*, 2807-2817.

Zeiger, W., Ito, D., Swetlik, C., Oh-hora, M., Villereal, M.L., and Thinakaran, G. (2011). Stanniocalcin 2 is a negative modulator of store-operated calcium entry. Mol Cell Biol *31*, 3710-3722.

Zhang, K., Shen, X., Wu, J., Sakaki, K., Saunders, T., Rutkowski, D.T., Back, S.H., and Kaufman, R.J. (2006). Endoplasmic reticulum stress activates cleavage of CREBH to induce a systemic inflammatory response. Cell *124*, 587-599.

Zhang, P., McGrath, B.C., Reinert, J., Olsen, D.S., Lei, L., Gill, S., Wek, S.A., Vattem, K.M., Wek, R.C., Kimball, S.R.*, et al.* (2002). The GCN2 eIF2alpha kinase is required for adaptation to amino acid deprivation in mice. Mol Cell Biol *22*, 6681-6688.

Zhou, H., Shen, D.F., Bian, Z.Y., Zong, J., Deng, W., Zhang, Y., Guo, Y.Y., Li, H., and Tang, Q.Z. (2011). Activating transcription factor 3 deficiency promotes cardiac hypertrophy, dysfunction, and fibrosis induced by pressure overload. PLoS One *6*, e26744.

Zhou, W., Levine, B.A., and Olson, M.S. (1993). Platelet-activating factor: a mediator of pancreatic inflammation during cerulein hyperstimulation. Am J Pathol *142*, 1504-1512.

Zhou, W.G., Chao, W., Levine, B.A., and Olson, M.S. (1990). Evidence for platelet-activating factor as a late-phase mediator of chronic pancreatitis in the rat. Am J Pathol *137*, 1501-1508.

Zinszner, H., Kuroda, M., Wang, X., Batchvarova, N., Lightfoot, R.T., Remotti, H., Stevens, J.L., and Ron, D. (1998). CHOP is implicated in programmed cell death in response to impaired function of the endoplasmic reticulum. Genes Dev *12*, 982-995.

8 « Appendices»

Appendix Figure A1. Activation of the PERK Pathway in Response to Pancreatitis is Altered in *Stc2*^{Tg} Mice. (A) Western blot analysis of PERK pathway members during pancreatitis (CIP) and treated with a saline control in wild type (WT) and *Stc2*^{Tg} (Tg) tissue. (B) Analysis of PERK phosphorylation in untreated and saline treated WT and *Stc2*^{Tg} tissue.

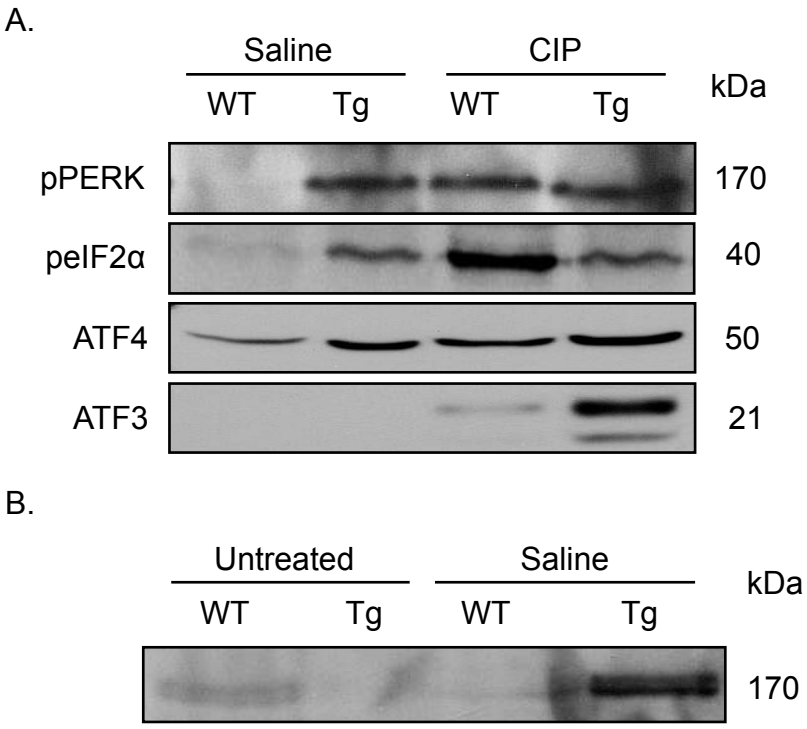

Appendix Figure A 1. Activation of the PERK Pathway in Response to Pancreatitis is Altered in *STC2*^{Tg} Mice.

Appendix Figure A2. XBP1 binds to region B of the *Mist1* promoter during CIP. (A) PCR analysis revealed that XBP1 binds region B of the Mist1 promoter only during CIP. (B) qPCR confirms XBP1 binding to region B during CIP. N = 2. IgG is used as a negative control.

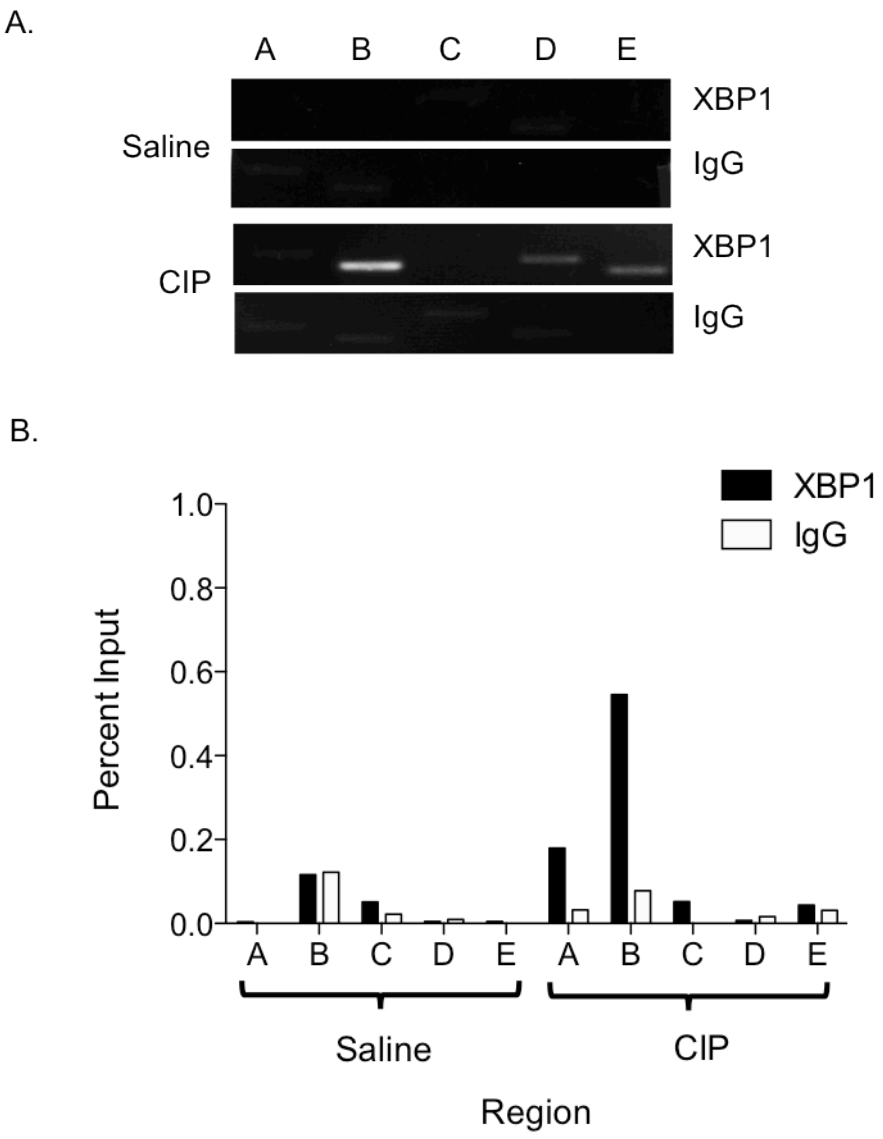

Appendix Figure A 2. XBP1 Binds to Region B of the *Mist1* Promoter During CIP.

Appendix Figure A 3. ATF3 is Not Required for *Gadd34* Expression During CIP. qRT-PCR revealed that the increase in *Gadd34* expression seen in wild type (WT) pancreatic tissue during CIP is present during CIP in mice lacking *Atf3* (*Atf3*$^{-/-}$).

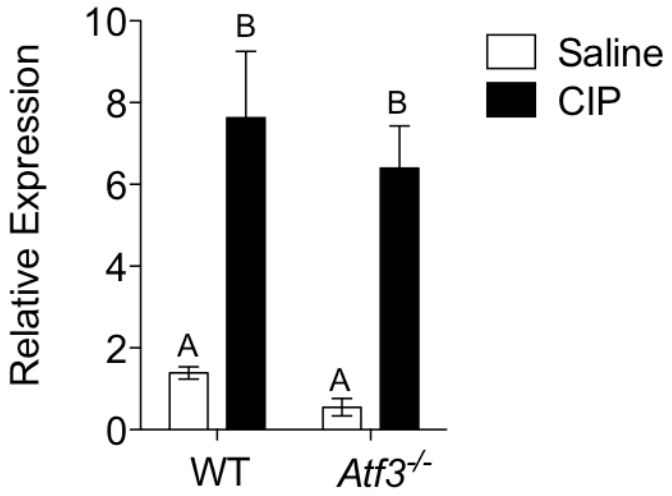

Appendix Figure A 3. ATF3 is not Required for *Gadd34* Expression During CIP.

9 « Curriculum Vitae»

Elena N. Fazio

EDUCATION

Sept. 2006 – Current	Ph.D. Candidate, Physiology and Developmental Biology University of Western Ontario, London, ON. Children's Health Research Institute Department of Physiology and Pharmacology with Developmental Biology Project: The transcriptional role of the unfolded protein response in pancreatic disease Advisor: C.L. Pin
March 2004-April 2006	M.Sc., Pharmacology and Toxicology University of Western Ontario, London, ON. Children's Health Research Institute Department of Physiology and Pharmacology Project: Altered endocrine function in mice lacking the exocrine-specific transcription factor Mist1 Advisor: C.L. Pin
1998-2002	B.Sc., Honours Pharmacology and Toxicology University of Western Ontario, London, ON.

RESEARCH EXPERIENCE:

May 2012 – Current	Postdoctoral Fellow London Regional Cancer Program, London ON London Health Sciences Centre Department of Oncology Advisors: T. Shepherd and G. DiMattia
Sept. 2002 – Feb. 2004	Commencement of Masters Thesis London Regional Cancer Program, London, ON University of Western Ontario Department of Physiology and Pharmacology Project: Activity of Thymine DNA Glycosylase and CREB Binding Protein in DNA Repair Advisor: M. Tini
May 2002 – Sept. 2002	Summer Research Student, London Health Sciences Centre London Regional Cancer Program, London ON Advisor: M. Tini
Sept 2001 – April 2002	Fourth Year Honours Thesis, Department of Pharmacology and Toxicology University of Western Ontario, London, ON Project: The role of Kiss-1 in trophoblast migration Advisor: T. D'Souza

May 2001 – Sept. 2001	Summer Research Student, Department of Paediatrics University of Western Ontario, London ON Advisor: T. D'Souza

SCHOLARSHIPS:

2010-11	Ontario Graduate Scolarship (OGS)
2009	Schulich Graduate Scholarship (SGS)
2008	Schulich Graduate Scholarship (SGS)
2007-10	Canadian Digestive Health Foundation/Canadian Institutes of Health Research (CDHF/CIHR) Doctoral Research Award
2007-08	Ontario Graduate Scholarship (OGS) - *Declined*
2007	Schulich Graduate Scholarship (SGS)
2007	Western Graduate Scholarship (WGRS)
2006-07	Department of Paediatrics Doctoral Research Award
2006-07	Western Graduate Research Scholarship (WGRS)
2003-04	Ontario Graduate Scholarship for Science and Technology
2002-03	Fuller Family Scholarship, London Regional Cancer Program
2002-03	Special University Scholarship, University of Western Ontario Tuition, approx.
2001-02	Lambton County University Scholarship
1998-02	University of Western Ontario Continuing Entrance Scholarship
1998-02	Dow Chemical Canada Scholarship
1998-02	Bayer Rubber Inc. Scholarship
1998-00	Carrothers Family Scholarship

OTHER ACADEMIC RECOGNITION:

2010	Department of Paediatrics Travel Award
2010	Children's Health Research Institute Travel Award
2010	Silver Medal: Canadian Institutes of Health Research - Canadian Student Health Research Forum (Winnipeg, MB)
2010	Schulich School of Medicine and Dentistry Honorarium (Selected as faculty representation at recruitment fair, Calgary AB and Edmonton AB)
2010	Moffat Research Day, First Prize: Molecular Biology
2009	Schulich School of Medicine and Dentistry Honorarium (Selected as faculty representation at recruitment fair, Calgary AB)
2009	Department of Paediatrics Travel Award
2008	Department of Physiology and Pharmacology Research Day, First Prize: Respiratory and Gastrointestinal Physiology
2008	Department of Physiology and Pharmacology: Mogenson Award (High achievement in the category of Physiology PhD)
2008	Department of Paediatrics Research Day: First Prize: Poster
2007	Department of Paediatrics Research Day: First Prize: Poster
2006	G. Murray Fraser Award: Top MSc Thesis
1998-02	University of Western Ontario Dean's Honour List

SCIENTIFIC PUBLICATIONS

Fazio, E.N (2012). XBP1. The Pancreapedia: Exocrine Pancreas Knowledge Base, DOI: 10.3998/panc.2012.1

Fazio, E.N., Mehmood, R., Pin, C.L. (2011) Chromatin Immunoprecipitation (ChIP) from pancreatic acinar cells and whole pancreatic tissue.

Submitted to Pancreapedia: Exocrine Pancreas Knowledge Base. Ann Arbor, MI: Publishing at the University of Michigan Library, August, 2011. This is a peer reviewed article requested by the Editors.

Fazio, E.N., DiMattia, G.E., Chadi, S.A., Kernohan, K., and Pin C.L. (2011). Stanniocalcin 2 alters PERK signaling and reduces cellular injury during cerulein induced pancreatitis in mice. *BMC Cell Biology.* 12:17.

Contribution to pulication: Conceived experimental design with C. Pin and G. DiMattia. Performed 95% of experimental work. Wrote manuscript.

Johnson, C.L., Weston, J.Y., Chadi. S.A., **Fazio, E.N**., Huff, M.W., Kharitonenkov, A., Köster, A., and Christopher L. Pin (2009) Fibroblast growth factor 21 reduces the severity of cerulein-induced pancreatitis in mice. *Gastroenterology.* **137:** 1795-1804.

Contribution to pulication: Performed pancreatitis experiments to generate tissue and blood for experimental analyses.

Kowalik A.S., Johnson, C.L., Chadi, S.A., Weston, J.Y., **Fazio, E.N.**, Pin, C.L. (2007) Mice lacking the transcription factor Mist1 exhibit an altered stress response and increased sensitivity to caerulein-induced pancreatitis. *American Journal of Physiology. Gastrointestinal and Liver Physiology*. **292(4)**: G1123-32.

Contribution to publication: performed a portion of experimental work.

Fazio. E.N., Pin, C.L. (2007) Mist1-null mice are resistant to streptozotocin-induced beta cell damage. *Biochemical and Biophysical Research Communications.* **353(3)**:823-828.

Contribution to publication: Conceived the study with C. Pin, performed all experimental work, wrote manuscript.

Fazio, E.N., Everest, M., Colman, R., Wang, R., Pin, C.L. (2005) Altered Glut-2 accumulation and β-cell function in mice lacking the exocrine-specific transcription factor Mist1. *Journal of Endocrinology.* **187**: 407-418.

Contribution to publication: Conceived experimental design with C. Pin, performed most of the experimental work, wrote manuscript.

SCIENTIFIC PRESENTATIONS

Platform

Fazio E.N., Johnson, C.L., Pin, C.L. Activating transcription factor 3 transcriptionally regulates cell differentiation during pancreatitis. London Health Research Day. March 2012

Fazio E.N., DiMattia G.E., Pin, C.L. The Molecular Role of the Unfolded Protein Response in Pancreatitis. European Pancreas Club, Stockholm, Sweden. June 2010

Fazio E.N., DiMattia G.E., Pin, C.L. The Molecular Role of the Unfolded Protein Response in Pancreatitis. Paediatric Research Day, London Health Sciences Centre. May 2010

Fazio E.N., DiMattia G.E., Pin, C.L. The Molecular Role of the Unfolded Protein Response in Pancreatitis. Developmental Biology Day, University of Western Ontario. May 2010

Fazio, E.N., DiMattia, G.E., Pin, C.L. Molecular stress mechanisms in the regenerating pancreas. Paediatric Research Day, Department of Paediatrics, London Health Sciences Centre. June 2009

Fazio, E.N., Wang, R., Pin, C.L. The Role of Exocrine-Specific Mist1 in the Mouse Endocrine Pancreas. Paediatric Research Day, Department of Paediatrics, London Health Sciences Centre. May 2005.

Recent Poster

Fazio, E.N., Cregan, S., Hai, T., Pin, C.L. A molecular role for the unfolded protein response in exocrine pancreas stress. FASEB Research Conference: From Unfolded Proteins in the Endoplasmic Reticulum to Disease. Saxton's River, Vermont, June 2011.

Fazio E.N., Pin, C.L. The Molecular Role of the Unfolded Protein Response in Pancreatitis. Canadian Student Health Research Forum, CIHR. Winnipeg. Manitoba. June 2010

Fazio E.N., DiMattia G.E., Pin, C.L. Molecular Stress Mechanisms in Pancreatic Injury. Moffat Research Day, University of Western Ontario. March 2010

Fazio, E.N., DiMattia, G.E., Chadi, S.A., Pin, C.L. The Role of Stanniocalcin 2 in the Pancreatic Unfolded Protein Response *in vivo***.** Physiology and Pharmacology Research Day. November 2009

Fazio, E.N., DiMattia, G.E., Pin, C.L. Molecular stress mechanisms in the regenerating pancreas. FASEB Research Conference: From Unfolded Proteins in the Endoplasmic Reticulum to Disease. Saxton's River, Vermont, June 2009

Fazio, E.N., and Pin, C.L. The role of Mist1 in Exocrine Pancreas Stress. Developmental Biology Day, University of Western Ontario. April, 2009.

Fazio, E.N., and Pin, C.L. The role of Mist1 in Exocrine Pancreas Stress. Physiology and Pharmacology Research Day, University of Western Ontario. November 2008.

Fazio, E.N., and Pin, C.L. The role of Mist1 in Exocrine Pancreas Stress. Paediatric Research Day, Department of Paediatrics, London Health Sciences Centre. May 2008.

Fazio, E.N., DiMattia, G.E., Drysdale, T.A., Kernohan, K., Giller, C., Chadi, S.A.,Weston., J.Y., Pin C.L. Stanniocalcin 2 in the Endoplasmic Reticulum Stress Response of the Pancreas. FASEB Summer Research Conference: From Unfolded Proteins in the Endoplasmic Reticulum to Disease. Indian Wells, California. August 2007.

Fazio, E.N., Gillier C., DiMattia, G.E., Pin, C.L. Stanniocalcin-2 is Important for Proper Pancreatic Development and Function. Paediatric Research Day, Department of Paediatrics, London Health Sciences Centre. May 2007.

TEACHING EXPERIENCE

September 2009 – January 2010	Lecturer Physiology 4690: Gastrointestinal Physiology University of Western Ontario London, ON
January 2004 – April 2004	Teaching Assistant Pharmacology 206b: Nursing Pharmacology University of Western Ontario/ Fanshawe College, London ON